



**İSTANBUL COMMERCE
UNIVERSITY**

GRADUATE SCHOOL OF NATURAL AND APPLIED SCIENCES

**SYSTEM IDENTIFICATION AND ESTIMATION OF DOMINANT
PARAMETERS OF AIRCRAFT LINEAR DYNAMICAL MODEL VIA
RECURSIVE LEAST SQUARE METHOD**

Mehmet ŞAHİN

**Supervisor
Prof. Dr. Muammer KALYON**

**MASTER'S THESIS
DEPARTMENT OF MECHATRONICS ENGINEERING
İSTANBUL - 2021**

ACCEPTANCE AND APPROVAL PAGE

On 05/07/2021 **Mehmet ŞAHİN** successfully defended the thesis, entitled "**System Identification and Estimation of Dominant Parameters of Aircraft Linear Dynamical Model via Recursive Least Square Method**" which he prepared after fulfilling the requirements specified in the associated legislations, before the jury members whose signatures are listed below. This thesis is accepted as a **MASTER'S THESIS** by Istanbul Commerce University, Graduate School of Natural and Applied Sciences **Mechatronics Engineering Department**.

Supervisor **Prof. Dr. Muammer KALYON**
Istanbul Commerce University

Jury Member **Assist. Prof. Dr. Vedat TAVAS**
Istanbul Commerce University

Jury Member **Assist. Prof. Dr. İlker ÜSTOĞLU**
Istanbul Technical University

Approval Date: 29/07/2021

Istanbul Commerce University, Graduate School of Natural and Applied Sciences, accordance with the 2nd article of the Board of Directors Decision dated 29/07/2021 and numbered 2021/317, "Mehmet ŞAHİN" who has determined to fulfill the course load and thesis obligation was unanimously decided to graduated.

Prof. Dr. Necip ŞİMŞEK
Head of Graduate School of Natural and Applied Sciences

DECLARATION OF CONFORMITY IN ACADEMIC AND ETHIC CODES

Istanbul Commerce University, Institute of Science, thesis writing in accordance with the rules of this thesis study,

- I have obtained all the information and documents in the thesis under the academic rules,
- I give all information and results in a visual, auditory and written manner in accordance with scientific code of ethics,
- in the case that the works of others are used, I have found the works in accordance with the scientific norms,
- I show all of the works I have cited as a source,
- I have not tampered with the data used,
- And that did not present any part of this thesis as a dissertation study at this university or at another university

I declare.

29/07/2021

Mehmet ŞAHİN

CONTENT

	Page
CONTENT	i
ABSTRACT	iii
ÖZET	iv
ACKNOWLEDGMENTS.....	v
LIST OF FIGURES	vi
LIST OF TABLES	viii
LIST OF ABBREVIATIONS.....	ix
1. INTRODUCTION	1
2. LITERATURE REVIEW	3
3. MATHEMATICAL MODEL OF AN AIRCRAFT	6
3.1. Definition of Aircraft State Space Vectors	7
3.1.1. Vector of aircraft velocity	8
3.1.2. Vector of aircraft position	9
3.1.3. Vector of forces and moments.....	10
3.1.4. Vector of actuator control input to aircraft.....	11
3.2. Rigid Body Equation of Motion	12
3.3. Rotational Kinematic Equation.....	18
3.4. Navigation Equation	18
3.5. Force Equations in Wind Axes	19
3.6. The Linarized Equations of Motion.....	21
3.6.1. The linarized longitudinal equations.....	21
3.6.2. The linarized lateral equations	26
4. SYSTEM IDENTIFICATION OF AN AIRCRAFT	33
4.1. Definition of System Identification	33
4.2. History of System Identification.....	36
4.3. System Identification Toolbox	37
4.3.1. Aircraft pitch transfer function estimation via toolbox.....	44
4.4. Parameter Estimation	46
4.4.1. Offline estimation	48
4.4.1.1. Bayesian model	48
4.4.1.2. Fisher model.....	49
4.4.1.2.1. Maximum likelihood method	49
4.4.1.3. Least square method	50
4.4.1.3.1. Estimation of aircraft control surfaces behavior via LSM... 54	
4.4.1.3.1.1. Elevator control surfaces behavior via LSM.....	57
4.4.1.3.1.2. Aileron control surfaces behavior via LSM.....	59
4.4.1.3.1.3. Rudder control surfaces behavior via LSM.....	61
4.4.2. Online estimation	63
4.4.2.1. Recursive least square method.....	63
4.4.2.1.1. Estimation of Aircraft Control Surfaces Behavior via RLSM .. 67	
4.4.2.1.1.1. Elevator control surfaces behavior via RLSM	67
4.4.2.1.1.2. Aileron control surfaces behavior via RLSM	69
4.4.2.1.1.3. Rudder control surfaces behavior via RLSM	71
4.4.2.2. Time-varying parameter	74
4.4.2.2.1. Exponentially Weighted Least Squares.....	74
4.4.2.2.2. Kalman filter	75

4.4.2.2.3. Sequential least square.....	77
4.4.3. Comparison of parameter estimation via RLSM and LSM	77
5. ESTIMATION OF DOMINANT PARAMETERS VIA LSM AND RLSM	85
5.1. Estimation Dominant Parameters via LSM.....	86
5.2. Estimation Dominant Parameters via RLSM.....	88
6. CONCLUSION AND RECOMMENDATIONS	91
REFERENCES.....	99
BIBLIOGRAPHY	101

ABSTRACT

M.Sc. Thesis

SYSTEM IDENTIFICATION AND ESTIMATION DOMINANT PARAMETERS OF AIRCRAFT LINEAR DYNAMICAL MODEL VIA RECURSIVE LEAST SQUARE METHOD

Mehmet ŞAHİN

**Istanbul Commerce University
Graduate School of Applied and Natural Sciences
Department of Mechatronic Engineering**

**Supervisor: Prof. Dr. Muammer KALYON
2021, 101 pages**

In order to examine the behavior of a system, its mathematical model must be extracted. System identification methods are needed to extract the mathematical model. Thus, with the system identification process, the mathematical models of systems with certain inputs and outputs are defined.

In this study, the analysis of the transfer functions, which are formed as a result of the behavior of an aircraft, with the system definition methods, in the MATLAB/Simulink program.

Parameter estimation methods were used as the system identification method and comparisons were made between the methods and correct results were tried to be achieved.

Parameter methods used in aviation are generally the methods that make real-time parameter estimation in order to give more accurate results. The first of these is the recursive least squares method, which is generally emphasized in this thesis. In addition, the least squares method, which is not used in real time, is explained in detail.

In order to prove that the recursive least squares method gives more accurate results, the analyzes made with both recursive least squares and least squares are compared and examined and ISE (Integral Square Error) table is prepared to observe the error rate. Thus, the success of the recursive least squares method has been observed and it has been understood that it gives more realistic results.

Keywords: Aerodynamic parameters, aircraft control surfaces, least square method, recursive least square method, system identification.

ÖZET

Yüksek Lisans Tezi

SİSTEM TANIMLAMA VE ÖZYİNELİ EN KÜÇÜK KARELER METODU İLE DOĞRUSAL DİNAMİK UÇAK MODELİNİN DOMİNANT PARAMETRELERİNİN TAHMİN EDİLMESİ

Mehmet ŞAHİN

İstanbul Ticaret Üniversitesi
Fen Bilimleri Enstitüsü
Mekatronik Mühendiliği Anabilim Dalı

Danışman: Prof. Dr. Muammer KALYON
2021, 101 sayfa

Bir sistemin davranışlarının incelenebilmesi için matematiksel modelinin çıkarılması gerekmektedir. Matematiksel modelin de çıkarılabilmesi için sistem tanımlama metodlarına ihtiyaç duyulur. Böylece sistem tanımlama işlemi ile belli giriş ve çıkışı olan sistemlerin matematiksel modelleri tanımlanmaktadır.

Bu çalışmada, bir hava aracının davranışları neticesinde oluşan transfer fonksiyonlarının sistem tanımlama metodları ile MATLAB/Simulink programında analizleri yapılmıştır.

Sistem tanımlama yöntemi olarak parametre tahmin metodları kullanılmış ve metodlar arasında kıyaslar gerçekleştirilmiştir ve doğru sonuçlara ulaşılmaya çalışılmıştır.

Havacılıkta kullanılan parametre metodları daha doğru sonuç vermesi açısından genelde gerçek zamanlı parametre tahmini yapan metodlardır. Bunların başında da bu tezde genel olarak üzerinde durulan özyineli en küçük kareler metodudur. Ayrıca gerçek zamanlı olarak kullanılmayan metod olan en küçük kareler metodu da detaylı şekilde anlatılmıştır.

Yapılan çalışmalarda özyineli en küçük kareler metodunun daha doğru sonuçlar verdiğinin ispatlanması için hem özyineli en küçük kareler hem de en küçük kareler ile yapılan analizler kıyaslanarak incelenmiş ve hata oranını gözlemleyebilmek için ISE (Integral Square Error) tablosu çıkarılmıştır. Böylece özyineli en küçük kareler metodunun başarısı görülmüş ve daha gerçeğe yakın sonuçlar verdiği anlaşılmıştır.

Anahtar Kelimeler: Aerodinamik parametreler, en küçük kareler metodu, özyineli en küçük kareler metodu, sistem tanımlama, uçak kontrol yüzeyleri.

ACKNOWLEDGMENTS

I would like to thank my precious thesis advisor Prof. Dr. Muammer KALYON, who guided me for this work and who did not spare his invaluable experience and invaluable advice throughout my master program.

I would like to thank my dear friend Ahmet Hulusi ÖZ, with whom I constantly exchanged ideas, had the opportunity to work together and mastered together. Also, I would like to thank another friend Sena KOÇAK, who is my colleague and has never withheld her help.

Finally, I would like to thank my dear family, my wife and especially my son, who have never withheld their love and support throughout my education and working life, and who always stood by me.

Mehmet ŞAHİN
ISTANBUL, 2021

LIST OF FIGURES

	Page
Figure 1.1. System definition.....	1
Figure 1.2. System model and parameter estimation algorithm.....	2
Figure 3.1. Aircraft freebody diagram	7
Figure 3.2. Body axis system	9
Figure 3.3. Stability and wind axes	9
Figure 3.4. The moments and forces vectors.....	10
Figure 3.5. Conventional aircraft.....	11
Figure 3.6. A proposed control configured vehicle.....	11
Figure 3.7. Definition of aerodynamic forces and moments.....	14
Figure 3.8. Rotation earth axes to body axes	16
Figure 3.9. Definition of aerodynamic angles	19
Figure 4.1. Representation of dynamic system.....	34
Figure 4.2. System identification of aircraft system.....	34
Figure 4.3. Definition of system identification	35
Figure 4.4. System identification procedure	36
Figure 4.5. System identification tool screen.....	38
Figure 4.6. System identification tool import data part	39
Figure 4.7. System identification tool data definition.....	40
Figure 4.8. System identification tool data views	41
Figure 4.9. System identification tool estimate part.....	41
Figure 4.10. System identification tool transfer function definition	42
Figure 4.11. System identification tool estimation progress viewer.....	42
Figure 4.12. System identification tool model views part	43
Figure 4.13. Estimation transfer function.....	43
Figure 4.14. System identification tool transfer function definition	44
Figure 4.15. System identification tool estimation progress viewer.....	45
Figure 4.16. System identification tool model views part	45
Figure 4.17. System identification tool model views part	46
Figure 4.18. Parameter estimation	47
Figure 4.19. Parameter Estimation Methods.....	48
Figure 4.20 Least square estimation.....	50
Figure 4.21. Least square method.....	51
Figure 4.22. Input-output relationship	52
Figure 4.23. Doublet input	56
Figure 4.24. MATLAB/Simulink Model for Elevator Control Surface	57
Figure 4.25. Elevator control surface behavior estimated via LSM	58
Figure 4.26. MATLAB/Simulink model for aileron control surface	59
Figure 4.27. Aileron control surface behavior estimated via LSM	60
Figure 4.28. MATLAB/Simulink model for rudder control surface	61
Figure 4.29. Rudder control surface behavior estimated via LSM	62
Figure 4.30. MATLAB/Simulink model for elevator control surface.....	68
Figure 4.31. Elevator control surface behavior estimated via RLSM	69
Figure 4.32. MATLAB/Simulink model for aileron control surface	70
Figure 4.33. Aileron control surface behavior estimated via RLSM	71
Figure 4.34. MATLAB/Simulink model for rudder control surface	72
Figure 4.35. Rudder control surface behavior estimated via RLSM	73

Figure 4.36 Kalman filter	75
Figure 4.37 Estimated via RLSM and LSM ($\theta/\delta e$)	79
Figure 4.38 Pole zero map for pitch transfer function.....	80
Figure 4.39 Estimated via RLSM and LSM ($\phi/\delta a$).....	81
Figure 4.40 Pole zero map for bank angle to aileron displacement	82
Figure 4.41 Estimated via RLSM and LSM ($\phi/\delta r$)	82
Figure 4.42 Pole zero map for bank angle to rudder displacement.....	83
Figure 5.1 MATLAB/Simulink model for $\alpha/\delta e$	87
Figure 6.1. Estimated via LSM for decreasing number of data ($\theta/\delta e$)	93
Figure 6.2. Estimated via LSM for decreasing number of data ($\phi/\delta a$).....	93
Figure 6.3. Estimated via LSM for decreasing number of data ($\phi/\delta r$).....	94
Figure 6.4. Estimated via LSM for increasing number of data ($\theta/\delta e$)	95
Figure 6.5. Estimated via LSM for increasing number of data ($\phi/\delta a$).....	95
Figure 6.6. Estimated via LSM for increasing number of data ($\phi/\delta r$).....	96

LIST OF TABLES

	Page
Table 4.1 ISE table for LSM and RLSM.....	84
Table 5.1 Estimated parameters via LSM.....	88
Table 5.2 Error table for parameters via LSM.....	88
Table 5.3 Estimated aerodynamic via RLSM.....	90
Table 5.4 Error table for parameters via RLSM.....	90
Table 6.1 Step-response characteristic values.....	97

LIST OF ABBREVIATIONS

A	Linear system and measurement matrices
B	Linear system and measurement matrices
b	Reference span
C	Linear system and measurement matrices
c	Reference chord
C_L	The coefficient of lift
C_{L0}	Equilibrium lift coefficient
C_D	The coefficient of drag
C_{D0}	Zero lift drag coefficient
C_Y	The coefficient fo sideforce
C_l	Coefficient of rolling moment
C_{l0}	Zero lift lift coefficient
$C_{L\alpha}$	Lift-curve slope
$C_{l\beta}$	Dihedral effect derivaitve (lateral stability)
C_{lp}	Proportional portion of lift coefficient signal
$C_{l\delta_e}$	Variation of lift coefficient with elevator deflection
C_M	Coefficient of pitching moment
C_N	Coefficient of yawing moment
$C_{Y\beta}$	General function of variables
$C_{Y\delta_r}$	General function of variables
C_{M0}	Pitching moment coefficient about aerodynamic centre of wing
$C_{M\alpha}$	Slope of $C_m - \alpha$ plot
$C_{N\beta}$	Weathercock effect derivative (directional satability)
C_{Np}	General function of variables
D	Aerodynamic force, the drag acting on the aircraft
DoF	Degree of freedom
C	Linear system and measurement matrices
DFT	Discrete Fourier Transform
F	Force vector
F_x	Force components along the body axes x,y,z
F_y	Force components along the body axes x,y,z
F_z	Force components along the body axes x,y,z
F_{x_s}	Force components along the stability axes x_s, y_s, z_s
F_{y_s}	Force components along the stability axes x_s, y_s, z_s
F_{z_s}	Force components along the stability axes x_s, y_s, z_s
FTR	Fourier Transform Regression
g	Gravitational
I	Moment of inertia
I_x	Roll moment of inertia
I_y	Pitch moment of inertia
I_z	Yaw moment of inertia
I_{xx}	Principle moment of inertia with respect to the x,y,z body axes
I_{yy}	Principle moment of inertia with respect to the x,y,z body axes
I_{zz}	Principle moment of inertia with respect to the x,y,z body axes
I_{xy}	Products of inertia

I_{xz}	Products of inertia
I_{yz}	Products of inertia
ISE	Integral Square Error
K	Gain matrix
K_e	Gain constant for elevator control surface
K_a	Gain constant for aileron control surface
K_r	Gain constant for rudder control surface
L,M,N	Moment component
L	Dimensional body axis aerodynamic rolling moment
LSM	Least Square Method
M	Dimensional body axis aerodynamic pitching moment
m	Mass
N	Dimensional body axis aerodynamic yawing moment
N	Number of time samples
P,Q,R	Component of rotational velocity
P	Covariance matrix
RLSM	Recursive Least Square Method
S	Reference area
s	Laplace variable
T	time
u	Input vector
U,V,W	Components of linear velocity
V	Total airspeed of the aircraft
V_p	Total aircraft velocity
V_0	Reference airspeed
v	Measurement noise
w	Undamped natural frequency
w_{ns}	Longitudinal motion short period approximation natural frequency
w_{np}	Longitudinal motion phugoid approximation natural frequency
w_{nr}	Lateral motion natural frequency
$w_{n\phi}$	Lateral motion natural frequency
x,y,z	Reference coordinates
x	State vector
ζ_s	Longitudinal motion short period approximation damping ratio
ζ_p	Longitudinal motion phugoid approximation damping ratio
τ_s	Longitudinal motion short period approximation time constant
τ_p	Longitudinal motion phugoid approximation time constant
$T_{\phi 1}$	Lateral motion time constant for aileron control surface
$T_{\phi 2}$	Lateral motion time constant for aileron control surface
ζ	Damping ratio
ζ_r	Lateral motion damping ratio
ζ_ϕ	Lateral motion damping ratio
$T_{\phi r_1}$	Lateral motion time constant for rudder control surface
$T_{\phi r_2}$	Lateral motion time constant for rudder control surface
ρ	Air density
α	Angle of attack
β	Side slip angle
γ	Flight path angle

γ_e	Equilibrium flight path angle
δ	perturbed quatity
δ_e	The deflection of the elevator control surface
δ_a	The deflection of the aileron control surface
δ_r	The deflection of the rudder control surface
Φ	The aircraft roll angle
Θ	The aircraft pitch angle
Ψ	The aircraft heading angle
ϵ	Prediction error matrix
Θ	Parameter vector
\mathcal{L}	Laplace transformation symbol

1. INTRODUCTION

Systems are structures based on observation or certain measurements, where there is an input or effect, and that generate an output or response according to input or effect. In Figure 1.1 shows the general structure of the system. Thus, the concept of system definition is defined as revealing systems and developing mathematical models for these systems. That is, system identification is the creation of a mathematical model as a result of measurements of input and output signals. In other words, system identification is a discipline that provides the most appropriate representation for a system and responds to the reverse problem when system behavior is examined as a result of many observations (Jategaonkar, 2006). The inverse problem, namely system identification, has been an essential element of identifying any system under consideration and having the knowledge to examine that system.

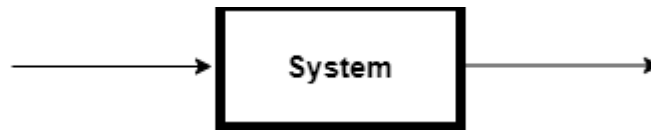


Figure 1.1. System definition

Aviation is one of the areas where system identification is used most widely and effectively. Generally, system identification is used for multiple applications such as flight analysis, flight control design, estimation of equations and parameters resulting from flight behavior, and verification of experimental data. We described the system in the previous paragraph. Accordingly, it is a system with entries and exits in the aircraft. performs the closest mathematical modeling job to this system in system identification. As a result of the collected experimental results, more than one data is processed and the functions that will occur for the analysis of the aircraft's behavior are defined.

In this thesis, various methods are mentioned to create mathematical models of systems. First, the system identification tool of the MATLAB/Simulink program was explained and the result of an aircraft on the equation of motion was

examined. Then, parameter estimation methods, which are the main mentality of the study, are explained. Figure 1.2 shows the creation of a system model with a general aircraft system and parameter estimation algorithm.

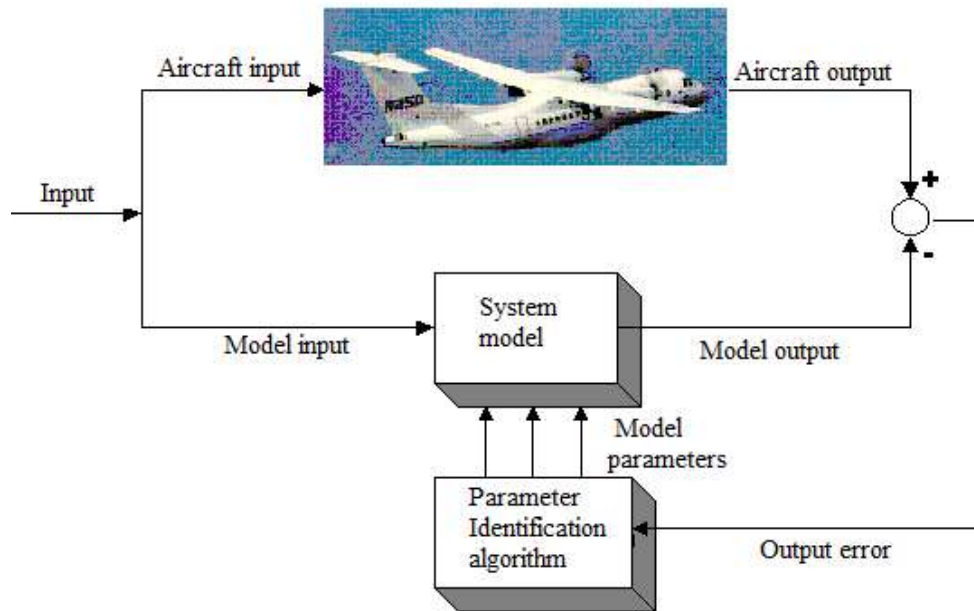


Figure 1.2. System model and parameter estimation algorithm

RLS method, which is one of the parameter estimation methods, is emphasized. Since the RLS method is a real time parameter estimation method, it is widely used in the aviation field in order to give more accurate results than other methods. For this reason, to show the effectiveness of the RLS method, analyzes were made on an aircraft with the LS method, which is a non-real-time parameter estimation method. In this context, the behavior functions resulting from the behavior of the aircraft control surfaces were extracted. These functions were examined with both LS and RLS and their comparisons were analyzed in MATLAB/Simulink program and the parameter estimation, which is the system definition, which generally expresses the essence of the study, was performed. In addition, pole zero maps were created in order to give information about the examined transfer functions and system. After the transfer functions were analyzed and estimated by both methods, some dominant aerodynamic parameters involved in the formation of these transfer functions were also estimated.

2. LITERATURE REVIEW

Evans (2001), explained various system identification techniques used in modeling dynamic equations of aircraft gas turbine engines. have used more than one system identification technique in their studies. They tried to explain the dynamic model of gas turbine engines used in aircraft with methods such as frequency identification method and least square method.

DeBusk et al. (2009), described the real-time definition of the dynamic model of an aircraft with instantaneous data received during flight. used the recursive FTR method to estimate the parameters of the dynamic model of an aircraft. They defined the FTR method in the frequency domain as an extension of the LS method and expressed the algorithm of the LS parameter estimation method.

Kamali et al. (2011), explained the analysis, evaluation and results of the RLS method, which is the parameter estimation method used in flight control and testing and in real-time applications. In their studies, they stated that online prediction algorithms are necessary for the reproducible flight control mechanism and that they come to the fore because of more efficient results in test processes. They described various parameter estimation algorithms and made comparisons on stabilized version of DFT and RLS method. They stated that the RLS method was more effective in dense and repetitive calculations and they made the estimation of an aircraft parameters by methods.

Scheper et al. (2013), made a system identification study to obtain a mathematical model of a fixed wing aircraft. In their work, they explained the aerodynamically model of the aircraft and the data acquisition to be used in system identification studies. Subsequently, they used the output error method, the maximum likelihood parameter approximation method, to estimate the model parameters.

Grauer and Morelli (2016), made the estimation of unknown parameters to create a mathematical model from the measured data for an aircraft using the RLS

method, one of the parameter estimation methods used in the aviation field. They also explained the LS method along with the RLS method in their work. They stated that the LS method is widely used in terms of simplicity and efficiency and firstly explained the algorithm of the LS method. They stated that LS method is used for parameter estimation after all data collection processes are completed, that is, after data is collected. Later on, they gave the algorithm of the RLS method due to the fact that the aircraft is also a dynamic system due to this reason and they explained that real-time parameter estimation can be made while collecting flight test data.

Qadri et al. (2016), explained the LS and RLS parameter estimation methods and the study of estimating the mathematical model of a waraircraft due to its complex and unpredictable motions. presented the calculation of aerodynamic parameters using both methods in their work. They firstly explained the dynamics, coordinate system and equation of motion of the waraircraft. Subsequently, they explained prediction algorithms, LS and RLS methods.

Hardier et al. (2016), followed the model parameters of the aircraft with the RLS method in terms of designing the flight control of a civil aircraft. In their studies, they worked in the frequency domain to monitor parameters that change over time and expressed the expressions in the frequency domain recursively.

Cetin (2018), explained the analysis of data collected with a flight simulation program for aircraft system modeling. made use of the system identification techniques used in the flow of time. The models obtained by the system identification method were compared with the data obtained from the simulation program and the accuracy of the model formed as a result of the system identification was observed.

Simmons (2018), explained the development of a flight dynamic model for a fixed wing unmanned aerial vehicle using the system identification technique. He explained that he uses various parameter estimation methods and the data collection system he uses to collect data before the stage of system identification.

Grauer and Boucher (2020), explained from measured input and output data to flight dynamic models and estimation of parameters in the model. They utilized the frequency domain approach in their studies and estimated the parameters using the maximum likelihood method.

3. MATHEMATICAL MODEL OF AN AIRCRAFT

Aircraft is a driven system that can move and rise while holding it in the air, with the help of air flow creating pressure under the wings. The main parts of the aircraft are the wings that keep the wings in the air, the tail to keep the wings in balance, the control surfaces that change the position and position of the aircraft, and the engine and propeller that provide the necessary propulsion. We need a mathematical model of the aircraft to be able to control the behavior that occurs as a result of all changes of these elements on the aircraft, and to model and observe the results. Hence, we need to know the mathematical models of aircraft so that we can examine and interpret the behavior of aircraft, so that we can control and model them.

The aircraft mathematical model becomes straightforward when the equations that make the aircraft move are understood. The equations that drive the aircraft can be derived mainly from the laws of kinetics and kinematics.

The first step in developing a 6 DoF (degree of freedom) nonlinear model for an aircraft is to develop the mathematical model that describes the aircraft dynamics and environment. The mathematical model consists of the development and explanation of aircraft motion equations (dynamic model) and aerodynamic force and moment equations. The following sections describe these equations. In Figure 3.1, the forces and angles that we will encounter while explaining the mathematical model of the aircraft are shown. In Figure 3.1, the equations that we will explain for the mathematical model of the aircraft, and the forces and angles that will appear. The mathematical model of the aircraft was constructed based on the book "Aircraft Control and Simulation" by Stevens, Lewis and Johnson (Stevens, et al. 2016) and "Aircraft System Identification: Theory and Practise" by Klein and Morielli (Klein and Morielli, 2006).

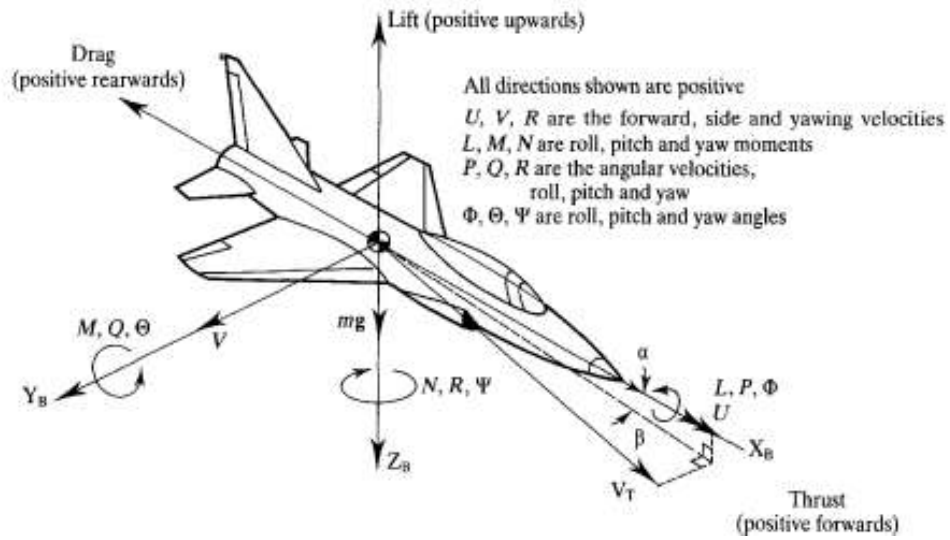


Figure 3.1. Aircraft freebody diagram (McLean, 1990)

3.1. Definition of Aircraft State Space Vectors

In this section, the equations of motion of a rigid aircraft are tried to be derived and expressed in state-space form:

$$\dot{X} = f(X, U)$$

X is the $(n \times 1)$ state vector, U is the $(m \times 1)$, and f is a vector-valued nonlinear function of the individual states and controls. This vector equation characterized the n first order, coupled simple differential equations.

$$\dot{X}_1 = f_1(X_1, X_2, \dots, X_n, U_1, \dots, U_m)$$

.

.

$$\dot{X}_n = f_n(X_1, X_2, \dots, X_n, U_1, \dots, U_m)$$

Where the f_i symbolize different nonlinear functions of the n state variables, X_i , and m inputs, U_i . After defining the state equation, an output equation of the general form is defined.

$$Y = g(X, U)$$

where Y is a $(p \times 1)$ output vector and g represents a set of nonlinear equations similar to f . The state variables, X_i , will be any set of variables that completely define the state.

Large symbols will be used for state, control, and output vectors and variables derived from them. because at this stage it will show the actual values of the aircraft variables.

$$\dot{X} = Ax + Bu$$

In this expression, the reason why the state and control vectors are expressed in lowercase indicates that they are perturbations from the equilibrium from equilibrium. As stated in the expression, the "*A-matrix*" is the square matrix in the state space form, and the "*B-matrix*" has the size determined by the number of states and controls.

The aircraft velocity, position, force and moment, actuator control input state space vectors are explained according to the logic of expressing the space state vectors in the following sections.

3.1.1. Vector of aircraft velocity

Parameters are defined by forming a aircraft velocity vector. Firstly, the aircraft velocity vector was constructed in order to derive the equations of motion. The meanings of the parameters were specified according to the motion of the aircraft to be used in the explanation of the dynamic equations of the aircraft. Velocity vector of the aircraft is depicted in (3.1).

$$\begin{bmatrix} u \\ v \\ w \\ p \\ q \\ r \end{bmatrix} = \begin{bmatrix} \text{velocity in forward direction} \\ \text{velocity in transverse direction} \\ \text{velocity in verticle direction} \\ \text{rate of roll motion} \\ \text{rate of pitch motion} \\ \text{rate of roll motion} \end{bmatrix} \quad (3.1)$$

3.1.2. Vector of aircraft position

This section describes the position vector of the state space form of the aircraft.

For aircraft it is common to use the following body-fixed coordinate systems:

- Body axes
- Stability axes
- Wind axes

In Figure 3.2 and Figure 3.3 shown the axis system of the aircraft. In Figure 3.3, α is the angle of attack and β is the side slip angle.

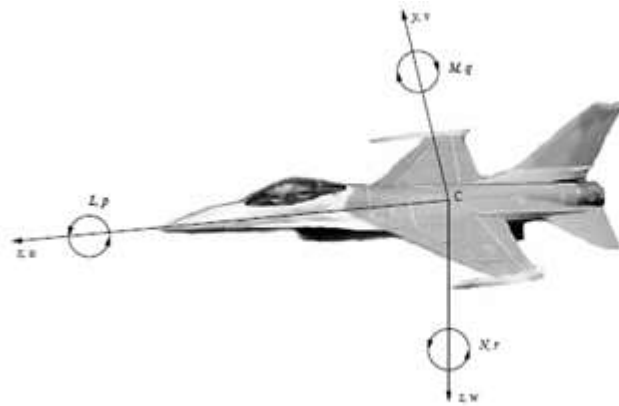


Figure 3.2. Body axis system

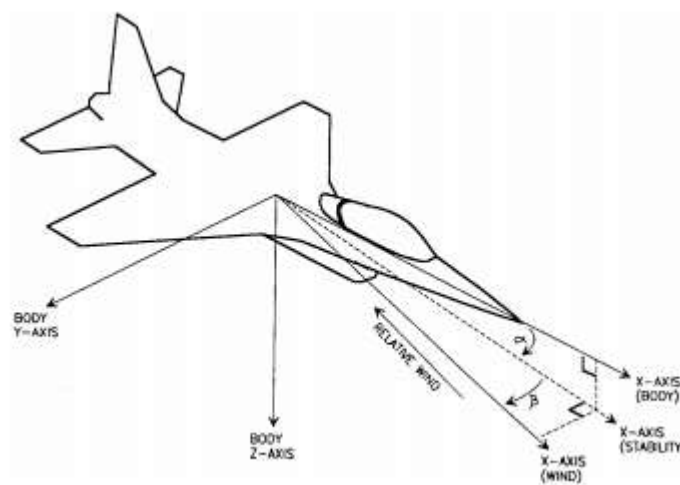


Figure 3.3. Stability and wind axes (Stevens and Lewis, 1992)

The angle of attack and the side slip angle are expressed by the velocity vectors described in the previous section and given in (3.2) and (3.3) respectively.

$$\tan \alpha = \frac{w}{u} \quad (3.2)$$

$$\sin \beta = \frac{v}{V} \quad (3.3)$$

Coordinates axes and Euler angles are also defined in (3.4).

$$\begin{bmatrix} X_e \\ Y_e \\ Z_e \\ \Phi \\ \theta \\ \psi \end{bmatrix} = \begin{bmatrix} \text{earth fixed } x \text{ axis} \\ \text{earth fixed } y \text{ axis} \\ \text{earth fixed } z \text{ axis} \\ \text{angle of roll} \\ \text{angle of pitch} \\ \text{angle of roll} \end{bmatrix} \quad (3.4)$$

3.1.3. Vector of forces and moments

In this section, the aircraft force and moment vectors are expressed in (3.5).

$$\begin{bmatrix} X \\ Y \\ Z \\ L \\ M \\ N \end{bmatrix} = \begin{bmatrix} \text{force in longitudinal direction} \\ \text{force in transverse direction} \\ \text{force in verticle direction} \\ \text{moment in rolling} \\ \text{moment in pitching} \\ \text{moment in yawing} \end{bmatrix} \quad (3.5)$$

In Figure 3.4 shown the force and moment axes on the aircraft.

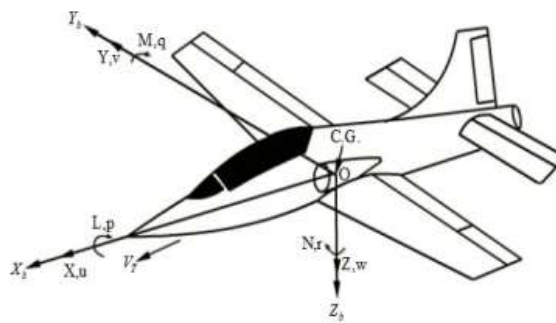


Figure 3.4. The moments and forces vectors

3.1.4. Vector of actuator control input to aircraft

In this section, the vector expression of the actuators given in (3.6) that could control on the aircraft is explained.

$$\begin{bmatrix} \delta_T \\ \delta_A \\ \delta_E \\ \delta_F \\ \delta_R \end{bmatrix} = \begin{bmatrix} thrust \\ aileron \\ elevator \\ flap \\ rudder \end{bmatrix} \quad (3.6)$$

In Figure 3.5 and Figure 3.6 shows these actuators on the aircraft.

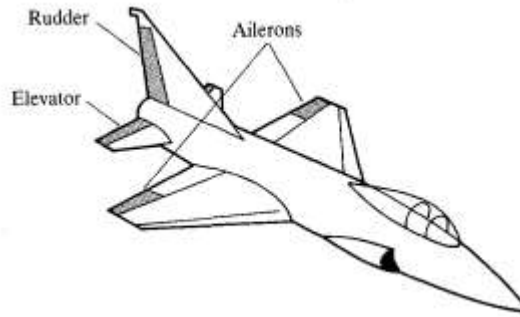


Figure 3.5. Conventional aircraft (McLean, 1990)

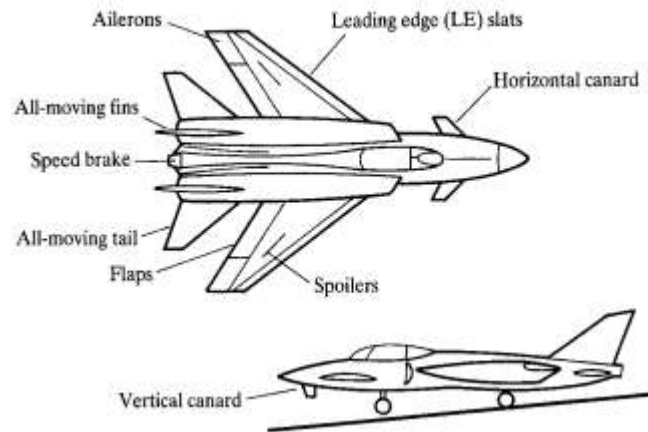


Figure 3.6. A proposed control configured vehicle (McLean, 1990)

3.2. Rigid Body Equation of Motion

Assuming the aircraft is a rigid body moving through space, it can be thought of as having six degrees of freedom in motion. By applying Newton's Second Law to this rigid body, equations of motion can be established in terms of translation and angular accelerations that occur as a result of some forces and moments applied to the aircraft.

In this section, kinematic equations of translation and rotation motion are obtained. Before obtaining the equations of translation and rotational motions, the second law of Newton was mentioned in (3.7) and (3.8).

$$F = \frac{d}{dt}(mV) \quad (3.7)$$

$$M = \frac{d}{dt}(I\omega) \quad (3.8)$$

where F is the force, mV is the linear momentum, m is the mass, V is the translational velocity, M is the moment, $I\omega$ is the angular momentum, ω is the angular velocity, and I is the inertia matrix. In (3.7) and (3.8) are vector equations describing translation and rotational motion. Each vector Equation expresses three scalar equations for vector components. Thus, six scalar Equations are formed for six degrees of freedom for aircraft motion. Below, the body axis components of the force, velocity, moment and angular velocity expressions in (3.7) and (3.8) are specified in $F = [F_x \ F_y \ F_z]^T$, $V = [u \ v \ w]^T$, $M = [M_x \ M_y \ M_z]^T$, $\omega = [p \ q \ r]^T$.

Therefore, the angular momentum expression is specified in (3.9) to be used in finding moment Equations.

$$I\omega = \begin{bmatrix} I_{xx} & -I_{xy} & -I_{xz} \\ -I_{yx} & I_{yy} & -I_{yz} \\ -I_{xz} & -I_{yz} & I_{zz} \end{bmatrix} \begin{bmatrix} p \\ q \\ r \end{bmatrix} \rightarrow I\omega = \begin{bmatrix} I_x p - I_{xz} r \\ I_y q \\ -I_{xz} p + I_z r \end{bmatrix} \quad (3.9)$$

The inertia matrix I symmetric matrix showed in (3.9) and where $I_{xy} = I_{yx} = I_{yz} = I_{zy} = 0$. So inertia matrix becomes like in Equation (3.10) as below.

$$I = \begin{bmatrix} I_{xx} & 0 & -I_{xz} \\ 0 & I_{yy} & 0 \\ -I_{xz} & 0 & I_{zz} \end{bmatrix} \quad (3.10)$$

For rotating axis system such as body axes, the derivative operator applied to vectors describes the rate of change of vector components expressed in the rotating system and the axis system rotation. This expression is explained in Equation (3.11).

$$\frac{d}{dt}(\cdot) = \frac{\delta}{\delta t}(\cdot) + \omega \times (\cdot) \quad (3.11)$$

In Equations (3.12) and (3.13) are formed by combining Equations (3.7) and (3.8). These equations are vector forms of the equations of motion expressed on the body axis.

$$F = m\dot{V} + \omega \times mV \quad (3.12)$$

$$M = I\dot{\omega} + \omega \times I\omega \quad (3.13)$$

The components of the force and moment equations in Equations (3.14) and (3.15) are found when the body axis components of Equation (3.9) and the body axis components are put into Equation (3.12) and (3.13) within the framework of the expressions in Equation (3.2-1) and (3.2-2) explained above.

Force Equations:

$$\begin{aligned} F_x &= m(\dot{u} + qw - rv) \\ F_y &= m(\dot{v} + ru - pw) \\ F_z &= m(\dot{w} + pv - qu) \end{aligned} \quad (3.14)$$

Moment Equations:

$$\begin{aligned} M_x &= \dot{p}I_x - \dot{r}I_{xz} + qr(I_z - I_y) - qpI_{xz} \\ M_y &= \dot{q}I_y + pr(I_x - I_z) + (p^2 - r^2)I_{xz} \end{aligned} \quad (3.15)$$

$$M_z = \dot{r}I_z + \dot{p}I_{xz} + pq(I_y - I_x) + qrI_{xz}$$

In Figure 3.8 shows aerodynamic forces and moments on the aircraft.

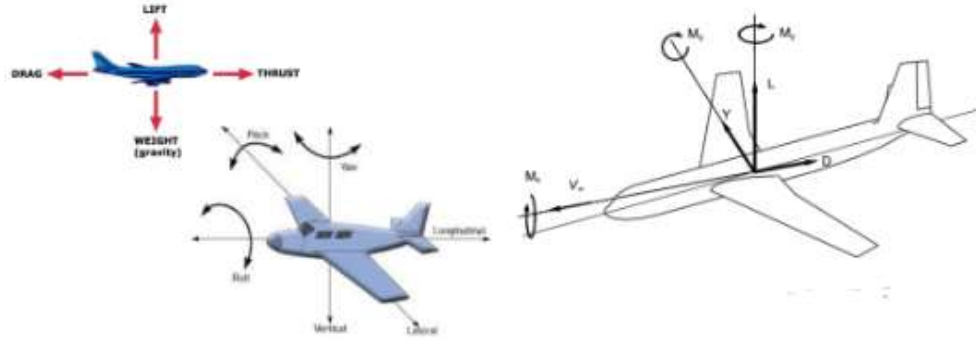


Figure 3.7. Definition of aerodynamic forces and moments

For aircrafts, the forces and moments applied to the left sides of the above equations are caused by aerodynamics, gravity and thrust. Since gravity moves approximately and the gravitational field is assumed to be uniform, there is no gravitational moment acting on the aircraft. Because of this reason, Equations (3.12) and (3.13) are expressed in equations (3.16) and (3.17) as follows.

$$F_A + F_T + F_G = m\dot{V} + \omega \times mV \quad (3.16)$$

$$M_A + M_T = I\dot{\omega} + \omega \times I\omega \quad (3.17)$$

The aerodynamic forces and moments affecting the airaircraft result from the relative motion of the air and the aircrafts. Components of aerodynamic forces and moments can be expressed in terms of dimensionless coefficients as in equations (3.18) and (3.19).

$$F_A = \bar{q}S \begin{bmatrix} C_x \\ C_y \\ C_z \end{bmatrix} \quad (3.18)$$

$$M_A = \bar{q}S \begin{bmatrix} bC_l \\ cC_m \\ bC_n \end{bmatrix} \quad (3.19)$$

where $\bar{q} = 0.5\rho V^2$ is the dynamic pressure, V is the airspeed (air relative velocity), ρ is the air density, S is the wing area, b is the wing span, and c is the mean aerodynamic chord length of the wing.

In general, the dimensionless aerodynamic force and moment coefficients are nonlinearly dependent on aircrafts translation and angular velocity vector components and control surface deviations and their time derivatives and/or other dimensionless quantities such as the Mach number and Reynolds number.

Aircrafts weight is considered constant in both magnitude and direction relative to earth axes, with O_{Z_E} moving along the earth axis. The components of the aircraft weight along the fuselage axes change with the orientation of the aircraft to the earth axis. The components of the aircraft weight along the fuselage axes change with the orientation of the aircraft to the earth axis. The gravitational components in the body axes are therefore dependent on the aircraft orientation with respect to the earth axis and can be defined based on the orientation of the body axes relative to the vehicle-carried earth axes. The most common way to explain aircraft orientation with respect to vehicle-carried body axes is to use Euler angles.

As shown in Figure 3.8, it is stated how the direction of a right-handed coordinate system can be defined relative to the other. The sequence of rotating the axis of Earth carried by the vehicle so that it is aligned with the body axis is completed by a yaw angle rotation ψ about the axis O_{Z_V} , followed by an angle of inclination rotation θ , around the axis y , a roll angle rotation ϕ around the body axis O_x .

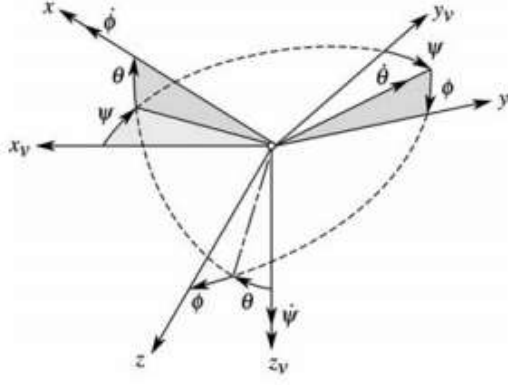


Figure 3.8. Rotation earth axes to body axes (Klein and Morielli, 2006)

The components of the gravity vector in body axes are found through the product of rotation matrices. As stated below, the components of the gravity vector in Equation (3.20) are obtained as a result of matrix multiplications.

$$F_G = \begin{bmatrix} g_x \\ g_y \\ g_z \end{bmatrix}_B = \begin{bmatrix} 1 & 0 & 0 \\ 0 & \cos\phi & \sin\phi \\ 1 & -\sin\phi & \cos\phi \end{bmatrix} \begin{bmatrix} \cos\theta & 0 & -\sin\theta \\ 0 & 1 & 0 \\ \sin\theta & 0 & \cos\theta \end{bmatrix} \begin{bmatrix} \cos\psi & \sin\psi & 0 \\ -\sin\psi & \cos\psi & 0 \\ 0 & 0 & 1 \end{bmatrix} \begin{bmatrix} 0 \\ 0 \\ g \end{bmatrix}_v = \begin{bmatrix} -g\sin\theta \\ g\cos\theta\sin\phi \\ g\cos\theta\cos\phi \end{bmatrix}$$

Additionally,

$$F_G = m \begin{bmatrix} g_x \\ g_y \\ g_z \end{bmatrix}_B = \begin{bmatrix} -mg\sin\theta \\ mg\cos\theta\sin\phi \\ mg\cos\theta\cos\phi \end{bmatrix} \quad (3.20)$$

Assuming that the thrust from the propulsion system moves along the x-body axis, the thrust appears only as a force exerted along the x-body axis and is expressed as in Equation (3.21).

$$F_T = \begin{bmatrix} T \\ 0 \\ 0 \end{bmatrix} \quad (3.21)$$

Sometimes it may be necessary to take into account the effect of rotating mass in the propulsion system, such as the propellers or rotors of jet engines. Gyroscopic terms associated with rotating mass are considered as applied moment because

the equations of motion were formulated assuming that the aircraft is a rigid body with no moving parts.

The angular momentum of the rotating mass in the body axes is expressed as in Equation (3.22) as follows.

$$h_p = \begin{bmatrix} I_p \Omega_p \\ 0 \\ 0 \end{bmatrix} \quad (3.22)$$

Where I_p is the inertia of the rotating mass and Ω_p is the angular velocity. Thus M_T is expressed as in Equation (3.23) as follows.

$$M_T = \frac{d}{dt}(h_p) = \omega \times h_p = \begin{bmatrix} 0 & -r & q \\ r & 0 & -p \\ -q & p & 0 \end{bmatrix} \begin{bmatrix} I_p \Omega_p \\ 0 \\ 0 \end{bmatrix} = \begin{bmatrix} 0 \\ I_p \Omega_p r \\ -I_p \Omega_p q \end{bmatrix} \quad (3.23)$$

As a result, by using the expressions above, the force and moment equations are obtained as in Equations (3.24) and (3.25) as follows.

Force Equations:

$$\begin{aligned} m\dot{u} &= m(rv - qw) + \bar{q}SC_x - mg\sin\theta + T \\ m\dot{v} &= m(pw - ru) + \bar{q}SC_y + mg\cos\theta\sin\phi \\ m\dot{w} &= m(qu - pv) + \bar{q}SC_z + mg\cos\theta\cos\phi \end{aligned} \quad (3.24)$$

Moment Equations:

$$\begin{aligned} \dot{p}I_x - \dot{r}I_{xz} &= \bar{q}SbC_l - qr(I_z - I_y) + qpI_{xz} \\ \dot{q}I_y &= \bar{q}ScC_m - pr(I_x - I_z) - (p^2 - r^2)I_{xz} + I_p\Omega_p r \\ \dot{r}I_z - \dot{p}I_{xz} &= \bar{q}SbC_n - pq(I_y - I_x) - qrI_{xz} - I_p\Omega_p q \end{aligned} \quad (3.25)$$

3.3. Rotational Kinematic Equation

Rotational kinematic equations are expressed in terms of the rate of change of Euler angles and the body axis components of angular velocity. Below is given in Equation (3.26).

$$\begin{bmatrix} p \\ q \\ r \end{bmatrix} = \begin{bmatrix} 1 & 0 & -\sin\theta \\ 0 & \cos\Phi & \sin\Phi\cos\theta \\ 0 & -\sin\Phi & \cos\Phi\cos\theta \end{bmatrix} \begin{bmatrix} \dot{\Phi} \\ \dot{\theta} \\ \dot{\psi} \end{bmatrix} \quad (3.26)$$

By inverting the expression in Equation (3.26), the Euler angles in Equation (3.27) are found.

$$\dot{\Phi} = p + \tan\theta(q\sin\Phi + r\cos\Phi)$$

$$\dot{\theta} = q\cos\Phi - r\sin\Phi \quad (3.27)$$

$$\dot{\psi} = \frac{q\sin\Phi + r\cos\Phi}{\cos\theta}$$

3.4. Navigation Equation

By expressing the aircraft velocity vector in the earth axes starting from the body axis components, the navigation equations are written as in Equation (3.28) as follows. The components are explained separately as in Equation (3.29), (3.30) and (3.31).

$$\begin{bmatrix} \dot{x}_E \\ \dot{y}_E \\ \dot{z}_E \end{bmatrix} = \begin{bmatrix} 1 & 0 & 0 \\ 0 & \cos\Phi & \sin\Phi \\ 0 & -\sin\Phi & \cos\Phi \end{bmatrix} \begin{bmatrix} \cos\theta & 0 & -\sin\theta \\ 0 & 1 & 0 \\ \sin\theta & 0 & \cos\theta \end{bmatrix} \begin{bmatrix} \cos\psi & \sin\psi & 0 \\ -\sin\psi & \cos\psi & 0 \\ 0 & 0 & 1 \end{bmatrix} \begin{bmatrix} u \\ v \\ w \end{bmatrix} \quad (3.28)$$

Therefore,

$$\dot{x}_E = u\cos\psi\cos\theta + v(\cos\psi\sin\theta\sin\Phi - \sin\psi\cos\Phi) + w(\cos\psi\sin\theta\cos\Phi + \sin\psi\sin\Phi) \quad (3.29)$$

$$\dot{x}_E = u \sin \psi \cos \theta + v(\sin \psi \sin \theta \sin \Phi + \cos \psi \cos \Phi) + w(\sin \psi \sin \theta \cos \Phi - \cos \psi \sin \Phi) \quad (3.30)$$

$$\dot{h} = u \sin \theta - v \cos \theta \sin \Phi - w \cos \theta \cos \Phi \quad (3.31)$$

where

$$h = \text{altitude} = -z_E$$

3.5. Force Equations in Wind Axes

The total velocity of the aircraft (V) was found in the previous sections is in the direction of the wind axis. To find the relationship between the fuselage axis and the wind axis, rotate the fuselage pivot system around the z-axis by a negative side slip angle unit (β); The resulting new coordinate system is then rotated by a positive angle of attack (α) around the new y-axis. In Figure 3.7, the rotation angles on the aircraft are specified.

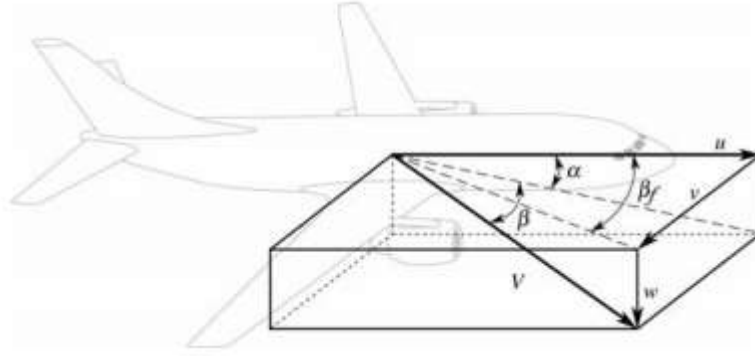


Figure 3.9. Definition of aerodynamic angles (Klein and Morielli, 2006)

The rotation matrix was specified in (3.32) to express the velocity vectors of the aircraft to the specified angle of attack (α) and side slip angles (β).

$$R_{body}^{wind} = \begin{bmatrix} \cos \beta \cos \alpha & \sin \beta & \cos \beta \sin \alpha \\ -\sin \beta \cos \alpha & \cos \beta & -\sin \beta \sin \alpha \\ -\sin \alpha & 0 & \cos \alpha \end{bmatrix} \quad (3.32)$$

Thus, velocity of the aircraft in body axis system is defined in (3.33) and (3.34).

$$V^{body} = R_{body}^{windT} V^{wind} \quad (3.33)$$

$$\begin{bmatrix} u \\ v \\ w \end{bmatrix} = \begin{bmatrix} V \cos(\beta) \cos(\alpha) \\ V \sin(\beta) \\ V \sin(\beta) \sin(\alpha) \end{bmatrix} \quad (3.34)$$

If the values of α and β are small enough such that $\cos \alpha = 1$ and $\sin \beta = \beta$, the expression in (3.35) is obtained from Equation (3.34).

$$\begin{aligned} u &= V \\ \alpha &= \tan^{-1} \frac{w}{u} \\ \beta &= \sin^{-1} \frac{v}{V} \end{aligned} \quad (3.35)$$

V is the airspeed and it is expressed in Equation (3.36).

$$V = \sqrt{u^2 + v^2 + w^2} \quad (3.36)$$

So, differentiating Equation (3.35) and (3.36) with respect to time gives in Equation (3.37) – (3.39).

$$\dot{V} = \frac{1}{V} (u\dot{u} + v\dot{v} + w\dot{w}) \quad (3.37)$$

$$\dot{\alpha} = \frac{u\dot{w} - w\dot{u}}{u^2 + w^2} \quad (3.38)$$

$$\begin{aligned} \dot{\beta} &= \frac{V\dot{v} - v\dot{V}}{V^2} \left[\frac{1}{\sqrt{1 - \left(\frac{v}{V}\right)^2}} \right] = \left[\frac{V\dot{v} - v\dot{V}}{V\sqrt{u^2 + w^2}} \right] \\ &= \frac{(u^2 + v^2 + w^2)\dot{v} - v(u\dot{u} + v\dot{v} + w\dot{w})}{V^2\sqrt{u^2 + w^2}} \\ &= \frac{(u^2 + w^2)\dot{v} - v(u\dot{u} + w\dot{w})}{V^2\sqrt{u^2 + w^2}} \end{aligned} \quad (3.39)$$

3.6. The Linarized Equations of Motion

The aircraft motion equations were derived above to be used in future studies. These equations need to be linearized so that they can be analyzed and examined comfortably in the sections to be explained later. For this reason, in this section, the equations of motion resulting from both the longitudinal and lateral sides of the aircraft are linearized since they are rather nonlinear. Highly nonlinear equations are linearized in order to easily analyze the mathematical explanations resulting from aircraft motion equations and behaviors (Howe, 1980). The purpose of linearization is that the least squares method, which will be explained later, can be applied easily on the equations formed as a result of the behavior of the aircraft control surfaces. Here, linearized equations have been derived.

3.6.1. The linarized longitudinal equations

First of all, the states used in longitudinal motion equations are determined in order to perform linearization. States of the longitudinal motions that are aircraft velocity (v_p), angular velocity pitch component (q), pitch angle (θ) and angle of attack (α). The equilibrium points of states are $v_p = v_{p0}$, $\alpha = \alpha_0 = 0$, $\theta = \theta_0 = 0$ and $q = 0$. After determining the states and equilibrium points for longitudinal motion, linearization of the longitudinal motion equations between Equation (3.40) and (3.43) is given below.

$$\dot{V}_p = \frac{-2g(C_{D0} + C_{D_{CL^2}} C_{L0}^2)}{V_{p0} C_L} V_p + g \left(1 - 2C_{D_{CL^2}} \frac{C_{L0}}{C_L} C_{L\alpha} + \frac{P_z}{m} \right) \alpha - g\theta \quad (3.40)$$

$$\dot{\alpha} = \frac{-g}{V_{p0}^2} \left(1 + \frac{C_{L0}}{C_L} + \frac{P_z}{mg} \right) V_p - \left(\frac{g}{V_{p0}} \frac{C_{L\alpha}}{C_L} + \frac{P_x}{mV_{p0}} \right) \alpha - \frac{g}{V_{p0}} \frac{C_{L\delta_e}}{C_L} \delta_e + q \quad (3.41)$$

$$\dot{q} = \frac{2mgcC_{M0}}{I_{yy}V_{p0}C_L} V_p + \frac{mgcC_{M\alpha}}{I_{yy}C_L} \alpha + \frac{mgc^2C_{M\dot{\alpha}}}{2I_{yy}V_{p0}C_L} \dot{\alpha} + \frac{mgc^2C_{MQ}}{2I_{yy}V_{p0}C_L} q + \frac{mgcC_{M\delta_e}}{I_{yy}C_L} \delta_e \quad (3.42)$$

$$\dot{\theta} = q \quad (3.43)$$

Equations between (3.40) - (3.43) can be stated as form of vector notation in Equation (3.44) as follows. Representation of A, B and C matrices in vector notation is given in equation (3.45).

$$C\dot{X} = AX + B\delta_e \rightarrow \begin{bmatrix} 1 & 0 & 0 & 0 \\ 0 & 1 & 0 & 0 \\ 0 & c_{32} & 1 & 0 \\ 0 & 0 & 0 & 1 \end{bmatrix} \begin{bmatrix} \dot{v}_p \\ \dot{\alpha} \\ \dot{q} \\ \dot{\theta} \end{bmatrix} = \begin{bmatrix} a_{11} & a_{12} & 0 & -g \\ a_{21} & a_{22} & 1 & 0 \\ a_{31} & a_{32} & a_{33} & 0 \\ 0 & 0 & 1 & 0 \end{bmatrix} \begin{bmatrix} v_p \\ \alpha \\ q \\ \theta \end{bmatrix} + \begin{bmatrix} 0 \\ b_2 \\ b_3 \\ 0 \end{bmatrix} \delta_e \quad (3.44)$$

where

$$C = \begin{bmatrix} 1 & 0 & 0 & 0 \\ 0 & 1 & 0 & 0 \\ 0 & c_{32} & 1 & 0 \\ 0 & 0 & 0 & 1 \end{bmatrix}, \quad A = \begin{bmatrix} a_{11} & a_{12} & 0 & -g \\ a_{21} & a_{22} & 1 & 0 \\ a_{31} & a_{32} & a_{33} & 0 \\ 0 & 0 & 1 & 0 \end{bmatrix}, \quad B = \begin{bmatrix} 0 \\ b_2 \\ b_3 \\ 0 \end{bmatrix} \quad (3.45)$$

C is invertible matrix. Therefore, it can be move to do right hand side of the Equation (3.44). Therefore, The A and B matrices are updated in Equation (3.46).

$$\hat{A} = C^{-1}A = \begin{bmatrix} a_{11} & a_{12} & 0 & -g \\ a_{21} & a_{22} & 1 & 0 \\ \hat{a}_{31} & \hat{a}_{32} & \hat{a}_{33} & 0 \\ 0 & 0 & 1 & 0 \end{bmatrix}, \quad \hat{B} = C^{-1}B = \begin{bmatrix} 0 \\ \hat{b}_2 \\ \hat{b}_3 \\ 0 \end{bmatrix} \quad (3.46)$$

Component of the A and B matrix detailed expressions can be obtained from the coefficient linearized longitudinal motion equations for $\dot{v}_p, \dot{\alpha}, \dot{q}, \dot{\theta}$ in Equation (3.40) - (3.43). Thus, the coefficients in the given matrix in Equation (3.46) are expressed in Equation (3.47) below with some assumptions. Some assumptions were made while generating the coefficients in Equation (3.47) (Howe, 1991). These assumptions are set out below.

- P_z is neglected, the z component of powerplant force
- $C_{L0} = C_L$
- $C_{M0} = 0$
- $C_D = C_{D0} + C_{DCL^2} C_{L0}$
- $\frac{P_x}{m} = \frac{gC_D}{C_L}$

The coefficients according to these assumptions are as follows.

$$\begin{aligned}
c_{32} &= -\frac{mgc^2 C_{M\dot{\alpha}}}{2I_{yy}V_{p_0}C_L} & a_{32} &= \frac{mgcC_{M\alpha}}{I_{yy}C_L} \\
a_{11} &= -\frac{2gC_D}{V_{p_0}C_L} & a_{33} &= \frac{mgc^2 C_{M\dot{Q}}}{2I_{yy}V_{p_0}C_L} \\
a_{12} &= g\left(1 - 2C_{D_{CL^2}}C_{L\alpha}\right) & a_{43} &= 1 \\
a_{14} &= -g & b_2 &= -\frac{g}{V_{p_0}}\frac{C_{L\delta_e}}{C_L} \\
a_{21} &= \frac{-2g}{V_{p_0}^2} & b_3 &= \frac{mgcC_{M\delta_e}}{I_{yy}C_L} \\
a_{22} &= -\frac{g}{V_{p_0}}\left(\frac{C_{L\alpha}}{C_L} + \frac{C_D}{C_L}\right) & \hat{a}_{31} &= -c_{32}a_{21} + a_{31} \\
a_{23} &= 1 & \hat{a}_{32} &= -c_{32}a_{22} + a_{32} \\
a_{31} &= 0 & \hat{a}_{33} &= -c_{32} + a_{33} \\
& & \hat{b}_3 &= -c_{32}b_2 + b_3
\end{aligned} \tag{3.47}$$

After the matrix coefficients defined above, the state equations can be rewritten as in Equation (3.48) - (3.51) below.

$$\dot{V}_p = a_{11}v_p + a_{12}\alpha + a_{14}\theta \tag{3.48}$$

$$\dot{\alpha} = a_{21}v_p + a_{22}\alpha + q + b_2\delta_e \tag{3.49}$$

$$\dot{q} = \hat{a}_{32}\alpha + \hat{a}_{33}q + \hat{b}_3\delta_e + \hat{a}_{31}v_p \tag{3.50}$$

$$\dot{\theta} = q \tag{3.51}$$

In addition, the states of (3.48) - (3.51) are expressed in the Laplace domain by performing the Laplace transform.

In this way, the linearized longitudinal equations of motion of an airplane together with laplace transforms will obtain the transfer function resulting from the behavior of the elevator control surface. Thus, the pitch transfer function which is the elevator displacement ratio of the pitch angle is expressed in Equations (3.52) and (3.53) below.

$$\frac{\theta}{\delta_e}(s) = \frac{(b_3 - c_{32}b_2)s^2 + [b_2(c_{32}a_{11} + a_{32}) - b_3(a_{11} + a_{22})]s + b_3(a_{11}a_{22} - a_{21}a_{12}) - b_2a_{32}a_{11}}{D(s)} \quad (3.52)$$

where

$$D(s) = s^4 + (c_{32} - a_{11} - a_{22} - a_{33})s^3 + [a_{11}a_{22} - a_{21}a_{12} + a_{33}(a_{11} + a_{22})c_{32}a_{11} - a_{32}]s^2 + [c_{32}a_{21}a_{14} + a_{32}a_{11} - a_{33}(a_{11}a_{22} - a_{21}a_{12})]s + a_{32}a_{21}a_{14} \quad (3.53)$$

In general, the pitch transfer function has been created. This function can also be expressed in the form in Equation (3.54) (Howe, 1980).

$$\frac{\theta}{\delta_e}(s) = K_e \frac{(\tau_s s + 1)(\tau_p s + 1)}{(\frac{1}{w_{ns}^2} s^2 + \frac{2\zeta_s}{w_{ns}} s + 1)(\frac{1}{w_{np}^2} s^2 + \frac{2\zeta_p}{w_{np}} s + 1)} \quad (3.54)$$

Longitudinal motion of the aircraft with the short-period and phugoid approximations may be expressed as the transfer function form in Equation (3.54). Input of this transfer is elevator displacement while output is pitch angle. The transfer function we find contains two complex conjugate root pair and damped oscillatory transients. According to the short period approach of the first root aircraft, undamped natural frequency w_{ns} , damping ratio ζ_s , τ_s and according to the second root phugoid approach, natural frequency w_{np} , damping ratio ζ_p , τ_p and the gain of our system are revealed. These expressions are explained in (3.55). The definition of the symbols used for this form of this transfer function explained in Equation (3.54) is given in Equation (3.55).

$$\begin{aligned} w_{np} &= \frac{\sqrt{2}g}{V_{p0}} \\ \zeta_p &= \frac{C_D}{\sqrt{2}C_L} \\ \tau_p &= \frac{V_{p0}C_L}{2gC_D} \end{aligned} \quad (3.55)$$

$$\begin{aligned}
w_{ns} &= \sqrt{\frac{mgc}{I_{yy}} \left(\left(\frac{-C_{M\alpha}}{C_L} \right) - \frac{gcC_{MQ}(C_{L\alpha} + C_D)}{2V_{p0}^2 CL^2} \right)} \\
\zeta_s &= \frac{g}{2w_{ns}V_{p0}} \left(\frac{C_{L\alpha} + C_D}{C_L} - \frac{mc^2 C_{MQ}C_{M\dot{\alpha}}}{2I_{yy}C_L} \right) \\
\tau_s &= \frac{c}{2V_{p0}} \left(\frac{C_{M\alpha}C_{L\delta_e}gc - 2V_{p0}^2 C_{M\delta_e}C_L}{C_{M\alpha}C_{L\delta_e}gc - (C_{L\alpha}C_D)C_{M\delta_e}gc} \right) \\
K_e &= \left(- \left(\frac{C_D(C_{D\alpha} + C_D)}{CL^2} + 1 - 2C_{D_{CL^2}}C_{L\alpha} \right) \frac{C_{M\delta_e}}{C_{M\alpha}} + \frac{C_{L\delta_e}C_D}{CL^2} \right)
\end{aligned}$$

After obtaining the pitch transfer function from the longitudinal motion equations, another transfer function derived from the longitudinal motion equations is the ratio of the angle of attack to the elevator displacement. With this transfer function, analysis of the behavior of an aircraft between the angle of attack and the elevator displacement can be realized. While finding this transfer function, the Equations between (3.47) - (3.51) described above are used. The necessary equations are made between the Equations (3.48) - (3.51) to obtain the transfer operator relating angle of attack to elevator displacement in the following Equation (3.56).

$$\frac{\alpha}{\delta_e}(s) = \frac{b_2s^3 + [b_3 - b_2(a_{11} + a_{33})]s^2 + a_{11}(b_2a_{33} - b_3)s + b_3a_{21}a_{14}}{D(s)} \quad (3.56)$$

where $D(s)$ as before is given by Equation (3.53). This transfer operator relating angle of attack to elevator displacement, extracted with the pitch transfer foundation, will be used in the description of the prediction methods described later.

3.6.2. The linearized lateral equations

After linearizing the longitudinal motion equations, the lateral motion equations will be linearized in this section for the analysis of the behaviors resulting from the aircraft's lateral motion. Before starting linearization, states should be determined as with longitudinal motion. States of the lateral motions that are side slip angle (β), roll rate (p), yaw rate (r) and bank angle (Φ). The equilibrium points of states determined in lateral motion are $\beta = 0, p = 0, r = 0$ and $\Phi = 0$. Thus, the linearized lateral motion Equations for $\dot{\beta}, \dot{p}, \dot{r}, \dot{\Phi}$ are expressed in Equation (3.57)- (3.60).

$$\dot{\beta} = \frac{gC_{Y\beta}}{V_{p0}C_L}\beta - r + \left(\frac{g}{V_{p0}}\right)\Phi + \left(\frac{gC_{Y\delta_r}}{V_{p0}C_L}\right)\delta_r \quad (3.57)$$

$$\dot{p} = \left(\frac{mgbC_{l\beta}}{I_{xx}C_L}\right)\beta + \left(\frac{mgb^2C_{lp}}{2I_{xx}V_{p0}C_L}\right)p + \left(\frac{mgb^2C_{lr}}{2I_{xx}V_{p0}C_L}\right)r + \frac{I_{xz}}{I_{xx}}\dot{r} + \left(\frac{mgbC_{l\delta_a}}{I_{xx}C_L}\right)\delta_a + \left(\frac{mgbC_{l\delta_r}}{I_{xx}C_L}\right)\delta_r \quad (3.58)$$

$$\dot{r} = \left(\frac{mgbC_{N\beta}}{I_{zz}C_L}\right)\beta + \left(\frac{mgb^2C_{Np}}{2I_{zz}V_{p0}C_L}\right)p + \left(\frac{mgb^2C_{Nr}}{2I_{zz}V_{p0}C_L}\right)r + \frac{I_{xz}}{I_{zz}}\dot{p} + \left(\frac{mgbC_{N\delta_a}}{I_{zz}C_L}\right)\delta_a + \left(\frac{mgbC_{N\delta_r}}{I_{zz}C_L}\right)\delta_r \quad (3.59)$$

$$\dot{\Phi} = p \quad (3.60)$$

The state equations that occur in the lateral motion of the aircraft have been expressed. These equations can also be expressed in vector representation. The vector representation is given below in Equation (3.61). Representation of A and B matrices in vector notation is given in equation (3.62).

$$C\dot{X} = AX + B\delta \rightarrow \begin{bmatrix} 1 & 0 & 0 & 0 \\ 0 & 1 & c_{23} & 0 \\ 0 & c_{32} & 1 & 0 \\ 0 & 0 & 0 & 1 \end{bmatrix} \begin{bmatrix} \dot{\beta} \\ \dot{p} \\ \dot{r} \\ \dot{\Phi} \end{bmatrix} = \begin{bmatrix} a_{11} & 0 & -1 & a_{14} \\ a_{21} & a_{22} & a_{23} & 0 \\ a_{31} & a_{32} & a_{33} & 0 \\ 0 & 1 & 0 & 0 \end{bmatrix} \begin{bmatrix} \beta \\ p \\ r \\ \Phi \end{bmatrix} + \begin{bmatrix} 0 & b_{12} \\ b_{21} & b_{22} \\ b_{31} & b_{32} \\ 0 & 0 \end{bmatrix} \begin{bmatrix} \delta_a \\ \delta_r \end{bmatrix} \quad (3.61)$$

where

$$C = \begin{bmatrix} 1 & 0 & 0 & 0 \\ 0 & 1 & c_{23} & 0 \\ 0 & c_{32} & 1 & 0 \\ 0 & 0 & 0 & 1 \end{bmatrix}, A = \begin{bmatrix} a_{11} & 0 & -1 & a_{14} \\ a_{21} & a_{22} & a_{23} & 0 \\ a_{31} & a_{32} & a_{33} & 0 \\ 0 & 1 & 0 & 0 \end{bmatrix}, B = \begin{bmatrix} 0 & b_{12} \\ b_{21} & b_{22} \\ b_{31} & b_{32} \\ 0 & 0 \end{bmatrix} \quad (3.62)$$

C is invertible matrix. Therefore, it can be move to do right hand side of the Equation (3.61). Therefore, The A and B matrices are updated in Equation (3.63).

$$\hat{A} = C^{-1}A = \begin{bmatrix} a_{11} & 0 & -1 & a_{14} \\ \hat{a}_{21} & \hat{a}_{22} & \hat{a}_{23} & 0 \\ \hat{a}_{31} & \hat{a}_{32} & \hat{a}_{33} & 0 \\ 0 & 1 & 0 & 0 \end{bmatrix}, \hat{B} = C^{-1}B = \begin{bmatrix} 0 & b_{12} \\ \hat{b}_{21} & \hat{b}_{22} \\ \hat{b}_{31} & \hat{b}_{32} \\ 0 & 0 \end{bmatrix} \quad (3.63)$$

Component of the A and B matrix detailed expressions can be obtained from the coefficient linearized lateral motion equations for $\dot{\beta}$, \dot{p} , \dot{r} , $\dot{\Phi}$ in Equation (3.57) - (3.60). Thus, the coefficients of A and B matrices in Equation (3.63) are expressed in Equation (3.64) below.

$$\begin{aligned} c_{23} &= -\frac{I_{xz}}{I_{xx}} & b_{12} &= \left(\frac{gC_Y\delta_r}{V_{p0}C_L}\right) \\ c_{32} &= -\frac{I_{xz}}{I_{zz}} & b_{21} &= \left(\frac{mgbC_{l\delta_a}}{I_{xx}C_L}\right) \\ a_{11} &= \frac{gC_Y\beta}{V_{p0}C_L} & b_{22} &= \left(\frac{mgbC_{l\delta_r}}{I_{xx}C_L}\right) \\ a_{14} &= \left(\frac{g}{V_{p0}}\right) & b_{31} &= \left(\frac{mgbC_{N\delta_a}}{I_{zz}C_L}\right) \\ a_{21} &= \left(\frac{mgbC_{l\beta}}{I_{xx}C_L}\right) & b_{32} &= \left(\frac{mgbC_{N\delta_r}}{I_{zz}C_L}\right) \\ a_{22} &= \left(\frac{mgb^2C_{lp}}{2I_{xx}V_{p0}C_L}\right) & \hat{a}_{21} &= -\frac{1}{c_{23}c_{32}-1}a_{21} + \frac{c_{23}}{c_{23}c_{32}-1}a_{31} \\ a_{23} &= \left(\frac{mgb^2C_{lR}}{2I_{xx}V_{p0}C_L}\right) & \hat{a}_{22} &= -\frac{1}{c_{23}c_{32}-1}a_{22} + \frac{c_{23}}{c_{23}c_{32}-1}a_{32} \\ a_{31} &= \left(\frac{mgbC_{N\beta}}{I_{zz}C_L}\right) & \hat{a}_{23} &= -\frac{1}{c_{23}c_{32}-1}a_{23} + \frac{c_{23}}{c_{23}c_{32}-1}a_{33} \\ a_{32} &= \left(\frac{mgb^2C_{Np}}{2I_{zz}V_{p0}C_L}\right) & \hat{a}_{32} &= \frac{c_{32}}{c_{23}c_{32}-1}a_{22} - \frac{1}{c_{23}c_{32}-1}a_{32} \\ a_{33} &= \left(\frac{mgb^2C_{NR}}{2I_{zz}V_{p0}C_L}\right) & \hat{b}_{21} &= -\frac{1}{c_{23}c_{32}-1}b_{21} + \frac{c_{23}}{c_{23}c_{32}-1}b_{31} \\ \hat{a}_{31} &= \frac{c_{32}}{c_{23}c_{32}-1}a_{21} - \frac{1}{c_{23}c_{32}-1}a_{31} & \hat{b}_{31} &= \frac{c_{32}}{c_{23}c_{32}-1}b_{21} - \frac{1}{c_{23}c_{32}-1}b_{31} \\ \hat{a}_{33} &= \frac{c_{32}}{c_{23}c_{32}-1}a_{23} - \frac{1}{c_{23}c_{32}-1}a_{33} & \hat{b}_{32} &= \frac{c_{32}}{c_{23}c_{32}-1}b_{22} - \frac{1}{c_{23}c_{32}-1}b_{32} \\ \hat{b}_{22} &= -\frac{1}{c_{23}c_{32}-1}b_{22} + \frac{c_{23}}{c_{23}c_{32}-1}b_{32} \end{aligned} \quad (3.64)$$

After the matrix coefficients defined above, the state equations can be rewritten as in Equation (3.65) - (3.68) below.

$$\dot{\beta} = a_{11}\beta - r + a_{14}\Phi + b_{12}\delta_r \quad (3.65)$$

$$\dot{p} = \hat{a}_{21}\beta + \hat{a}_{22}p + \hat{a}_{23}r + \hat{b}_{21}\delta_a + \hat{b}_{22}\delta_r \quad (3.66)$$

$$\dot{r} = \hat{a}_{31}\beta + \hat{a}_{32}p + \hat{a}_{33}r + \hat{b}_{31}\delta_a + \hat{b}_{32}\delta_r \quad (3.67)$$

$$\dot{\Phi} = p \quad (3.68)$$

Thus, the states of (3.65) - (3.68) are expressed in the Laplace domain by performing the Laplace transform.

Then, Equation (3.69) and Equation (3.70) expressions can be obtained when the Equations in (3.65) - (3.68) are adjusted within themselves in order to derive the desired transfer functions.

$$\begin{aligned} & [s^2 - (a_{11} + a_{33})s + (a_{31} + a_{33}a_{11})]r \\ & = [-c_{32}s^3 + (a_{32} + c_{32}a_{11})s^2 - a_{32}a_{11}s + a_{31}a_{14}]\Phi + (b_{31}s - b_{31}a_{11})\delta_a \\ & + (b_{32}s + a_{31}b_{12} - b_{32}a_{11})\delta_r \end{aligned} \quad (3.69)$$

$$\begin{aligned} & [(a_{31} - a_{21}c_{32})s^2 + (a_{21}a_{32} - a_{31}a_{32})s]\Phi \\ & = [(a_{21} - a_{31}c_{23})s + a_{31}a_{23} - a_{21}a_{33}]r + (a_{31}b_{21} - a_{21}b_{31})\delta_a + (a_{31}b_{22} \\ & - a_{21}b_{32})\delta_r \end{aligned} \quad (3.70)$$

After reaching these expressions, in order to simplify the expressions in Equation (3.69) and (3.70), the coefficients in the expressions are expressed in Equation (3.71) in the following format.

$$\begin{aligned} a_1 &= -(a_{11} + a_{33}) & b_3 &= b_{32} \\ a_0 &= a_{31} + a_{33}a_{11} & b_2 &= a_{31}b_{12} - b_{32}a_{11} \end{aligned}$$

$$\begin{aligned}
c_3 &= -c_{32} & d_2 &= a_{31} - a_{21}c_{32} \\
c_2 &= a_{32} + c_{32}a_{11} & d_1 &= a_{21}a_{32} - a_{31}a_{22} \\
c_1 &= -a_{32}a_{11} & k_1 &= a_{21} - a_{31}c_{23} \\
c_0 &= a_{31}a_{14} & k_0 &= a_{31}a_{23} - a_{21}a_{33} \\
b_1 &= b_{31} & b_4 &= a_{31}b_{21} - a_{21}b_{31} \\
b_0 &= -b_{31}a_{11} & b_4 &= a_{31}b_{21} - a_{21}b_{31}
\end{aligned} \tag{3.71}$$

Thus, in order to make examinations in the lateral motion, the ratio of the bank angle found in Equation (3.72) and (3.73) below to both aileron displacement and rudder displacement is determined as a result of the equations above.

$$\begin{aligned}
\Phi(s) = & \frac{(b_4 + b_1k_1)s^2 + [b_4a_1 + b_0k_1]s + (b_4a_0 + b_0k_0)}{D_1(s)} \delta_a \\
& + \frac{(b_5 + b_3k_1)s^2 + [b_5a_1 + b_2k_1 + b_3k_0]s + (b_5a_0 + b_2k_0)}{D_1(s)} \delta_r
\end{aligned} \tag{3.72}$$

where

$$\begin{aligned}
D_1(s) = & (d_2 - c_3k_1)s^4 + (d_2a_1 + d_1 - c_2k_1 - c_3k_0)s^3 \\
& + [a_0d_2 + a_1d_1 - c_1k_1 - c_2k_0]s^2 + [a_0d_1 - c_1k_0 - c_0k_1]s + c_0k_0
\end{aligned} \tag{3.73}$$

Thus, the transfer function, which generally results from the lateral motion of an aircraft, has been found. The analysis of the behavior of this transfer function bank angle is based on the changes of both aileron and rudder displacement. also, this transfer function can be expressed in a separate form. In other words, the ratio of the bank angle to the aileron displacement and the ratio of the bank angle to the rudder displacement are explained separately below (Howe, 1980). First, the ratio of bank angle to aileron displacement in Equation (3.74) is given below.

$$\frac{\Phi}{\delta_a} = -K_a \frac{\frac{s^2}{w_{n\phi}^2} + \frac{2\zeta_{\phi}s}{w_{n\phi}} + 1}{(T_{\phi 1}s + 1)(T_{\phi 2}s + 1)(\frac{s^2}{w_{nr}^2} + \frac{2\zeta_r s}{w_{nr}} + 1)} \tag{3.74}$$

Lateral motion of the aircraft with the dutch-roll and spiral mode approximations may be expressed as the transfer function form in Equation (3.6.2-21). Input of this transfer

is aileron displacement while output is bank angle. As was done when expressing the pitch transfer function before, this equation was obtained in its plain form with some approximations. The dutch roll and spiral mode approaches we used in the lateral motion of the aircraft were used to obtain this equation. The time constants $T_{\phi 1}$ and $T_{\phi 2}$ are for the rolling motion, $w_{n\phi}$ and w_{nr} are the natural frequency, ζ_ϕ and ζ_r are the damping ratio, and the gain value is the gain of our system. These expressions are explained in (3.75). The definition of the symbols used for this form of this transfer function explained in Equation (3.74) is given in Equation (3.75).

$$\begin{aligned}
T_{\phi 1} &= \frac{-2I_{xx}V_{p0}C_L}{mgb^2C_{lP}} \\
T_{\phi 2} &= \frac{V_{p0}}{g} \left(\frac{C_{lP}C_{N\beta} - C_{NP}C_{l\beta}}{C_{lR}C_{N\beta} - C_{NR}C_{l\beta}} \right) \\
w_{nr} &= \sqrt{\frac{mgbC_{N\beta}}{I_{zz}C_L}} \\
\zeta_r &= \frac{g}{\frac{mgbC_{N\beta}V_{p0}}{I_{zz}C_L}} \left(\frac{mgb^2C_{NR}}{2I_{zz}C_L} + \frac{C_{Y\beta}}{C_L} \right) \\
K_a &= - \left(\frac{mgb^2C_{N\beta}mgC_{l\delta_a}}{I_{zz}C_L I_{xx}C_L} - \frac{mgb^2C_{l\beta}mgC_{N\delta_a}}{I_{zz}C_L I_{xx}C_L} \right) \left(\frac{mgbC_{N\beta}}{I_{zz}C_L} + \frac{mgb^2C_{NR}gC_{Y\beta}}{I_{zz}C_L 2V_{p0}C_L V_{p0}} \right) \\
&\quad + \frac{mgbC_{N\delta_a}gV_{p0}C_{Y\beta}}{I_{zz}C_L V_{p0}C_L} \left(\frac{mgbC_{N\beta}mgb^2C_{lR}}{I_{zz}C_L 2I_{xx}V_{p0}C_L} - \frac{mgbC_{l\beta}mgb^2C_{NR}}{I_{xx}C_L 2I_{zz}V_{p0}C_L} \right) \\
w_{n\phi} &= - \sqrt{K_a \frac{1}{\left[\frac{mgb^2C_{N\beta}mgC_{l\delta_a}}{I_{zz}C_L I_{xx}C_L} - \frac{mgb^2C_{l\beta}mgC_{N\delta_a}}{I_{zz}C_L I_{xx}C_L} + \frac{mgbC_{N\delta_a}}{I_{zz}C_L} \left(\frac{mgbC_{l\beta}}{I_{xx}C_L} + \frac{mgbC_{N\delta_a}I_{xx}}{I_{zz}C_L I_{xx}} \right) \right]}}
\end{aligned} \tag{3.75}$$

$$\zeta_\phi = -w_{n\phi} \frac{1}{K_a} \left[-\frac{mgb^2 C_{N\beta} mg C_{l\delta_a}}{I_{zz} C_L I_{xx} C_L} - \frac{mgb^2 C_{l\beta} mg C_{N\delta_a}}{I_{zz} C_L I_{xx} C_L} \right. \\ \left. + \frac{mgb C_{N\delta_a}}{I_{zz} C_L} \left(\frac{g C_{Y\beta}}{V_{p0} C_L} + \frac{mgb^2 C_{NR}}{2 I_{zz} V_{p0} C_L} \right) \right. \\ \left. - \frac{mgb C_{N\delta_a} g V_{p0} C_{Y\beta}}{I_{zz} C_L V_{p0} C_L} \left(\frac{mgb C_{l\beta}}{I_{xx} C_L} + \frac{mgb C_{N\delta_a} I_{xz}}{I_{zz} C_L I_{xx}} \right) \right. \\ \left. + \frac{mgb C_{l\beta}}{I_{xx} C_L} \left(\frac{mgb C_{N\beta} mgb^2 C_{lR}}{I_{zz} C_L 2 I_{xx} V_{p0} C_L} - \frac{mgb C_{l\beta} mgb^2 C_{NR}}{I_{xx} C_L 2 I_{zz} V_{p0} C_L} \right) \right]$$

After explaining the ratio of bank angle to aileron displacement as above, this time again in bear form, the ratio of bank angle to rudder displacement is explained below in Equation (3.76).

$$\frac{\phi}{\delta_r} = K_r \frac{(T_{\phi r_1} s + 1)(-T_{\phi r_2} s + 1)}{(T_{\phi 1} s + 1)(T_{\phi 2} s + 1) \left(\frac{s^2}{w_{nr}^2} + \frac{2\zeta_r s}{w_{nr}} + 1 \right)} \quad (3.76)$$

While analyzing the aileron control surface behavior, the states in the lateral motion of the aircraft and the equations resulting from the linearization were extracted. Here again, we will reach the transfer function, which is the ratio of bank angle to rudder displacement in (3.6.2-19), using those equations. As we have done before when expressing the pitch transfer function and the transfer function of the ratio of the bank angle to aileron displacement, this equation is also simply obtained by some approximation. In order to obtain this equation, the dutch roll and spiral mode approaches that we use in the lateral motion of the aircraft are used. $T_{\phi 1}$, $T_{\phi 2}$, w_{nr} and ζ_r values expressed above have the same value here as they were the behavior of the bank angle before. In addition, $T_{\phi r_1}$ and $T_{\phi r_2}$ time constants and the gain of our system are defined here. These expressions are explained in (3.75) and (3.77). Parameter of the Equation (3.76) is presented in Equation (3.77).

$$K_r = \left(\frac{mgb C_{N\beta}}{I_{zz} C_L} \frac{mgb C_{l\delta_r}}{C_L I_{xx}} - \frac{mgb C_{l\beta}}{I_{xx} C_L} \frac{mgb C_{N\delta_r}}{C_L I_{zz}} \right) \left(\frac{mgb C_{N\beta}}{I_{zz} C_L} + \frac{mgb^2 C_{NR}}{2 I_{zz} C_L V_{p0}} \frac{g C_{Y\beta}}{C_L V_{p0}} \right) \\ + \left(\frac{mgb C_{N\beta}}{I_{zz} C_L} \frac{mgb^2 C_{lR}}{2 I_{xx} C_L V_{p0}} - \frac{mgb C_{l\beta}}{C_L I_{xx}} \frac{mgb^2 C_{NR}}{C_L} \right) \left(\frac{mgb C_{N\beta}}{I_{zz} C_L} \frac{g C_{Y\delta_r}}{C_L V_{p0}} - \frac{mgb C_{N\delta_r}}{C_L I_{zz}} \frac{g C_{Y\beta}}{C_L V_{p0}} \right) \quad (3.77)$$

$$T_{\phi r_1} = -\left[\frac{mgbC_{N\beta}}{I_{zz}C_L}\frac{mgbC_{l\delta_r}}{C_L I_{xx}} - \frac{mgbC_{l\beta}}{I_{xx}C_L}\frac{mgbC_{N\delta_r}}{C_L I_{zz}} + \frac{mgbC_{N\delta_r}}{C_L I_{zz}}\left(\frac{mgbC_{l\beta}}{C_L I_{xx}} + \frac{mgbC_{N\beta I_{xz}}}{I_{zz}C_L I_{xx}}\right)\right]\frac{1}{D}$$

$$D = \left[\frac{mgbC_{N\beta}}{I_{zz}C_L}\frac{mgbC_{l\delta_r}}{C_L I_{xx}} - \frac{mgbC_{l\beta}}{I_{xx}C_L}\frac{mgbC_{N\delta_r}}{C_L I_{zz}}\left(-\left(\frac{gC_{Y\beta}}{C_L V_{p0}} + \frac{mgb^2 C_{NR}}{2I_{zz}C_L V_{p0}}\right)\right) + \left(\frac{mgbC_{l\beta}}{C_L I_{xx}} - \frac{mgbC_{N\beta I_{xz}}}{I_{zz}C_L I_{xx}}\right)\left(\frac{mgbC_{N\beta}}{I_{zz}C_L}\frac{gC_{Y\delta_r}}{C_L V_{p0}} - \frac{mgbC_{N\delta_r}}{C_L I_{zz}}\frac{gC_{Y\beta}}{C_L V_{p0}}\right) + \frac{mgbC_{N\delta_r}}{I_{zz}C_L}\left(\frac{mgbC_{N\beta}}{I_{zz}C_L}\frac{mgb^2 C_{lR}}{2I_{xx}C_L V_{p0}} - \frac{mgbC_{l\beta}}{C_L I_{xx}}\frac{mgb^2 C_{NR}}{C_L}\right)\right] + K_r$$

Thus, the transfer functions resulting from both the longitudinal and lateral motions of an aircraft are expressed. These transfer functions will be analyzed using system identification methods in the following sections and it will be examined whether the same result is given with the original data. Therefore, in this section, the mathematical model of the aircraft has been derived and the transfer functions to be analyzed are created by linearizing the nonlinear equations.

4. SYSTEM IDENTIFICATION OF AN AIRCRAFT

In this section, what the system definition is, its history, the description of the system definition tool in the MATLAB program and how the system identification is used on the aircraft are explained. By explaining the parameter estimation methods, the equations resulting from the behavior of aircraft control surfaces with online and offline parameter estimation methods are estimated. In this chapter, the system identification procedure for the aircrafts was explained based on the book “Aircraft System Identification: Theory and Practise” by Klein and Morelli (Klein and Morelli, 2006).

4.1. Definition of System Identification

System identification creates mathematical models of any dynamical system based on the behavior of input and output signals. The estimated models are then utilized to examine the behavior of the dynamic system. System identification tries to develop a significant mathematical model that relates the inputs of the system with the outputs using the experimental data measured from the system. As observed in Figure 4.1 and Figure 4.2, the inputs and outputs of the system are generally known as the system definition process and the model of the dynamic system emerges. In other words, when the input values that will enter our system and the behavior of our system as output are known, our system can be defined and the state equation of our system is found. The dynamical system represented via state space approach may be seen in Figure 4.1 A dynamic system is a mathematical relationship between the input and output variables of the system.

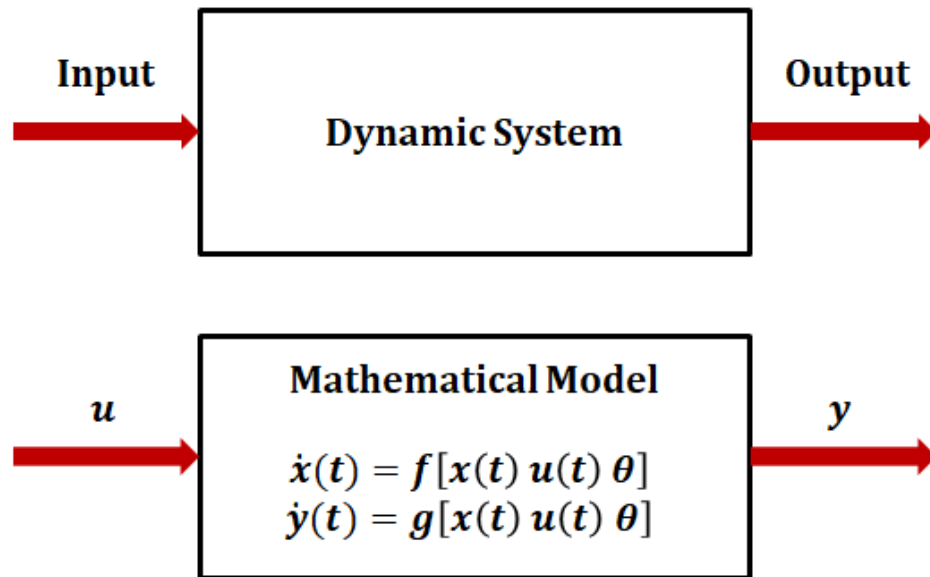


Figure 4.1. Representation of dynamic system

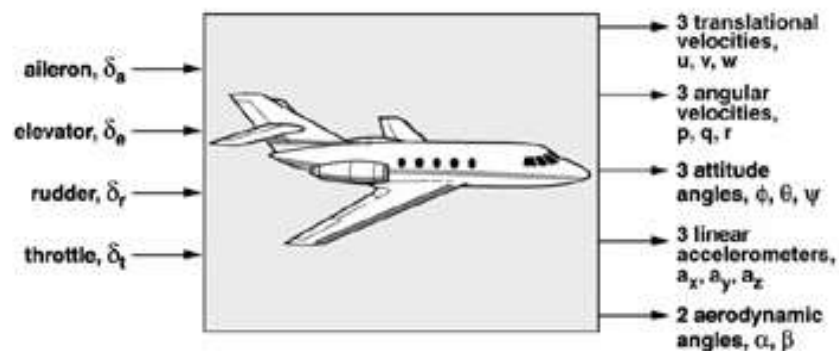


Figure 4.2. System identification of aircraft system

Three different types of problems are encountered in system theory, with the other two being any of the input, output and model functions described above. The three problems that arise according to the state of these parameters are the simulation, control and definition of the dynamic system. These three problems are below.

- 1) Simulation problem by giving the input u and system functions f and g and finding the output y .
- 2) The control problem is to give output y and system functions f and g and find the input u .

- 3) The identification problem is to find the system functions f and g by giving the input u and the output z .

System identification is concerned with the determination of the mathematical model structure that corresponds to the generally unknown dynamic system. For a given model, the parameters within the model are quantified by applying a numerical, usually statistical procedure. Basically, this part of the model building process is called “parameter estimation” as seen in the Figure 4.3. In order to evaluate the model suitability, the "model validation" step comes after the parameter estimation stage. If it turns out that the defined model does not meet the requirements, the model structure must be changed again and the process must be repeated from the beginning. Therefore, system identification is generally an iterative process that is significantly required.

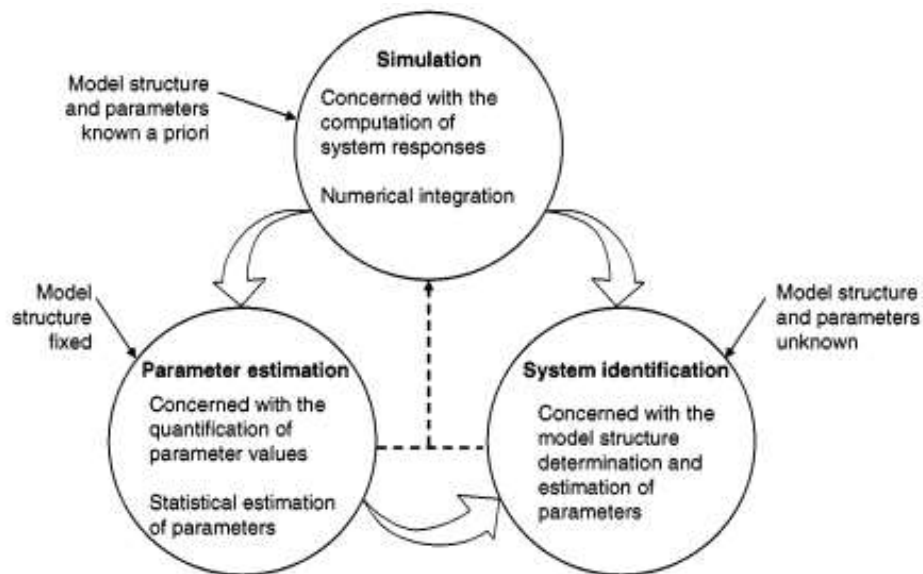


Figure 4.3. Definition of system identification (Jategaonkar, 2006)

In Figure 4.4, showed the system identification prodecure stage. The system identification process starts by making experiments to collect data on the system while determining the measurements of system inputs and outputs. After data is collected, general equations that describe a model or system are developed. Then the unknown parameters in the created model limits are tried to be determined.

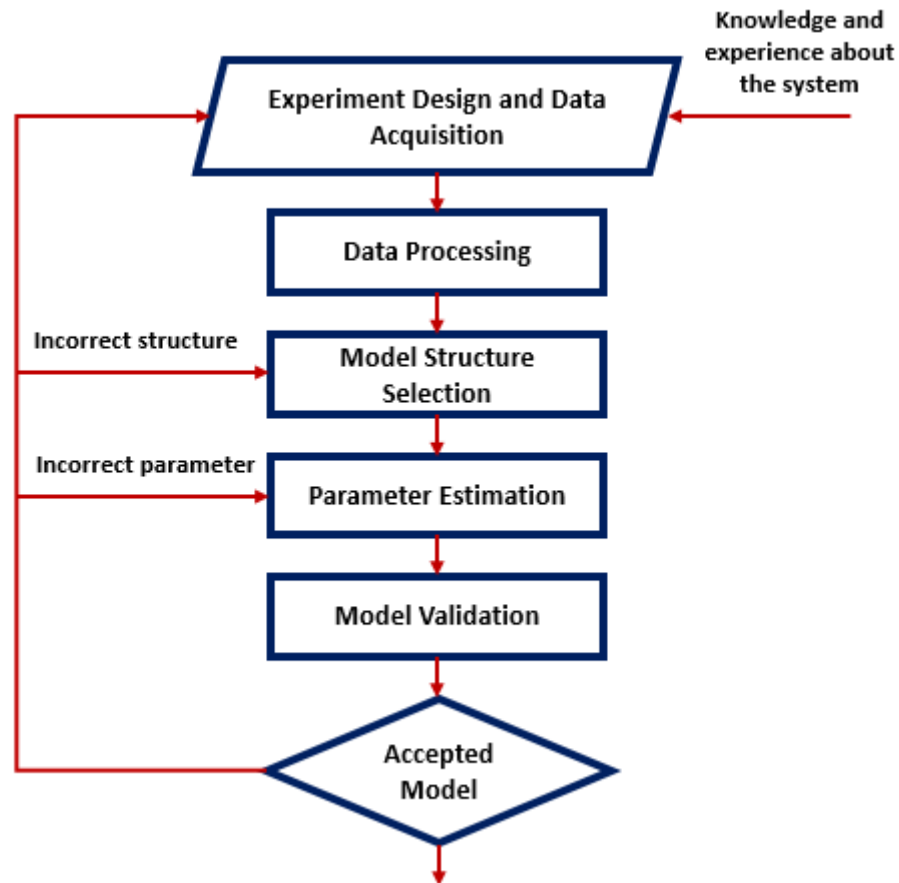


Figure 4.4. System identification procedure

4.2. History of System Identification

The term system identification was coined by Lotfi Zadeh in 1962. Zadeh introduced the term system identification as “the determination on the basis of input and output, of a system within a specified class of systems, to which the system under test is equivalent” (Zadeh, 1962). The earliest studies in system identification were created by statistics and time series communities. System description has its roots in the studies, “Theory of the Motion of Heavenly Bodies Moving about the Sun in Conic Sections” the theory stationary stochastic processes was developed during the period 1920 to 1970 (Gauss, 1809). In the 1960s, the model-based control era and the work of expressing the systems as state space functions began. At that time, various techniques were used to express physical systems in this way. The need for system definition has arisen due to the increasing pressure to apply these modern techniques to areas where models are not available in physics.

Then, system identification is defined as the task of creating a dynamic model in state space and input/output types that can predict the output signals of a dynamic system.

The studies “Effective construction of linear state variable models from input-output functions” (Ho and Kalman, 1965) and “Numerical identification of linear dynamic systems from normal operating records” (Aström and Bohlin, 1965) may be stated as one of the fundamental researches related to system identification.

4.3. System Identification Toolbox

In this section, the tool of MATLAB program is used as a system identification tool. The system identification toolbox enables mathematical models of dynamic systems to be created from measured input-output data. Thanks to the tool, we obtain dynamic systems that can be modeled simply. Also we can use time-domain and frequency-domain input-output data to define continuous-time and discrete-time transfer functions, process models, and state-space models.

Using the MATLAB program system definition tool, examples are made on some systems and the use of the tool is shown. The screen demonstrated in Figure 4.5 appears when the program's tool is opened for the first time. Using the system identification tool, we will be able to accomplish below tasks.

- Import data from the MATLAB workspace into the system identification toolbox.
- Plot the data.
- Process data by removal offsets from the input and output signals.
- Estimate, validate, and compare linear models.
- Export models to the MATLAB workspace.

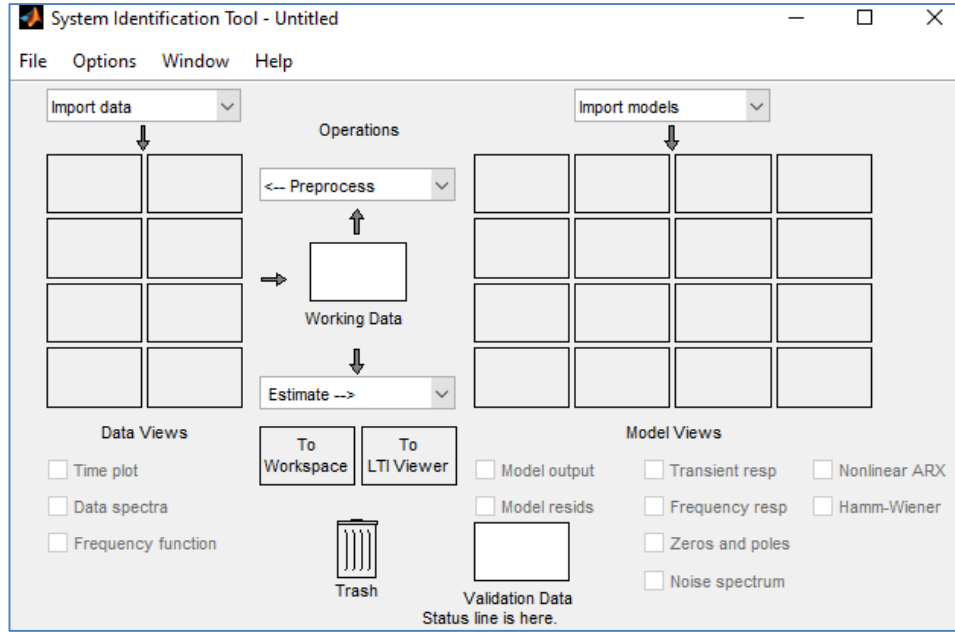


Figure 4.5. System identification tool screen

In order to better comprehend the tool in the MATLAB program and to use its functions, a sample system has been determined, and the program visuals and how it works are given on it. An example transfer function determined is given in Equation (4.1). In this transfer function, y is output and u is input. Also the transfer function is expressed in the laplace domain and s is the laplace variable.

$$\frac{y}{u} = \frac{100}{s^2 + 25s + 100} \quad (4.1)$$

In order to express the output in the specified butransfer function, an input must be defined. As seen in Equation (4.2), the unit step function is defined as input to the system.

$$u = 1 \quad (4.2)$$

After the input is determined, the transfer function, which is its counterpart in the laplace dominant, is expressed in Equation (4.3) below.

$$y = \frac{1}{s} \frac{100}{s^2 + 25s + 100} \quad (4.3)$$

Thus, the output of the determined system is indicated in the time domain in Equation (4.4) as follows.

$$y(t) = 6.66(e^{-5t} - e^{-20t}) + 1 \quad (4.4)$$

Thus, using the system identification tool, we have obtained the input and output values that we will define to the tool to find the transfer function that I have determined as an example. In matlab script part, we can define output function, input value and time interval. After opening the system identification tool, we first call the data according to the type of data from the 'import data' section as shown in Figure 4.6.

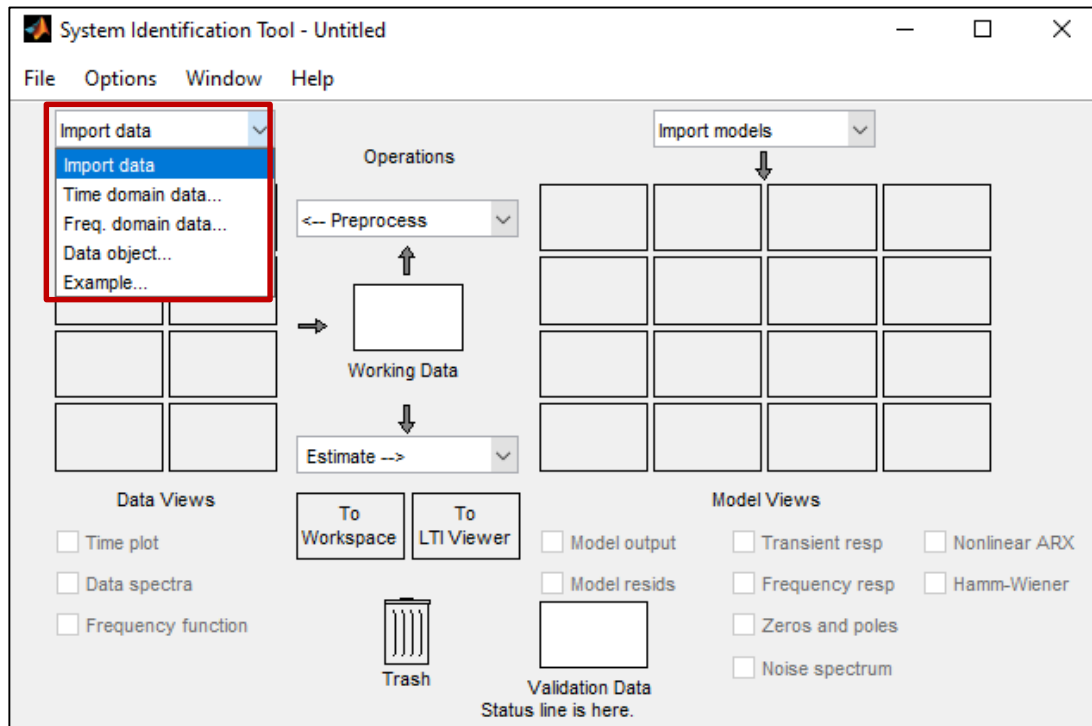


Figure 4.6. System identification tool import data part

After importing the data, we enter the input output values defined in the MATLAB workspace and the starting time and sampling interval while sampling from our

output data on the screen in Figure 4.7. The sampling time is the time between consecutive data samples in your experiment and must be the numerical time interval at which your data is sampled in any units.

The image shows a software window titled "Import D...". It contains the following sections:

- Data Format for Signals:** A dropdown menu currently showing "Time-Domain Signals".
- Workspace Variable:** Two input fields. "Input:" is set to "u" and "Output:" is set to "y".
- Data Information:** Three input fields. "Data name:" is set to "mydata", "Starting time" is set to "0", and "Sampling interval:" is set to "0.01". Below these is a "More" button.
- Buttons:** A grid of four buttons at the bottom: "Import", "Reset", "Close", and "Help".

Figure 4.7. System identification tool data definition

After clicking the import button, the defined input output values come to the data screen in the Figure 4.8. More than one data can be imported from the data screen. The data to be analyzed is dragged to the 'working data' section.

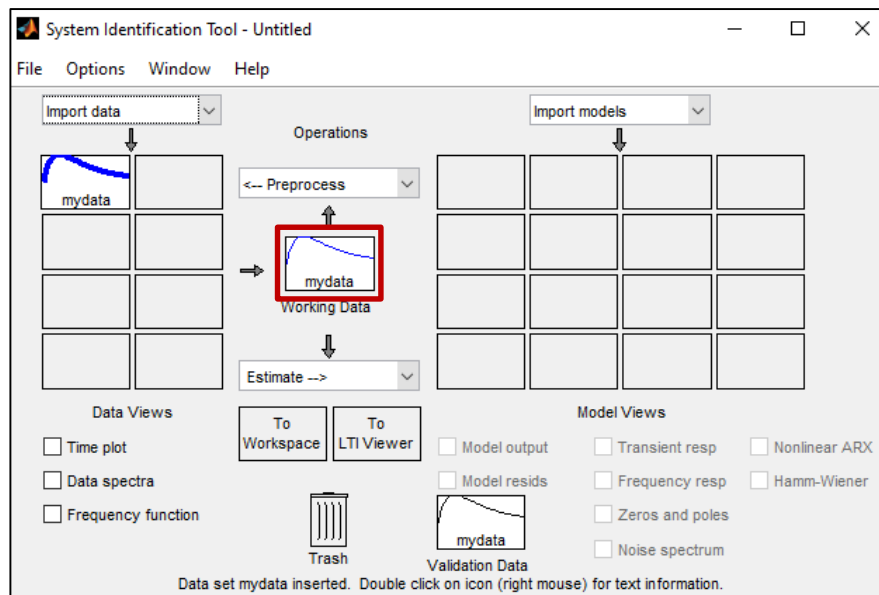


Figure 4.8. System identification tool data views

After dragging the data to the working area, the desired model type is selected from the 'estimate' part shown in Figure 4.9. In the example above, since the system is taken as a transfer function, the transfer function model has been selected here.

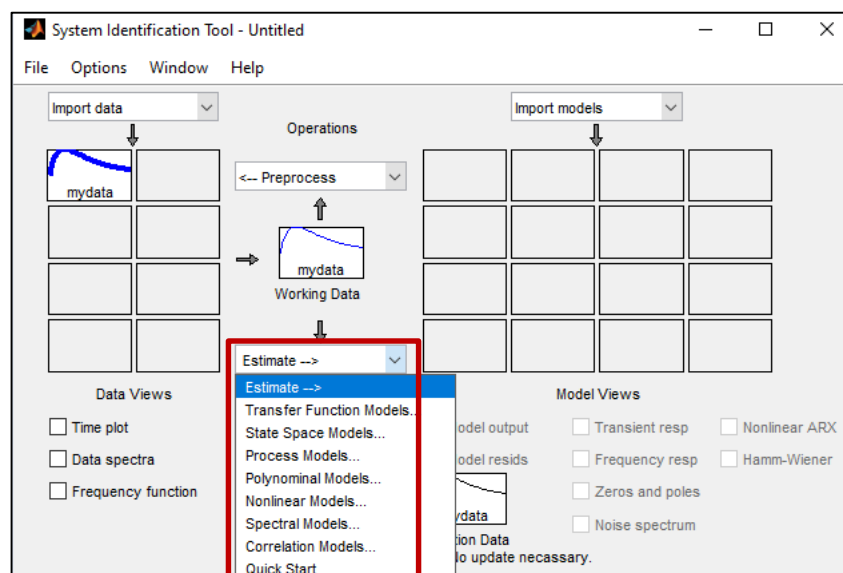


Figure 4.9. System identification tool estimate part

In Figure 4.10, the pole and zero numbers of our system are entered and the 'estimate' button is clicked.

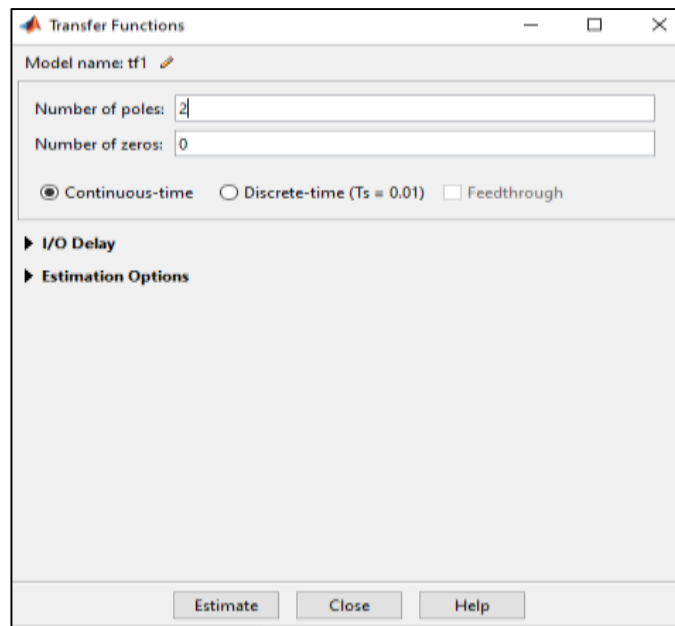


Figure 4.10. System identification tool transfer function definition

In Figure 4.11, The transfer function definition process screen appears and it is seen how successfully the data are estimate.

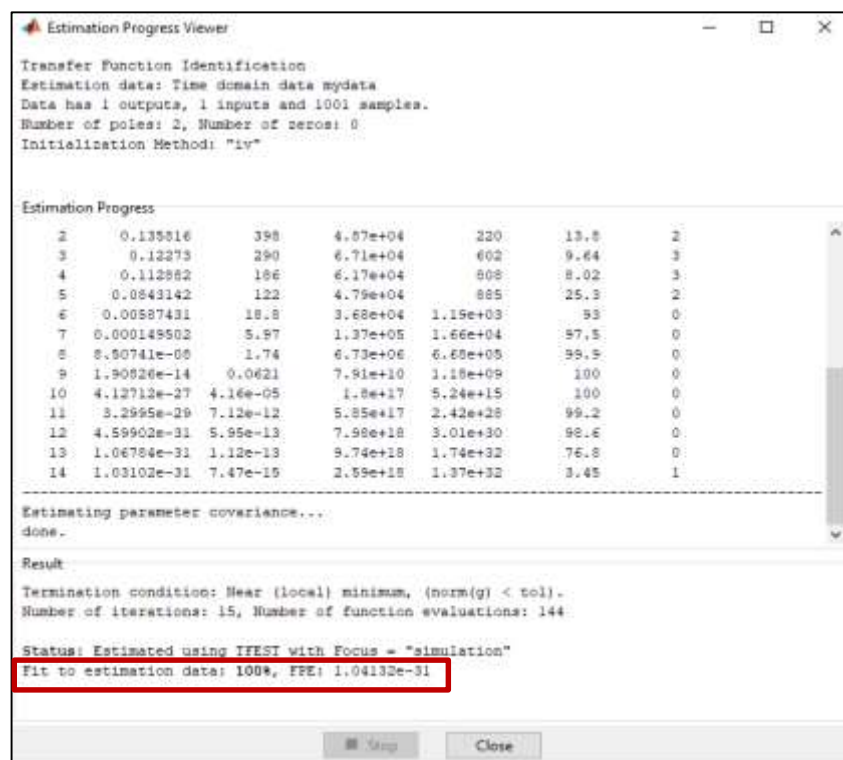


Figure 4.11. System identification tool estimation progress viewer

In Figure 4.12, the model with estimate comes to the 'model views' section and by right clicking, the transfer function, which is estimate, is found as seen in Figure 4.13.

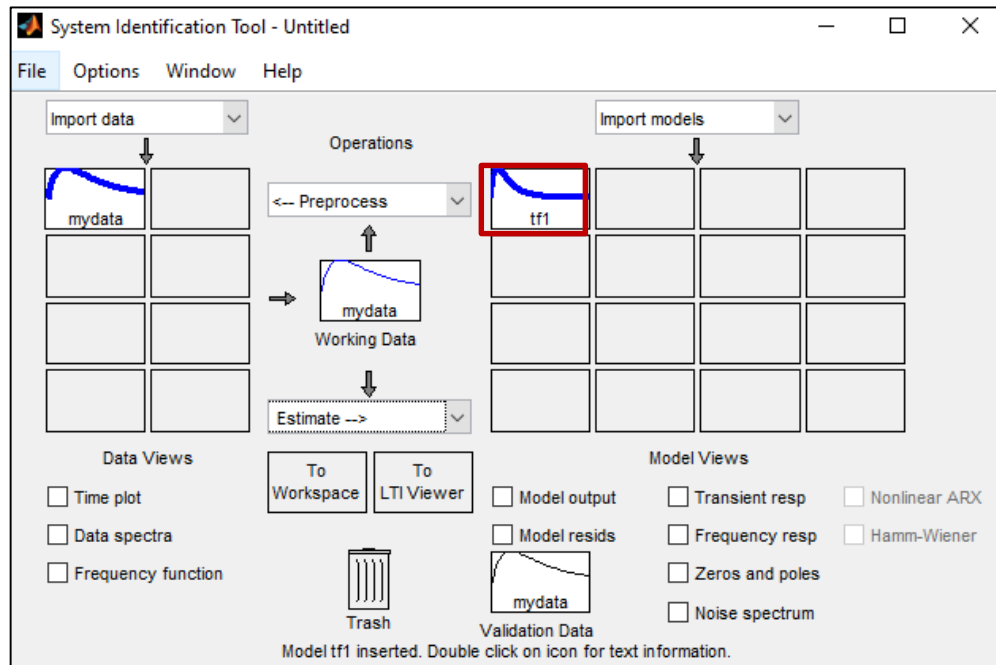


Figure 4.12. System identification tool model views part

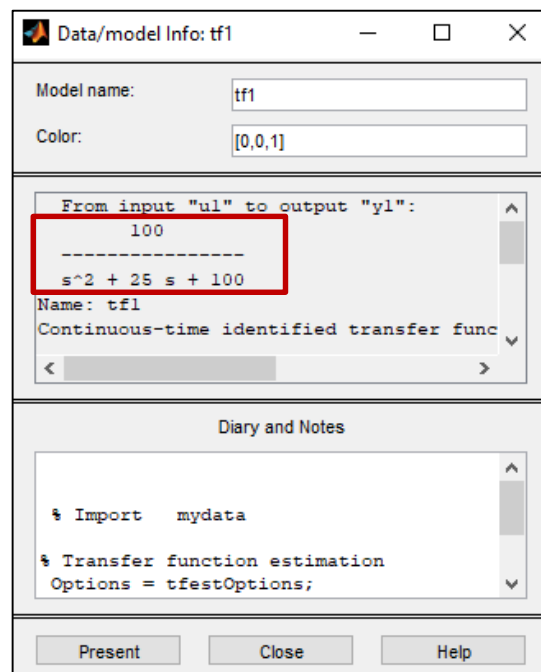


Figure 4.13. Estimation transfer function

4.3.1. Aircraft pitch transfer function estimation via toolbox

In the section above, based on the transfer function of a simple system, it was explained how to obtain the transfer function of the system by using the system identification tool after the input and output values determined. In this context, the use of system identification tool was explained with this example.

In this section, the pitch transfer function as the behavior of the aircraft elevator control surface was obtained using the system definition tool. The pitch transfer function is as follows in Howe lecture notes (Howe, 1980). The transfer function to be examined in (4.5) and the specified input expression in (4.6) are given.

$$\frac{\theta}{\delta_e} = \frac{-26(53.2s^2 + 39.1s + 1)}{55.8s^4 + 112s^3 + 1815s^2 + 48.2s + 1} \quad (4.5)$$

$$u = 0.1sint \quad (4.6)$$

In Figure 4.14 has defined the pole and zero numbers of our model.

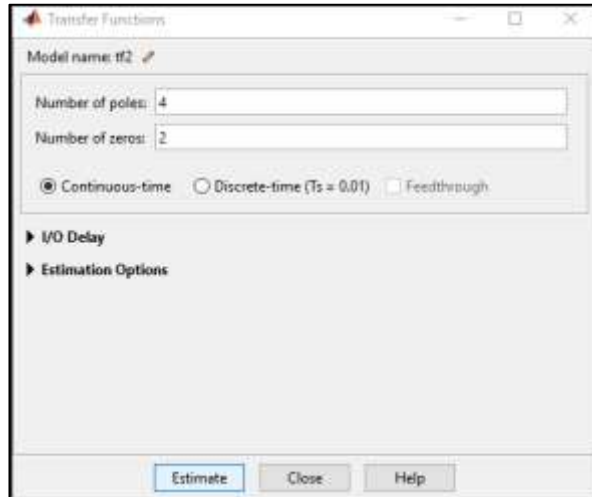


Figure 4.14. System identification tool transfer function definition

As seen in Figure 4.15, the success rate of the estimate result of the examined pitch transfer function using the system definition tool is specified.

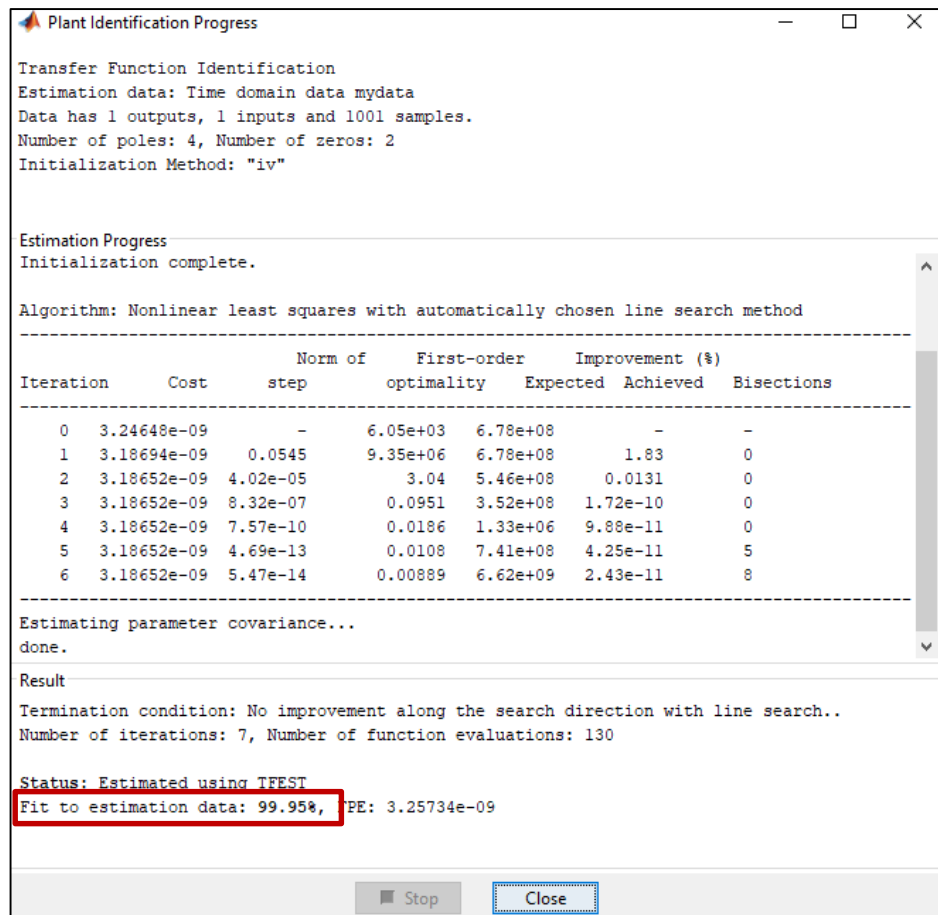


Figure 4.15. System identification tool estimation progress viewer

In Figure 4.16 has seen the behavior of our model after being estimate on the 'model views' screen.

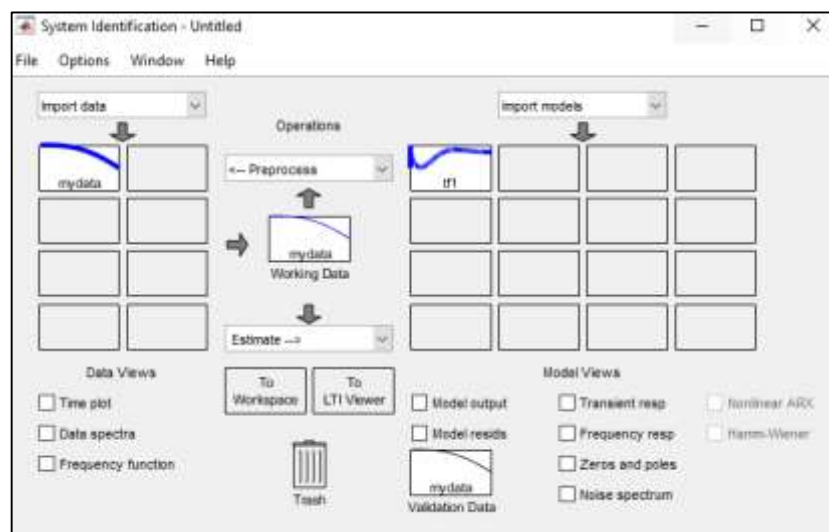


Figure 4.16. System identification tool model views part

Finally, as can be seen in the Figure 4.17, the transfer function that our system estimates with the system identification tool was found.

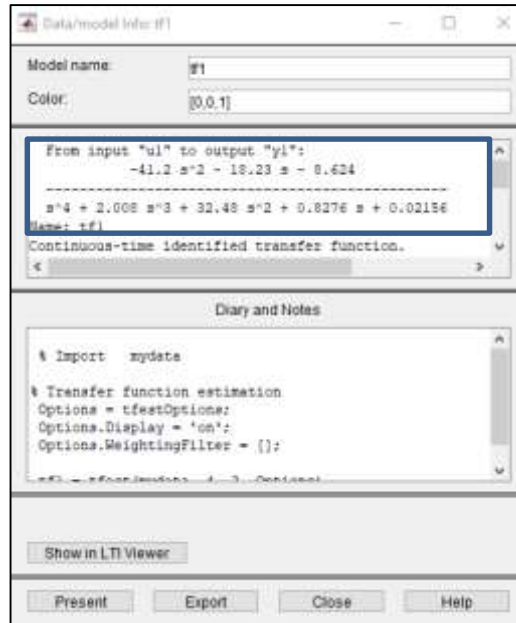


Figure 4.17. System identification tool model views part

4.4. Parameter Estimation

The parameter estimation process is a type of system identification that deals with estimating the values of parameters based on measured empirical data with a random component. When estimating parameters, a basic physical setting is described in such a way that their values affect the distribution of the measured data. Parameter estimation is finding the values of unknown model parameters in a default model structure. For parameter estimation, a model structure to be estimated with unknown parameters (θ), a mathematical model for the measurement process, Observations or measurements (z), assumptions about uncertainty in model parameters and measurement noise are required (v). When y is output as follows Equatio (4.7), the model is linear.

$$y = H\theta \quad (4.7)$$

where the matrix H is assumed to be known. Then the measurement equation can be expressed as in Equation (4.8).

$$z = H\theta + v \quad (4.8)$$

Figure 4.18 shows how the parameter approach is in general. In this figure, data collection, which is the mentality of the parameter estimation, is a system that will be estimate and the process of the most estimation process and the emergence of the model is shown.

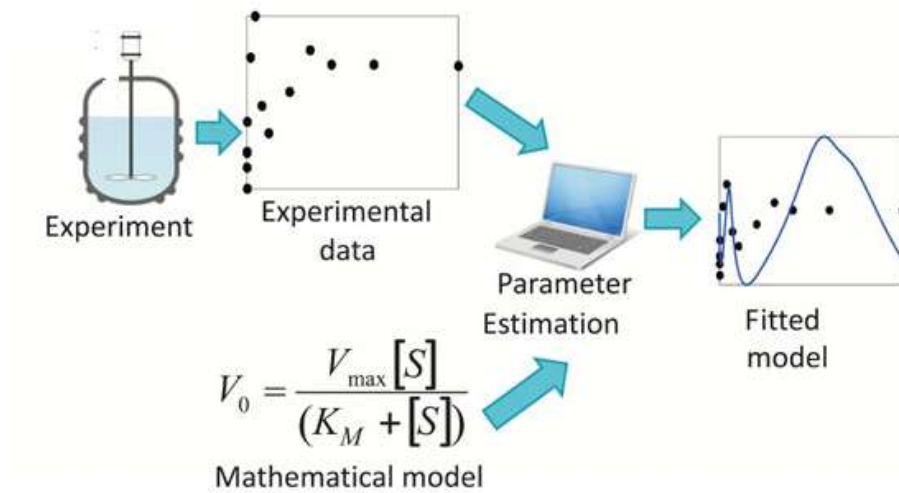


Figure 4.18. Parameter estimation (Remli, et al. 2017)

Below, in the classification created in Figure 4.19, various parameter estimation methods are shown. While this classification was made, more than one method was classified as online and offline. Parameter estimation methods expressed in this way will be explained as the subject progresses.

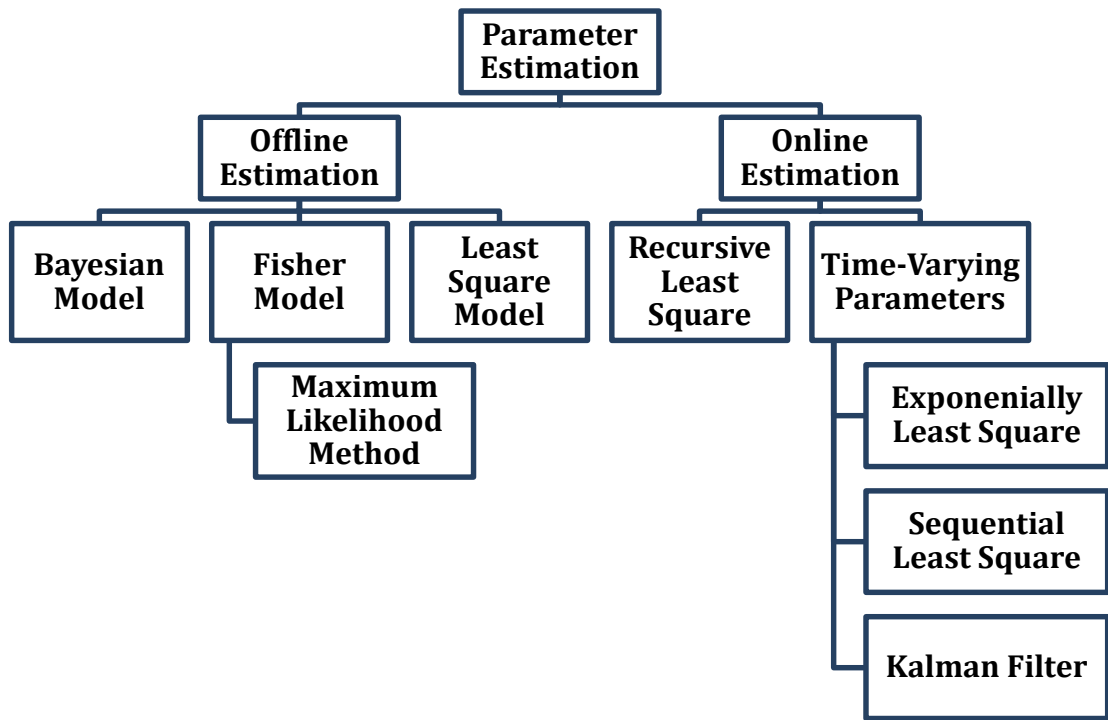


Figure 4.19. Parameter Estimation Methods

4.4.1. Offline estimation

Collect all the input/output data and then estimate the model parameter. In other words, data analysis or offline parameter estimation methods used after the flight.

4.4.1.1. Bayesian model

Bayesian model follows from the Bayesian estimation theory explained. A model where you use the probability to represent all uncertainty in the model, representing both the uncertainty about the output and the uncertainty about the input in the model. θ is a vector of random variables with probability density $p(\theta)$. v is a random vector with probability density $p(v)$. The bayesian model is expressed in Equation (4.9).

$$P(\theta | z) = \frac{p(z | \theta)p(\theta)}{p(z)} \quad (4.9)$$

4.4.1.2. Fisher model

Fisher Model is based on the estimation theory using the concept of a likelihood function. θ is a vector of unknown constant parameters. v is a random vector with probability density $p(v)$.

$$L(z; \theta) = p(z | \theta)$$

Common estimator for the Fisher model is the maximum likelihood (ML) estimator, which is equal to the value of u that maximizes $L(z; u)$ for given z .

4.4.1.2.1. Maximum likelihood method

Our aim in applying the Maximum Likelihood method is to estimate the parameters of the stack to which the data we have belongs. Because it is generally very difficult to know the real value of the parameter of the stack. Here, the Maximum Likelihood Method is just one of many solutions that can be applied to overcome this difficulty. This technique used for estimating the parameters of a given distribution, using some observed data. Maximum Likelihood Method, unlike Bayes model, sees parameters as a fixed point. In other words, the result of the operation is a fixed number.

For example, let us have samples drawn from a certain stack in the form of $Z_N = [z(1)z(2) \dots z(N)]^T$. The maximum likelihood method is expressed in Equation (4.10).

$$\begin{aligned} L[Z_N; \theta] &= L[z(1)z(2) \dots z(N); \theta] \\ &= L[z(N)|Z_{N-1}; \theta]L[Z_{N-1}; \theta] \\ &\quad \cdot \\ &= \prod_{i=1}^N L[z(i)|Z_{i-1}; \theta] \end{aligned} \quad (4.10)$$

4.4.1.3. Least square method

Creating a curve or mathematical function that best fits a set of data points is known as curve fitting. For a given data set, fitting curves of a particular type are generally not unique. The best fit curve with minimum deviations from all data points can be obtained by the least squares method (Molugaram and Rao, 2017). The least squares method is a standard regression method used to write the mathematical connection between two physical quantities that vary depending on each other as an equation that is as realistic as possible. In other words, this method serves to find a function curve that will pass "as close as possible" to the data points obtained from the measurement result. As can be seen in Figure 4.20, if it is desired to express the connection between two axes as a single linear equation, a line must be found to pass as close to these points as possible. The Least Squares Method consists of the coefficients in our linear equation that minimize the sum of the squares of the distances between the points on the line and the scattering points as a result of the approximation.

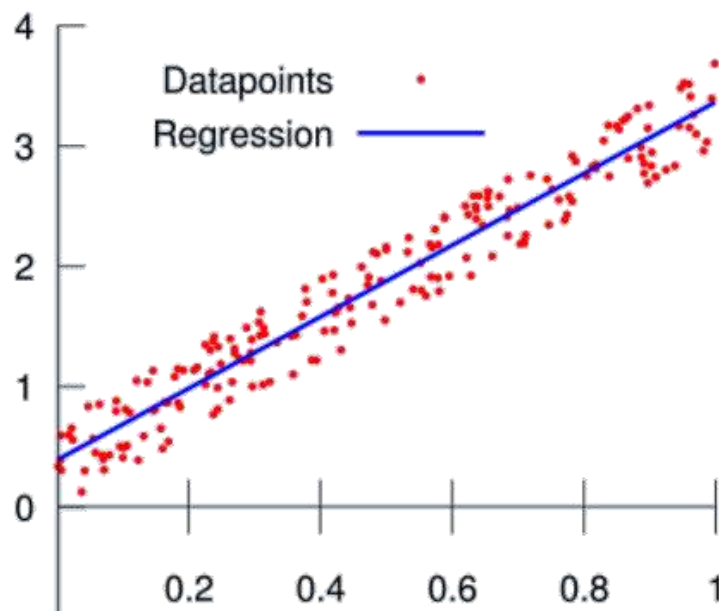


Figure 4.20 Least square estimation

In order to explain the least squares method better in general, it is defined over the sample data points. Assume that the data points are $(x_1, y_1), (x_2, y_2), \dots, (x_n, y_n)$ where x is the independent variable, y is the dependent variable and n is the number of data points. As can be seen in Equation (4.11) below, the error occurring in the result of the curve fitted at each data point is shown.

$$\begin{aligned}
 e_1 &= y_1 - f(x_1), \\
 e_2 &= y_2 - f(x_2), \\
 &\cdot \\
 &\cdot \\
 &\cdot \\
 e_n &= y_n - f(x_n)
 \end{aligned}
 \tag{4.11}$$

According to the definitions above, this error should be minimum, ie it should be $\sum_1^n e_i^2 = \sum_1^n [y_i - f(x_i)]^2$. As can be seen in Figure 4.21, the representation of the general definition is given. that is, values around a curve and estimated values calculated by LS method are explained on the figure.

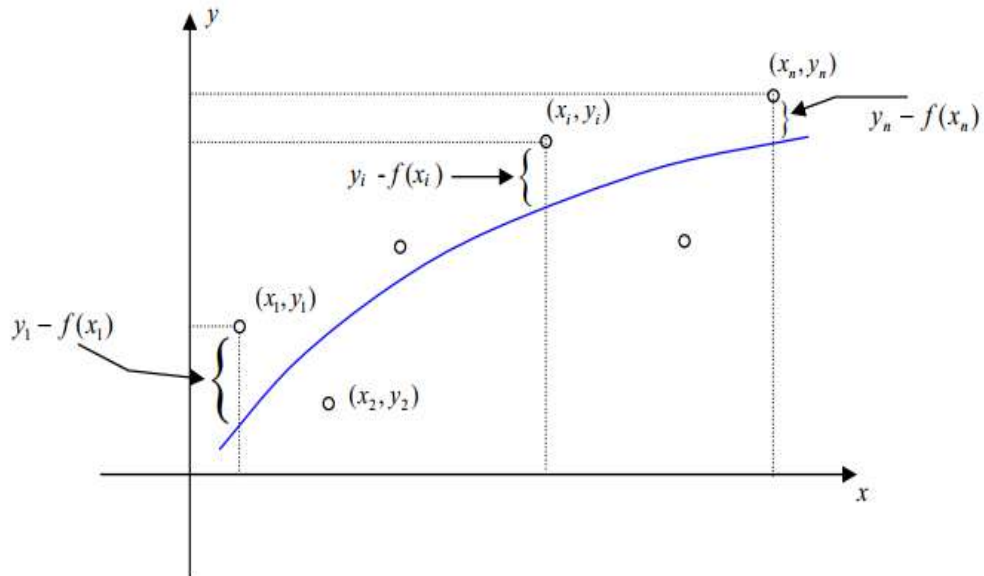


Figure 4.21. Least square method

The general definition of the least squares method has been briefly explained above. Now, the algorithm logic will be expressed in detail and the sense of finding the unknown parameters with which algorithm will be expressed. It will be used to estimate the parameters, which are the coefficients of transfer functions resulting from the behavior of aircraft control surfaces, which are the general rationale of this thesis and will be explained later.

As mentioned, in order to use this method, a system must have an input and output to this system. When performing a design, there is an input-output relation to the plant of that system and an existing transfer function in the plant as shown in Figure 4.22 (Chen and Tomizuka, 2014).

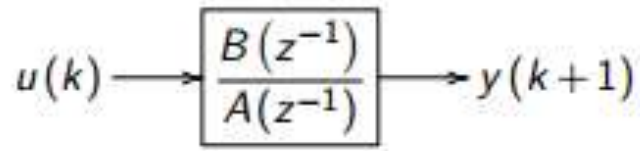


Figure 4.22. Input-output relationship (Chen and Tomizuka, 2014)

The elements of the transfer function given in the plant given in Figure 4.29 are expressed in Equation (4.12). From here, the input-output relationship will be determined and the algorithm of the least square method will be given gradually.

$$B(z^{-1}) = b_0 + b_1 z^{-1} + \dots + b_m z^{-m} \quad (4.12)$$

$$A(z^{-1}) = 1 + a_1 z^{-1} + \dots + a_n z^{-n}$$

After determining the elements of the mathematical function, the input and output elements are determined. $y(k+1)$ is a linear combination of $y(k), \dots, y(k+1-n)$ and $u(k), \dots, u(k-m)$ and is expressed in Equation (4.13).

$$y(k+1) = - \sum_{i=1}^n a_i y(k+1-i) + \sum_{i=0}^m b_i u(k-i) \quad (4.13)$$

After specifying the transfer function in Equation (4.13), the unknown parameter and regressor vector are defined. Regression is a method for modeling the relationship between a scalar response and one or more explanatory variables. $\theta = [a_1, a_2, \dots, a_n, b_0, b_1, \dots, b_m]^T$ and the regressor vector $\phi(k) = [-y(k), \dots, -y(k+1-n), u(k), u(k-1), \dots, u(k-m)]^T$ are the parameter vector that must be defined in the transfer function. The general system model expressing the relationship between the unknown parameter vector and the regressor vector is expressed in Equation (4.14).

$$y(k+1) = \theta^T \phi(k) \quad (4.14)$$

$\phi(k)$ and $y(k+1)$ are measured and known values. The main purpose is to find the unknown parameter vector θ . That is, the θ to be found by estimating here. Estimated version of the parameter vector $\hat{\theta}^T = [\hat{a}_1, \hat{a}_2, \dots, \hat{a}_n, \hat{b}_0, \hat{b}_1, \dots, \hat{b}_m]^T$. At time k is expressed as Equation (4.15), and estimation can be performed.

$$\hat{y}(k+1) = \hat{\theta}^T \phi(k) \quad (4.15)$$

where

$$\hat{\theta}^T = [\hat{a}_1(k), \hat{a}_2(k), \dots, \hat{a}_n(k), \hat{b}_0(k), \hat{b}_1(k), \dots, \hat{b}_m(k)]^T$$

As stated at the beginning of the subject, the error should be minimized as a result of the curve fitting, which is the general purpose. In this context, the error function J_k in Equation (4.4.1.3-6) defined below should be minimized.

$$J_k = \sum_{i=1}^k [y(i) - \hat{\theta}^T(k) \phi(i-1)]^2 \quad (4.16)$$

The solution of equation (4.16) is given in equation (4.17).

$$J_k = \sum_{i=1}^k [y(i)^2 + \hat{\theta}^T(k) \phi(i-1) \phi^T(i-1) \hat{\theta}(k) - 2y(i) \phi^T(i-1) \hat{\theta}(k)]^2 \quad (4.17)$$

Since the error function J_k is desired to be minimum, the partial derivative of the function J_k to the unknown parameter vector must be 0 ($\partial J_k / \partial \theta(k) = 0$). From here, the parameter vector found by applying the least square method is expressed as in Equation (4.18).

While θ is found here, the matrix inversion method has been applied. This matrix inversion method can be applied only when the coefficient matrix is a square matrix and non-singular. Thus, ϕ is square and non-singular matrix. If matrix determinant is equal non-zero, this matrix is non-singular. Since ϕ is non-singular, ϕ^{-1} exists and $\phi^{-1} \phi = \phi \phi^{-1} = I$. Where I is identity matrix ($\phi \theta = y \rightarrow \phi^{-1}(\phi \theta) = \phi^{-1} y \rightarrow \theta = \phi^{-1} y$).

$$\hat{\theta}(k) = F(k) \sum_{i=1}^k \phi(i-1)y(i) \quad (4.18)$$

where

$$F(k) = \left[\sum_{i=1}^k \phi(i-1)\phi^T(i-1) \right]^{-1}$$

As a result, all parameters are obtained using Equation (4.18). Thus, as the advantage of the least square method, derivatives are not taken separately for each parameter. Solve each parameter with the expression in equation (4.18).

4.4.1.3.1. Estimation of aircraft control surfaces behavior via LSM

The definition, algorithm and working sense of the least squares method are explained above. In this section, the parameter estimation will be made about how close the transfer functions formed as a result of the linearized aircraft motion equations previously described in the mathematical modeling section to their original state with the least-squares method. The parameter estimation process will be performed for the transfer functions of all three aircraft control surface behaviors: elevator, aileron and rudder. The original forms of the transfer

functions to be obtained in the estimation process were created according to the flight data in the Howe lecture notes (Howe, 1980).

Before starting to examine the transfer functions explained in the mathematical modeling section, a transfer function representation in general and the representation of unknown parameters, known and measurable data through this transfer function are expressed. In general, system equation in (4.19), system output in (4.20) and the matrix structure of our system in (4.21), unknown parameters $(\alpha, \beta, \gamma, a, b, c, d)$ matrix, output and regressor vector matrix are shown as follows (4.22).

$$\frac{y}{u} = \frac{\alpha s^2 + \beta s + \gamma}{s^4 + as^3 + bs^2 + cs + d} \quad (4.19)$$

$$y^{(4)} = -a\ddot{y} - b\dot{y} - cy - dy + \alpha\ddot{u} + \beta\dot{u} + \gamma u \quad (4.20)$$

$$\begin{bmatrix} \ddot{y}_1 & \ddot{y}_1 & \dot{y}_1 & y_1 & \ddot{u}_1 & \dot{u}_1 & u_1 \\ \ddot{y}_2 & \ddot{y}_2 & \dot{y}_2 & y_2 & \ddot{u}_2 & \dot{u}_2 & u_2 \\ \ddot{y}_3 & \ddot{y}_3 & \dot{y}_3 & y_3 & \ddot{u}_3 & \dot{u}_3 & u_3 \\ . & . & . & . & . & . & . \\ . & . & . & . & . & . & . \\ . & . & . & . & . & . & . \\ . & . & . & . & . & . & . \end{bmatrix} \begin{bmatrix} -a \\ -b \\ -c \\ -d \\ \alpha \\ \beta \\ \gamma \end{bmatrix} = \begin{bmatrix} y^{(4)}_1 \\ y^{(4)}_2 \\ y^{(4)}_2 \\ . \\ . \\ . \\ . \end{bmatrix} \quad (4.21)$$

Therefore,

$$\Phi = \begin{bmatrix} \ddot{y}_1 & \ddot{y}_1 & \dot{y}_1 & y_1 & \ddot{u}_1 & \dot{u}_1 & u_1 \\ \ddot{y}_2 & \ddot{y}_2 & \dot{y}_2 & y_2 & \ddot{u}_2 & \dot{u}_2 & u_2 \\ \ddot{y}_3 & \ddot{y}_3 & \dot{y}_3 & y_3 & \ddot{u}_3 & \dot{u}_3 & u_3 \\ . & . & . & . & . & . & . \\ . & . & . & . & . & . & . \\ . & . & . & . & . & . & . \\ . & . & . & . & . & . & . \end{bmatrix} \theta = \begin{bmatrix} -a \\ -b \\ -c \\ -d \\ \alpha \\ \beta \\ \gamma \end{bmatrix} \quad y = \begin{bmatrix} y^{(4)}_1 \\ y^{(4)}_2 \\ y^{(4)}_2 \\ . \\ . \\ . \\ . \end{bmatrix} \quad (4.22)$$

Thus, it has been shown what kind of mantacite is applied while making future examinations.

In this section, the transfer functions resulting from the behavior of all three control surfaces will be tried to be estimated by the least squares method. While performing the estimation process, the algorithm and model created in the MATLAB/Simulink program will be used. When creating the model, the pitch transfer function obtained in the mathematical modeling section above was also created for the transfer functions, which are the ratio of the bank angle to aileron and rudder displacement. Doublet input is defined for elevator, aileron and rudder displacements which are the inputs of the systems. Doublet inputs are used to denote side pulses (Klein and Morelli, 2006). The graph in Figure 4.23 below can be shown as an example of doublet input.

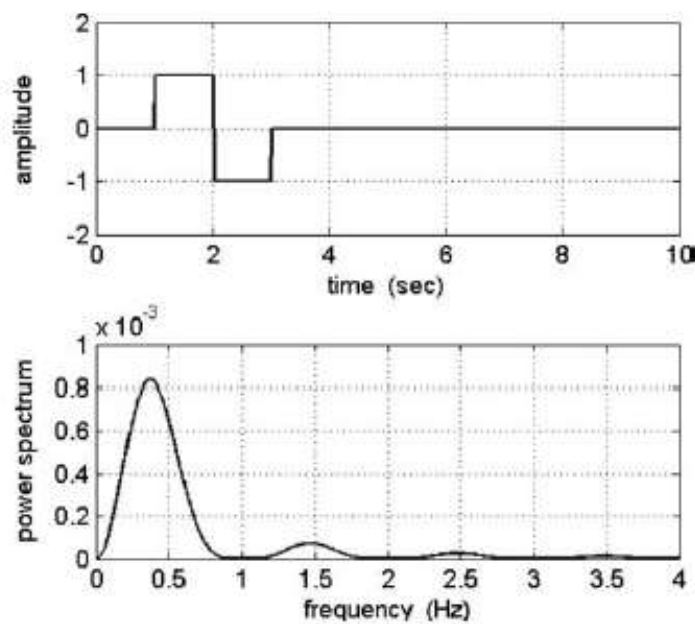


Figure 4.23. Doublet input (Klein and Morelli, 2006)

4.4.1.3.1.1. Elevator control surfaces behavior via LSM

Here, firstly, the transfer function resulting from the behavior of the elevator control surface will be analyzed. This situation, which occurs as a result of the longitudinal motion of an aircraft, has been described before. The pitch transfer function in Equation (3.52) and (3.53) or (3.54) will be estimated by the least squares method. In order to run the algorithm of the least squares method created in the MATLAB/Simulink program, a model was created as shown in Figure 4.24, which also provides the input of the original data.

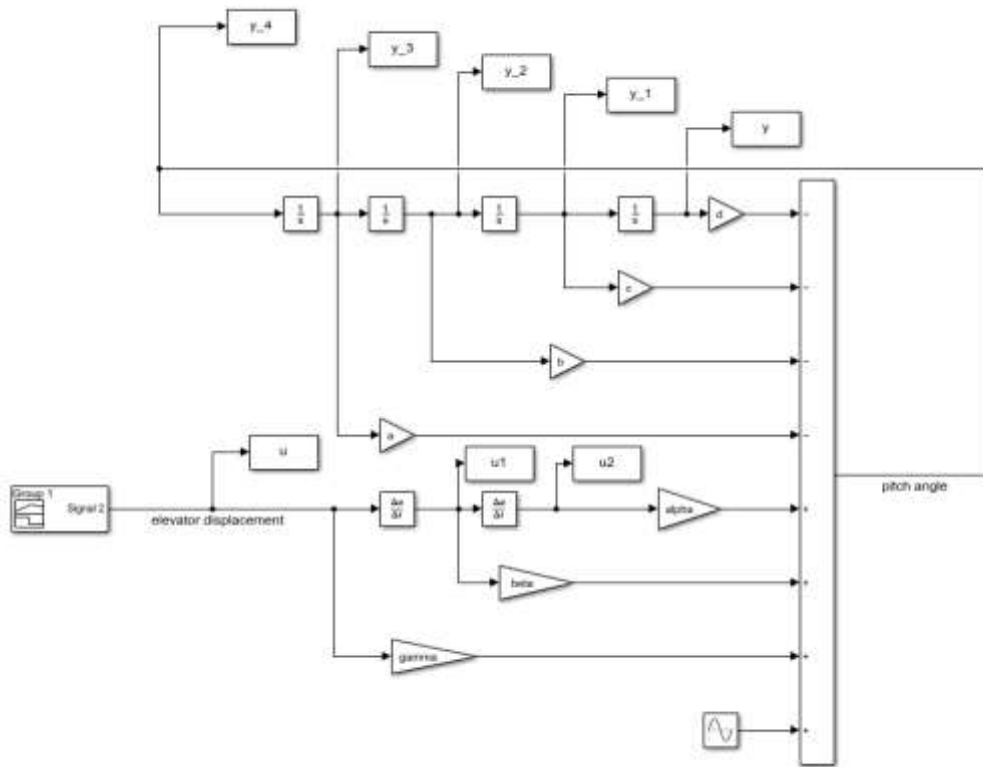


Figure 4.24. MATLAB/Simulink Model for Elevator Control Surface

Below, the pitch transfer function created with the original data is given in Equation (4.23).

$$\left(\frac{\theta}{\delta_e}\right)_{ORJ} = \frac{-24.7885s^2 - 18.2186s - 0.4659}{s^4 + 2.0072s^3 + 32.5269s^2 + 0.8638s + 0.0179} \quad (4.23)$$

When the model in Figure 4.24 and the algorithm created in the MATLAB program are run, the estimated transfer function obtained by the least squares method is obtained in Equation (4.24) below.

$$\left(\frac{\theta}{\delta_e}\right)_{LSM} = \frac{-24.7885s^2 - 18.2191s - 0.4447}{s^4 + 2.0072s^3 + 32.5269s^2 + 0.864s + 0.0186} \quad (4.24)$$

Thus, the pitch transfer function resulting from the longitudinal motion of an aircraft was estimated by the least squares method. The graph in Figure 4.25 was again created in the MATLAB/Simulink program in order to see the graphical comparison of both transfer functions by using the original transfer function and the transfer function estimated by the least squares method.

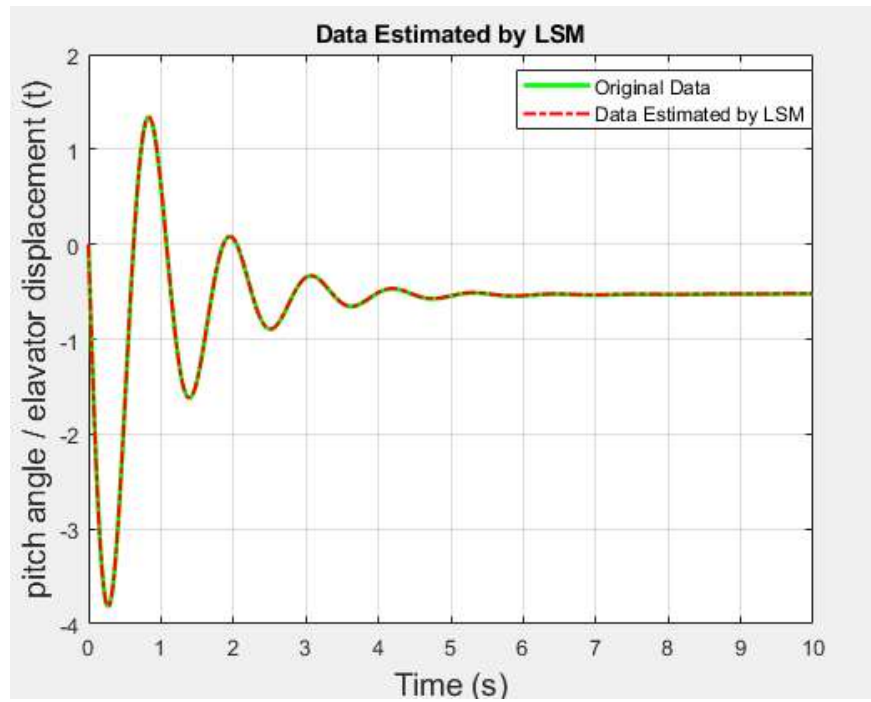


Figure 4.25. Elevator control surface behavior estimated via LSM

With this graph created in the time domain obtained, the approach of the least squares method used with the original form of the transfer function is seen.

4.4.1.3.1.2. Aileron control surfaces behavior via LSM

After examining the transfer function resulting from the longitudinal motion of an aircraft, transfer functions resulting from the lateral motion of an aircraft will be examined. Firstly, the transfer function, which is the ratio of the bank angle resulting from the behavior of the aileron control surface to the aileron displacement, is discussed. Here again, the transfer functions previously found in the mathematical modeling section will be used. Least squares method will be applied using previously found Equation (3.72) and (3.73) or Equation (3.74). In order to run the algorithm of the least squares method created in the MATLAB/Simulink program, a model was created as shown in Figure 4.26, which also provides the input of the original data.

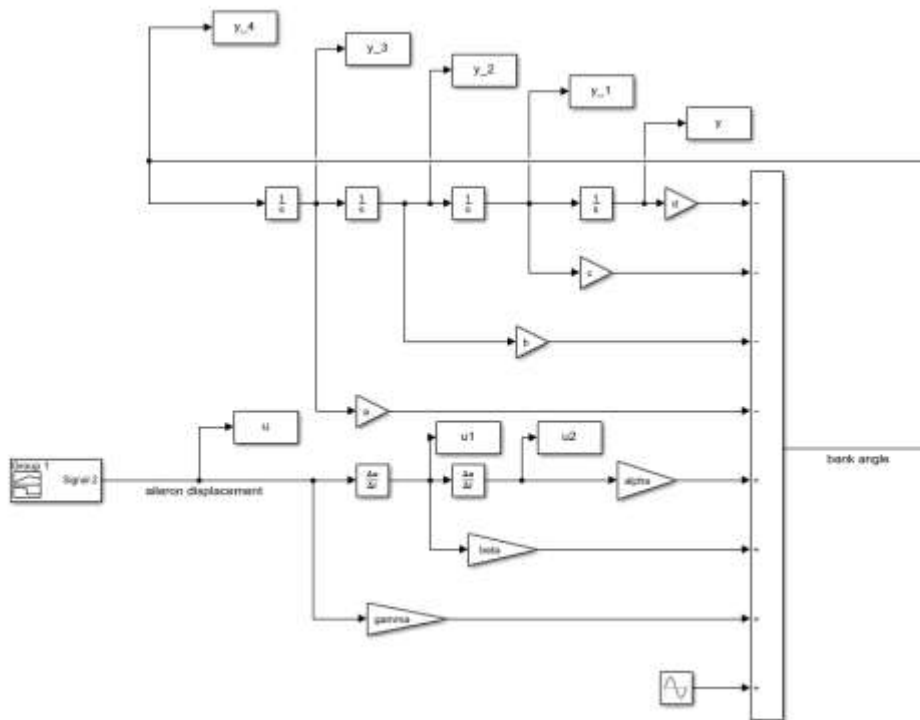


Figure 4.26. MATLAB/Simulink model for aileron control surface

Below is given the transfer function, which is the ratio of the bank angle to aileron displacement, first created with the original data in Equation (4.25).

$$\left(\frac{\phi}{\delta_a}\right)_{ORJ} = \frac{26.8666s^2 + 0.4725s + 94.0527}{s^4 + 1.8683s^3 + 3.6856s^2 + 6.2648s - 0.0085} \quad (4.25)$$

When the model in Figure 4.26 and the algorithm created in the MATLAB program are run, the estimated transfer function obtained by the least squares method is obtained in Equation (4.26) below.

$$\left(\frac{\phi}{\delta_a}\right)_{LSM} = \frac{26.8666s^2 + 0.4721s + 94.0737}{s^4 + 1.8683s^3 + 3.6856s^2 + 6.2649s - 0.0087} \quad (4.26)$$

Thus, the from bank angle to aileron displacement ratio transfer function resulting from the lateral motion of an aircraft was estimated by the least squares method. The graph in Figure 4.27 was again created in the MATLAB/Simulink program in order to see the graphical comparison of both transfer functions by using the original transfer function and the transfer function estimated by the least squares method.

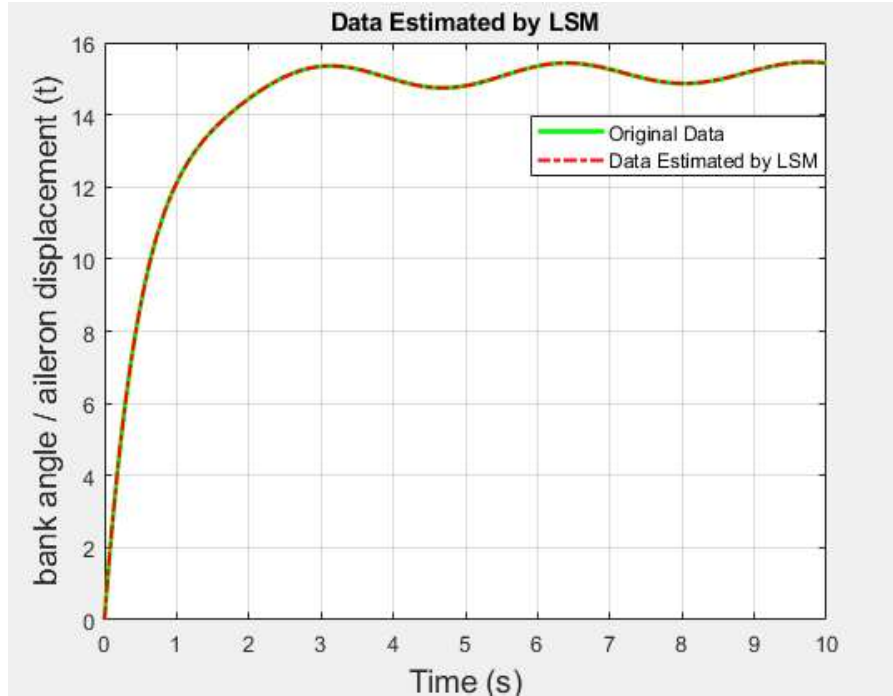


Figure 4.27. Aileron control surface behavior estimated via LSM

With this graph created in the time domain obtained, the approach of the least squares method used with the original form of the transfer function is seen.

4.4.1.3.1.3. Rudder control surfaces behavior via LSM

Again, the transfer function resulting from the behavior of the rudder control surface resulting from the lateral motion of an aviator will be examined. The least squares method was applied by using Equation (3.72) and (3.73) or (3.76) expressions in the mathematical modeling section. In order to run the algorithm of the least squares method created in the MATLAB/Simulink program, a model was created as shown in Figure 4.28, which also provides the input of the original data.

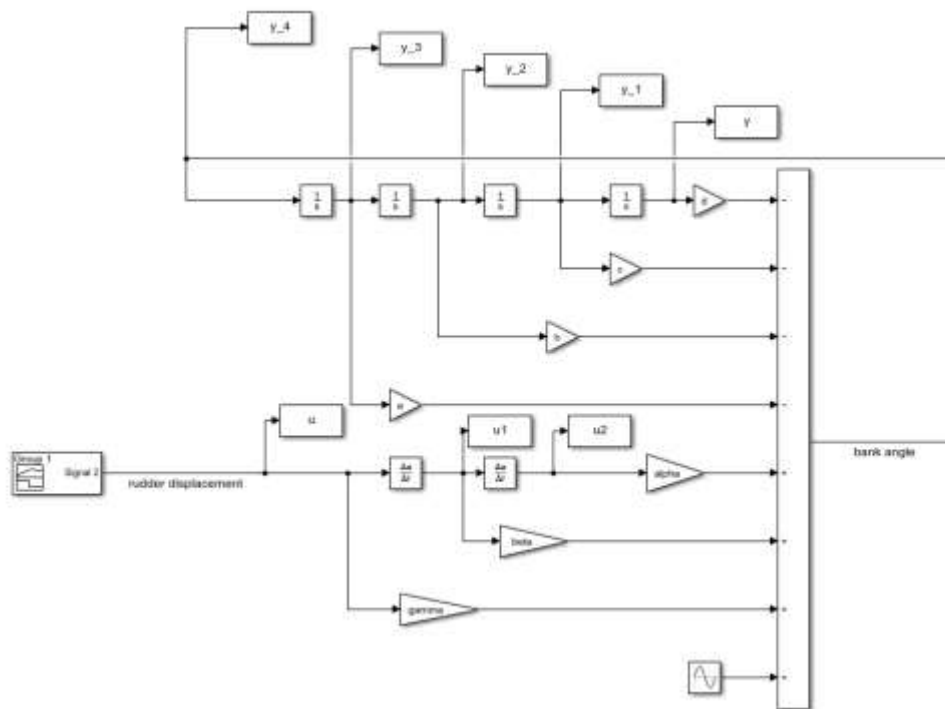


Figure 4.28. MATLAB/Simulink model for rudder control surface

Below is given the transfer function, which is the ratio of the bank angle to aileron displacement, first created with the original data in Equation (4.27).

$$\left(\frac{\phi}{\delta_r}\right)_{ORJ} = \frac{0.5749s^2 - 0.2124s - 4.2481}{s^4 + 1.8683s^3 + 3.6856s^2 + 6.2648s - 0.0085} \quad (4.27)$$

When the model in Figure 4.28 and the algorithm created in the MATLAB program are run, the estimated transfer function obtained by the least squares method is obtained in Equation (4.28) below.

$$\left(\frac{\phi}{\delta_r}\right)_{LSM} = \frac{0.5749s^2 - 0.2128s - 4.2263}{s^4 + 1.8678s^3 + 3.6850s^2 + 6.2636s - 0.0031} \quad (4.28)$$

Thus, the from bank angle to rudder displacement ratio transfer function resulting from the lateral motion of an aircraft was estimated by the least squares method. The graph in Figure 4.29 was again created in the MATLAB/Simulink program in order to see the graphical comparison of both transfer functions by using the original transfer function and the transfer function estimated by the least squares method.

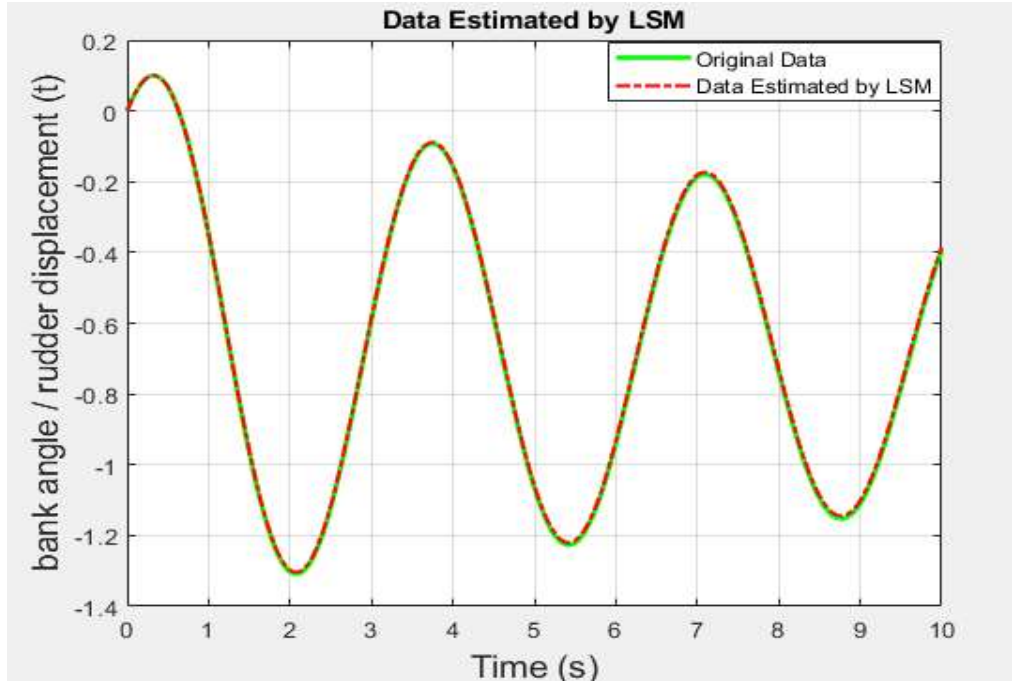


Figure 4.29. Rudder control surface behavior estimated via LSM

With this graph created in the time domain obtained, the approach of the least squares method used with the original form of the transfer function is seen.

4.4.2. Online estimation

Estimate the parameters of a model when new data is available during the operation of the model. Offline parameter estimation techniques were applied after the flight after data collection was completed. These are parameter estimation methods that give intermediate results when new data is received during the flight and during the experiment, that is, during data collection. It enables parameter estimates to be calculated in real time without the need to process the entire data set as additional measurements are added. It is also advantageous in terms of specifying model structure inadequacy and / or identifiability problems through time variations in parameter estimates and error boundaries. It is a stronger type of parameter estimation method in terms of monitoring parameters that change over time (Klein and Morelli, 2006).

4.4.2.1. Recursive least square method

It is an iterative least squares method used as a real time parameter estimation method. It is similar to the least squares method in general logic. It differs from the least squares method in that it is a method that can get results in real time, that is, during the experiment. Because in the least squares method, the process starts after the data is completely collected, and if a new data is received after data collection is completed, the parameter estimation is made from the first data again. However, the part that makes this method advantageous is that when new data arrives, it is not necessary to do all the operations from the beginning, and the last incoming data is processed. The general mentality of the recursive least squares method prevents the rework of old data, making the procedure efficient for real-time processing. Thus, it can be applied more conveniently to aircraft systems with variable dynamics with the recursive least squares method, which is a real time parameter estimation. With this method, the unknown parameters will be estimated, as is done in the least squares method. While doing this, the algorithm, which is similar to the algorithm of the least squares method but has some differences due to its repetition, will be explained. The recursive least squares method makes real-time estimates according to the least squares

method. The data flow can be fast and the data model can change instantaneously due to the dynamic nature of an aircraft system. Therefore, it is more convenient to update the prediction of the previous unknown parameters $\theta(k)$ for the new row of data than to re-analyze all data for each future data. $\theta(k)$ estimation process in Equation (4.18) was specified above with the least squares method. Now, the approach and algorithm of the recursive least squares method will be explained below in case of recursively new data. . While explaining the algorithm of the RLS method, the k index, which is also used in the description of the LS method, is used. k index represents the number of data lines. While describing the LS method, assuming that there are k data lines, the result of the unknown parameters was expressed in Equation (4.18). Now assuming that new measurements are made, that is, when a new data arrives in k rows of data, the function J_k in Equation (4.16) will be updated to $(k + 1)$, $u(k + 1)$ and $y(k + 1)$ and the expression in Equation (4.29) will appear. Thus, in the light of these mentioned situations, how the RLS method will be applied and what kind of an algorithm it has will be explained below.

$$J_{k+1} = \sum_{i=1}^{k+1} [y(i) - \hat{\theta}^T(k+1)\phi(i-1)]^2 \quad (4.29)$$

Thus, the updated version of the parameter matrix in Equation (4.18) found with the LS method above is expressed in Equation (4.30) below.

$$\hat{\theta}(k+1) = F(k+1) \sum_{i=1}^{k+1} \phi(i-1)y(i) \quad (4.30)$$

where

$$F(k+1) = \left[\sum_{i=1}^{k+1} \phi(i-1)\phi^T(i-1) \right]^{-1}$$

From Equation (4.16), the following Equation (4.31).

$$\sum_{i=1}^k \phi(i-1)y(i) = F(k)^{-1} \hat{\theta}(k) \quad (4.31)$$

From Equation (4.30), the following Equation (4.32) is expressed.

$$\sum_{i=1}^{k+1} \phi(i-1)y(i) = \sum_{i=1}^k \phi(i-1)y(i) + \phi(k)y(k+1) \quad (4.32)$$

Equation (4.30) according to the expression in Equation (4.32) is expressed as in Equation (4.33) as follows.

$$\hat{\theta}(k+1) = F(k+1)[F(k)^{-1} \hat{\theta}(k) + \phi(k)y(k+1)] \quad (4.33)$$

The $F(k)$ expression previously explained is stated below to remind you again.

$$F(k) = \left[\sum_{i=1}^k \phi(i-1)\phi^T(i-1) \right]^{-1}$$

$F(k)$ expression contains $F(k)^{-1}$ as seen in Equation (4.34) as below.

$$F(k)^{-1} = \sum_{i=1}^k \phi(i-1)\phi^T(i-1) \quad (4.34)$$

According to the expression found in Equation (4.34), the expression $F(k+1)^{-1}$ is expressed in Equation (4.35) as follows.

$$F(k+1)^{-1} = \sum_{i=1}^{k+1} \phi(i-1)\phi^T(i-1) = F(k)^{-1} + \phi(k)\phi^T(k) \quad (4.35)$$

Thus, $F(k)^{-1}$ expression is found as in Equation (4.36).

$$F(k)^{-1} = F(k + 1)^{-1} - \phi(k)\phi^T(k) \quad (4.36)$$

Thus, Equation (4.33) is updated as follows in Equation (4.37) and (4.38) as a result of the expressions stated above.

$$\hat{\theta}(k + 1) = F(k + 1)[(F(k + 1)^{-1} - \phi(k)\phi^T(k))\hat{\theta}(k) + \phi(k)y(k + 1)] \quad (4.37)$$

$$\hat{\theta}(k + 1) = \hat{\theta}(k) + F(k + 1)\phi(k)[y(k + 1) - \hat{\theta}^T(k)\phi(k)] \quad (4.38)$$

Therefore, $\hat{\theta}(k + 1) = \hat{\theta}(k) + [\text{correction term}]$, the expressions in correction terms are gain and error. Where $\text{gain} = F(k + 1)\phi(k)$ and $\text{error} = y(k + 1) - \hat{\theta}^T(k)\phi(k)$. Then Express Equation (4.39) from equation (4.36) to express $F(k + 1)$ iteratively.

$$F(k + 1) = [F(k)^{-1}\phi(k)\phi^T(k)]^{-1} \quad (4.39)$$

Then Equation (4.40) is then expressed using the Matrix Inversion Lemma rule for Equation (4.39).

$$F(k + 1) = F(k) - F(k)\phi(k)[\phi^T(k)F(k)\phi(k) + I]^{-1}\phi^T(k)F(k) \quad (4.40)$$

Thus $F(k + 1)$ can be expressed in the form in Equation (4.41) as follows.

$$F(k + 1) = F(k) - \frac{F(k)\phi(k)\phi^T(k)F(k)}{1 + \phi^T(k)F(k)\phi(k)} \quad (4.41)$$

Finally, Equation (4.38) is updated like $\hat{\theta}(k + 1)$ in Equation (4.42).

$$\hat{\theta}(k + 1) = \hat{\theta}(k) + \left[\frac{F(k)\phi(k)\phi^T(k)F(k)}{1 + \phi^T(k)F(k)\phi(k)}\right]\phi(k)[y(k + 1) - \hat{\theta}^T(k)\phi(k)] \quad (4.42)$$

Thus, the unknown parameters were found by applying the algorithm logic of the RLS method. With this method, as explained above, the method and logic applied according to the new line of data are expressed.

After the expression of the parameter matrix is found, the Matrix Inversion Lemma method used when passing from Equation (4.39) to Equation (4.40) expression is also expressed below.

Matrix Inversion Lemma: if A is nonsingular, B and C have compatible dimensions, then

$$(A + BC)^{-1} = A^{-1} - A^{-1}B(CA^{-1}B + I)^{-1}CA^{-1}$$

4.4.2.1.1. Estimation of Aircraft Control Surfaces Behavior via RLSM

Previously, the estimation of transfer functions resulting from the behavior of aircraft control surfaces was carried out using the least squares method. In this section, transfer functions arising from the behavior of aircraft control surfaces will be analyzed using the recursive least squares method, and a comparison with the original data and graphical results will be presented. In this context, as in the LS method, examinations were carried out in all three control surfaces in this method. Here again, the original forms of the transfer functions to be obtained in the estimation process were created according to the flight data in the Howe lecture notes (Howe, 1980).

4.4.2.1.1.1. Elevator control surfaces behavior via RLSM

First, we started with the transfer function, which again results from the behavior of the elevator control surface. The formation process of the transfer function is expressed in the mathematical modeling part, as it is also mentioned in the LS method. This situation, which occurs as a result of the longitudinal motion of an aircraft, has been described before. The pitch transfer function in Equation (3.52) and (3.53) or (3.54) will be estimated by the least squares method. In order to run the algorithm of the least squares method created in the MATLAB/Simulink program, a model was created as shown in Figure 4.30, which also provides the input of the original data.

graphical comparison of both transfer functions using the original transfer function and the transfer function estimated by the recursive least squares method.

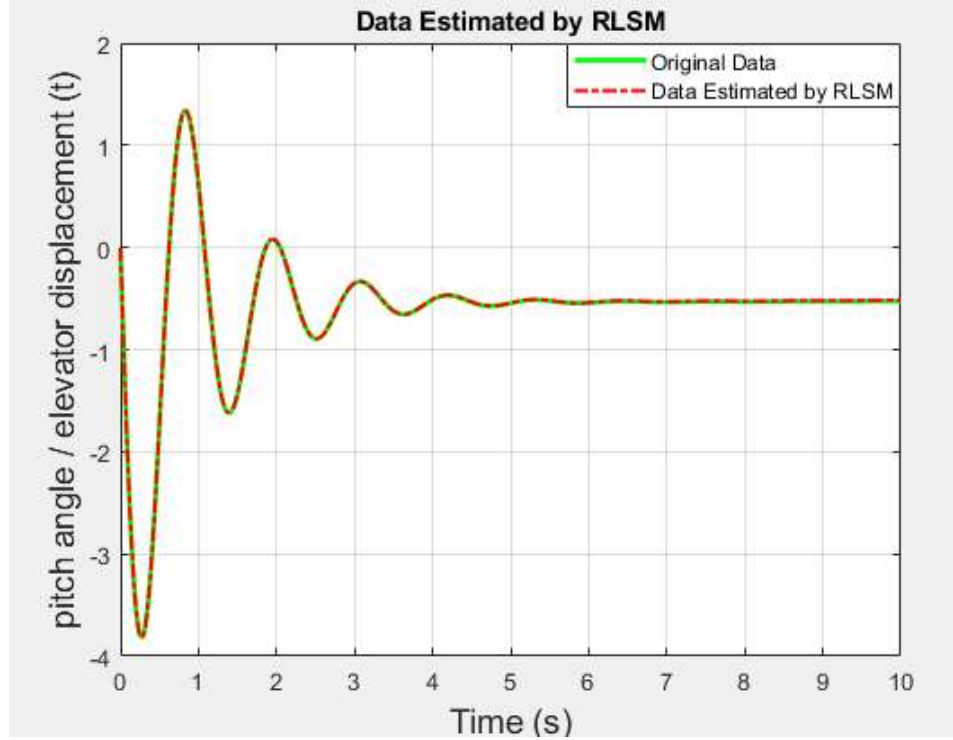


Figure 4.31. Elevator control surface behavior estimated via RLSM

With this graph created in the time domain obtained, the approach of the recursive least squares method used with the original form of the transfer function is seen.

4.4.2.1.1.2. Aileron control surfaces behavior via RLSM

After the transfer function estimation due to the longitudinal motion of an aircraft is performed, the estimation of the transfer functions resulting from the lateral motion of an aircraft will also be performed. First, the transfer function, which is the ratio of the angle of bank resulting from the behavior of the blade control surface to the blade displacement, is investigated. Here again, the transfer functions previously found in the mathematical modeling section will be used. Recursive Least Squares Method will be applied using the previously found Equations (3.72) and (3.37) or Equation (3.74). In order to run the algorithm of

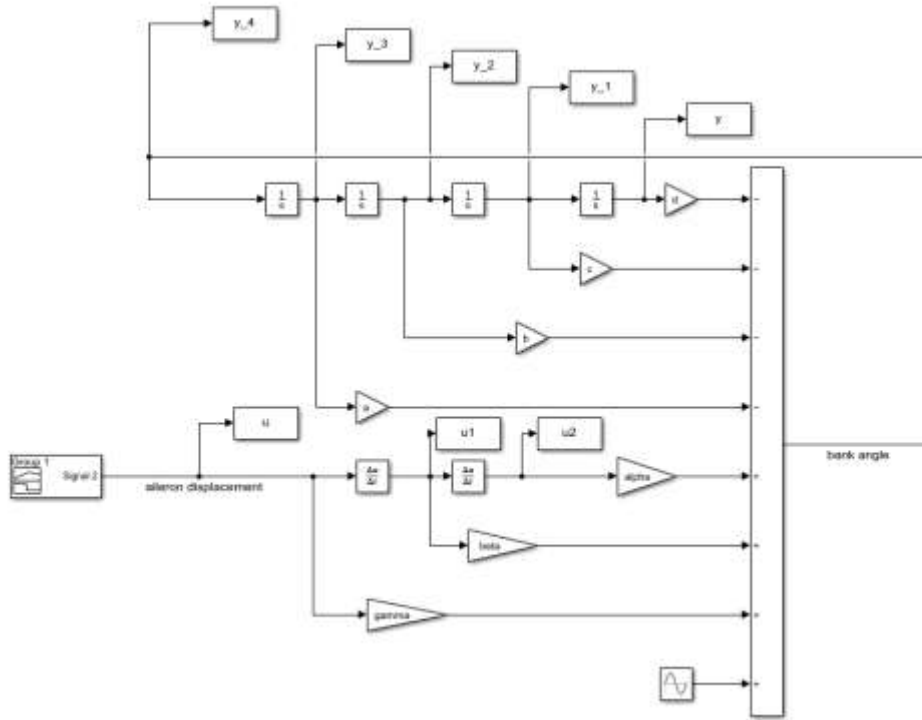


Figure 4.32. MATLAB/Simulink model for aileron control surface

Below is given the transfer function, which is the ratio of the bank angle to aileron

$$\left(\frac{\phi}{\delta_a}\right)_{ORI} = \frac{26.8666s^2 + 0.4725s + 94.0527}{s^4 + 1.8683s^3 + 3.6856 + 6.2648s - 0.0085} \quad (4.45)$$

When the model in Figure 4.32 and the algorithm created in the MATLAB

$$\left(\frac{\phi}{\delta_a}\right)_{RLSM} = \frac{26.8666s^2 + 0.4722s + 94.0603}{s^4 + 1.8683s^3 + 3.6856 + 6.2648s - 0.0085} \quad (4.46)$$

Thus, the from bank angle to aileron displacement ratio transfer function resulting from the lateral motion of an aircraft was estimated by the recursive least squares method. The graph in Figure 4.33 was again created in the MATLAB/Simulink program in order to see the graphical comparison of both transfer functions by using the original transfer function and the transfer function estimated by the recursive least squares method.

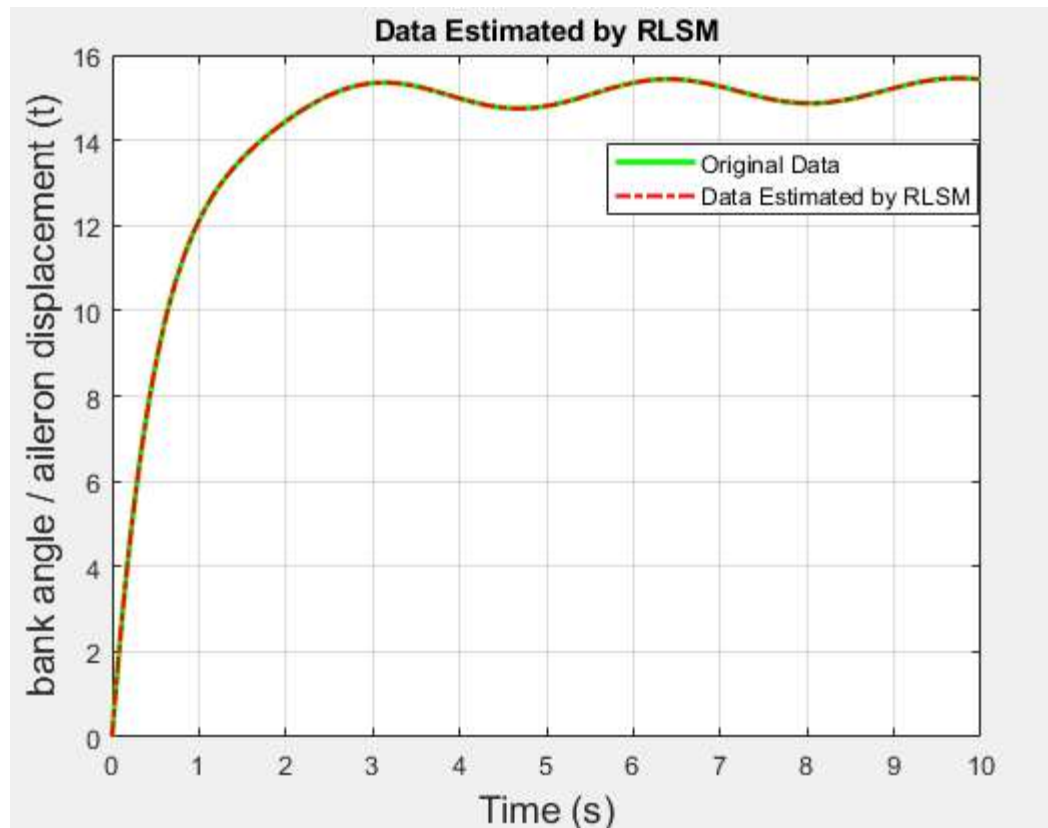


Figure 4.33. Aileron control surface behavior estimated via RLSM

With this graph created in the time domain obtained, the approach of the recursive least squares method used with the original form of the transfer function is seen.

4.4.2.1.1.3. Rudder control surfaces behavior via RLSM

Again, the transfer function resulting from the behavior of the rudder control surface resulting from the lateral motion of an aviator will be examined. The recursive least squares method was applied by using Equation (3.72) and (3.73)

or (3.76) expressions in the mathematical modeling section. In order to run the algorithm of the recursive least squares method created in the MATLAB/Simulink program, a model was created as shown in Figure 4.34, which also provides the input of the original data.

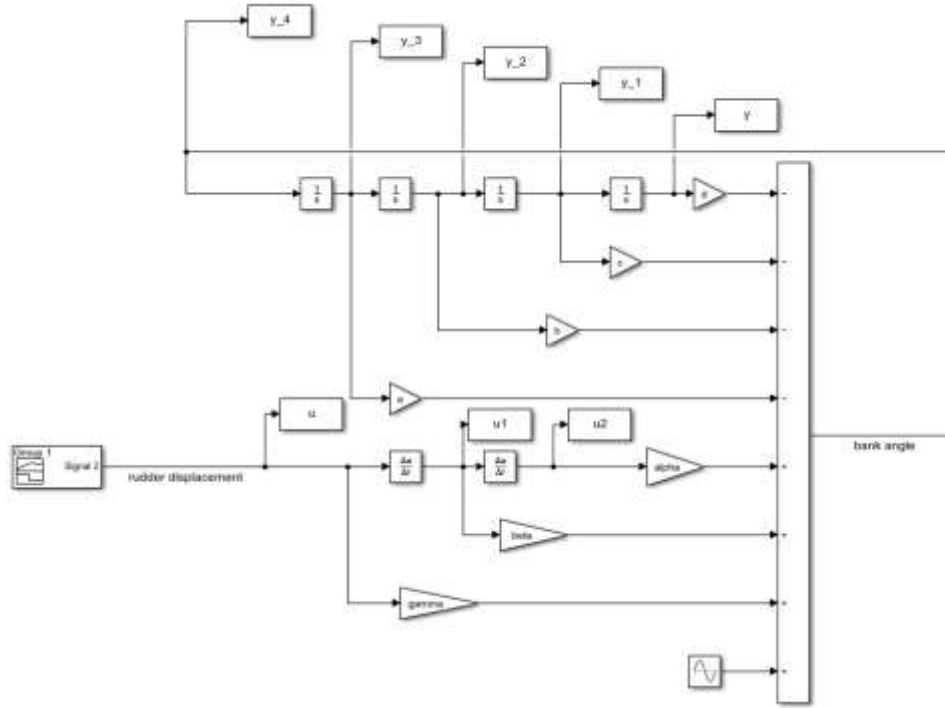


Figure 4.34. MATLAB/Simulink model for rudder control surface

Below is given the transfer function, which is the ratio of the bank angle to aileron displacement, first created with the original data in Equation (4.47).

$$\left(\frac{\phi}{\delta_r}\right)_{ORJ} = \frac{0.5749s^2 - 0.2124s - 4.2481}{s^4 + 1.8683s^3 + 3.6856s^2 + 6.2648s - 0.0085} \quad (4.47)$$

When the model in Figure 4.34 and the algorithm created in the MATLAB program are run, the estimated transfer function obtained by the least squares method is obtained in Equation (4.48) below.

$$\left(\frac{\phi}{\delta_r}\right)_{RLSM} = \frac{0.5749s^2 - 0.1868s - 4.2416}{s^4 + 1.868s^3 + 3.6859s^2 + 6.2648s - 0.0082} \quad (4.48)$$

Thus, the from bank angle to rudder displacement ratio transfer function resulting from the lateral motion of an aircraft was estimated by the recursive least squares method. The graph in Figure 4.34 was again created in the MATLAB/Simulink program in order to see the graphical comparison of both transfer functions by using the original transfer function and the transfer function estimated by the recursive least squares method.

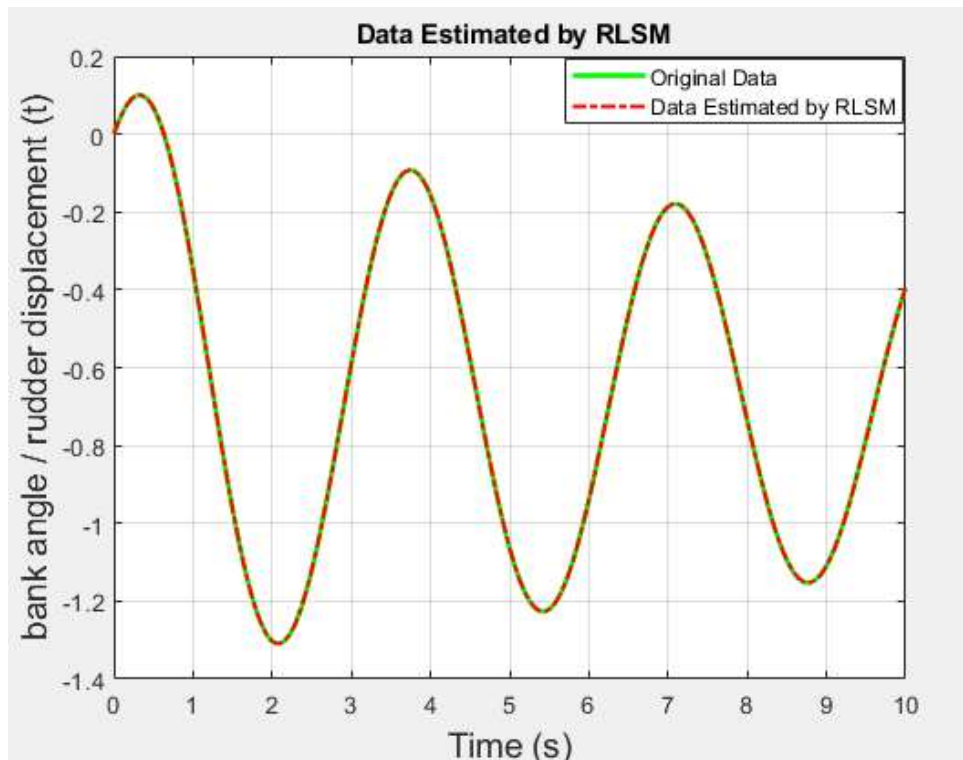


Figure 4.35. Rudder control surface behavior estimated via RLSM

With this graph created in the time domain obtained, the approach of the recursive least squares method used with the original form of the transfer function is seen.

Thus, the transfer functions resulting from the behavior of all three control surfaces were estimated by using the recursive least squares method as well as the least squares method.

4.4.2.2. Time-varying parameter

Other online parameter estimation methods are time varying parameter estimation methods. they are applied when the parameters change over time. ie the parameters are not fixed, they are used when the model parameters change over time. To express these methods, a few changes have been made in the algorithm of the recursive least square method, which is the online parameter estimation method described earlier. These methods are briefly discussed below.

4.4.2.2.1. Exponentially Weighted Least Squares

In this method, the model parameters do not remain constant but gradually change according to a determined weight over time. The general function of this method is expressed as follows in (4.49).

$$J(\theta) = 0.5 \sum_{i=k-m}^k \lambda^{k-i} [z(i) - x^T(i)\theta]^2 \quad (4.49)$$

Where m refers to the number of past values weighted with the tops of the λ value in the data set. The aim is to minimize this function. The algorithm to be created minimizes the result of the function, which is our goal. The algorithm of this method is expressed by developing the algorithm of the recursive least square method described in (4.50) to (4.52).

$$\hat{\theta}_{k+1} = \hat{\theta}_k K_{k+1} [z_{k+1} - X_{k+1}^T \hat{\theta}_k] \quad (4.50)$$

$$K_{k+1} = P_k x_{k+1} (\lambda + 1 + x_{k+1}^T P_k x_{k+1})^{-1} \quad (4.51)$$

$$P_{k+1} = \frac{1}{\lambda} [P_k - P_k x_{k+1} (\lambda + x_{k+1}^T P_k x_{k+1})^{-1} x_{k+1}^T P_k] \quad (4.52)$$

Therefore $\hat{\theta}_{k+1}$, K_{k+1} and P_{k+1} expressions are updated.

4.4.2.2. Kalman filter

In a dynamic system represented by the state space model, it is the filter that can predict the state of the system from the input and output information together with the previous information of the model. Although it is named as a filter; an algorithm that predicts the next state of the system based on previous states. It also allows you to estimate as close to reality as possible from noisy and imprecise data. In Figure 4.36 shows the working mechanism of the kalman filter. In general the algorithm of Kalman filter (4.53) to (4.68) is described.

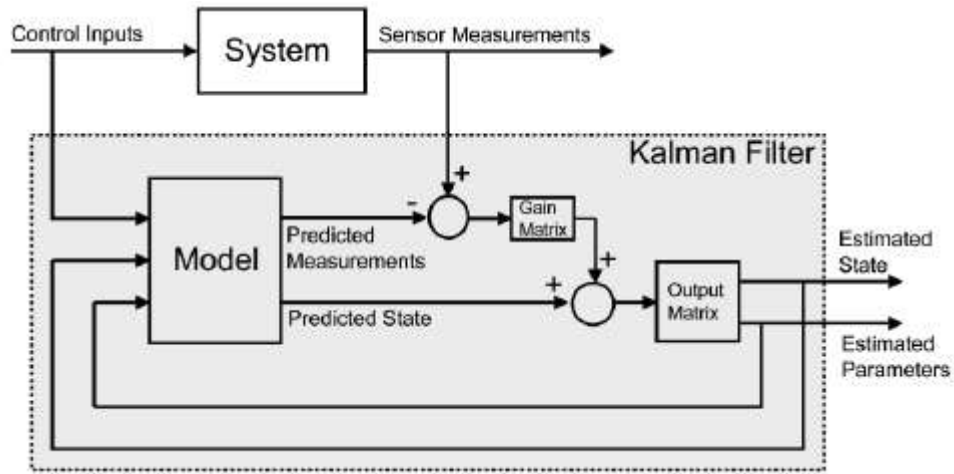


Figure 4.36 Kalman filter (Charles, et al. 2008)

Kalman filters are used to predict states based on dynamical systems in the form of state spaces. The process model defines the progress of the state from time $k - 1$ to time k as:

$$\theta_k = \Phi_{k-1}\theta_{k-1} + w_{k-1} \quad (4.53)$$

where Φ_{k-1} state transition matrix applied to vector θ_{k-1} , w_{k-1} is the noise vector and E denotes expected value. The relationship between k states and measurements in the current time step is matched with the measurement model described as:

$$z_k = x_k^T \theta_k + v_k \quad (4.54)$$

where z_k is the measurement vector, X is the measurement matrix, and v_k is the measurement noise vector.

$$E[w_k w_k^T] = Q_k \delta_{kl}$$

$$E[v_k v_k^T] = \sigma^2 \delta_{kl} \quad (4.55)$$

$$\hat{\theta}_{k \setminus k-1} = \Phi_{k-1} \hat{\theta}_{(k-1) \setminus k-1} \quad (4.56)$$

$$P_{k \setminus k-1} = \Phi_{k-1} P_{(k-1) \setminus k-1} \Phi_{k-1}^T + Q_{k-1} \quad (4.57)$$

$$\hat{\theta}_{k \setminus k} = \hat{\theta}_{(k \setminus k-1)} + K_k [z_k - x_k^T \hat{\theta}_{k \setminus k-1}] \quad (4.58)$$

$$P_{k \setminus k} = [I - K_k x_k^T] P_{k \setminus k-1} \quad (4.59)$$

$$K_k = P_{k \setminus k-1} x_k [x_k^T P_{k \setminus k-1} x_k + \sigma^2_k]^{-1} \quad (4.60)$$

Where P state covariance matrix, state vector of the kalman filter in this case is the parameter vector θ , Q noise covariance matrix and σ^2 noise covariance are constant. $\Phi_k = I$ is implemented to simplify the algorithm.

$$\hat{\theta}_k = \hat{\theta}_{k-1} + w_{k-1} \quad (4.61)$$

Thus, Kalman filter equations are expressed as follows.

$$\hat{\theta}_{(k \setminus k-1)} = \hat{\theta}_{(k-1) \setminus k-1} = \hat{\theta}_{k-1} \quad (4.62)$$

$$P_{k \setminus k-1} = P_{(k-1) \setminus k-1} + Q \quad (4.63)$$

$$\hat{\theta}_k = \hat{\theta}_{k-1} + K_k [z_k - x_k^T \hat{\theta}_{k-1}] \quad (4.64)$$

$$P_{k \setminus k} = [I - K_k x_k^T] P_{k \setminus k-1} \quad (4.65)$$

$$K_k = P_{k \setminus k-1} x_k [x_k^T P_{k \setminus k-1} x_k + \sigma_k^2]^{-1} \quad (4.66)$$

If $w_k = 0$ and $Q = 0$, state model is

$$\theta_k = \theta_{k-1} \quad (4.67)$$

$$P_{k \setminus k-1} = P_{k-1 \setminus k-1} = P_{k-1} \quad (4.68)$$

4.4.2.2.3. Sequential least square

The least square solution applied the function in Equation (4.49) the result is as follows in (4.69) to (4.74).

$$\hat{\theta}_k = [M_{k_\lambda}]^{-1} S_{k_\lambda} \quad (4.69)$$

$$\text{Cov}[\hat{\theta}_k] = \sigma^2 [M_{k_\lambda}]^{-1} \quad (4.70)$$

$$M_{k_\lambda} = \sum_{i=k-m}^k \lambda^{k-i} x_i x_i^T \quad (4.71)$$

$$S_{k_\lambda} = \sum_{i=k-m}^k \lambda^{k-i} x_i z_i \quad (4.72)$$

M_{k_λ} and S_{k_λ} are updated recursively and expressed as follows.

$$M_{k_\lambda} = \lambda M_{(k-1)_\lambda} + x_k x_k^T \quad (4.73)$$

$$S_{k_\lambda} = \lambda S_{(k-1)_\lambda} + x_k z_k \quad (4.74)$$

4.4.3. Comparison of parameter estimation via RLSM and LSM

The parameter estimation methods used for parameter estimation, offline and online, and the general mentality of the use of estimation operations with these methods have been expressed in the above sections. Two methods frequently

used in these, namely RLS and LS methods, were emphasized and samples were carried out within the framework of estimation of transfer functions resulting from the behavior of an aircraft control surfaces with both methods. Once again, offline methods were non-real-time methods. In other words, they are the methods used after data analysis is completed after the flight is completed. Online methods, on the other hand, are methods that are used in real time and can be used for any new data that may come during flight. In this section, the online parameter estimation method RLS was compared with the offline parameter estimation method LS in parallel with the above. While comparing these two methods, graphically overlapping outputs were drawn in MATLAB/Simulink program and analyzed.

Firstly, the comparison process was started with the pitch transfer function generated as a result of the behavior of the elevator control surface. This transfer function has previously been done with both methods. Now, in order to see the accuracy of the methods with each other, the overlapping process in Figure 4.37 has been performed.

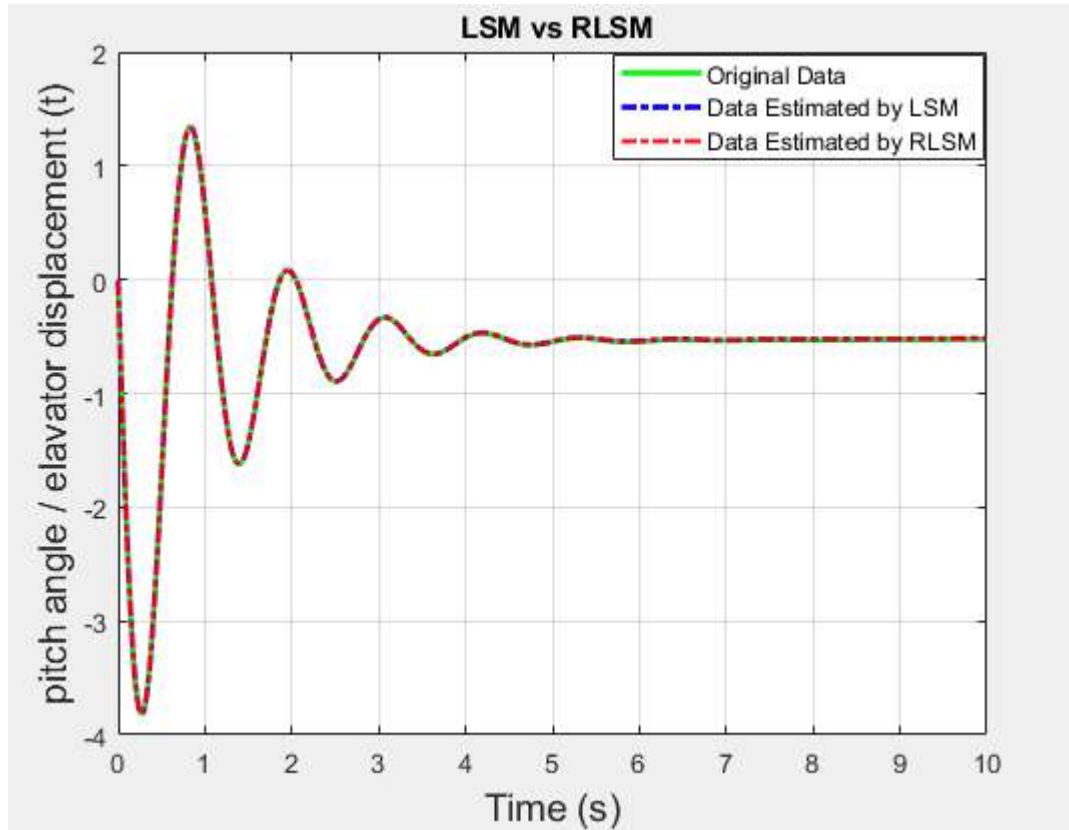


Figure 4.37 Estimated via RLSM and LSM (θ/δ_e)

Thus, estimate graphic obtained by both methods was created. For this pitch transfer function, which is also examined in terms of providing information about the transferred functions or the system, the pole zero map has been extracted as the original form, obtained by LS and RLS methods. This pole zero map is given in Figure 4.38 below.

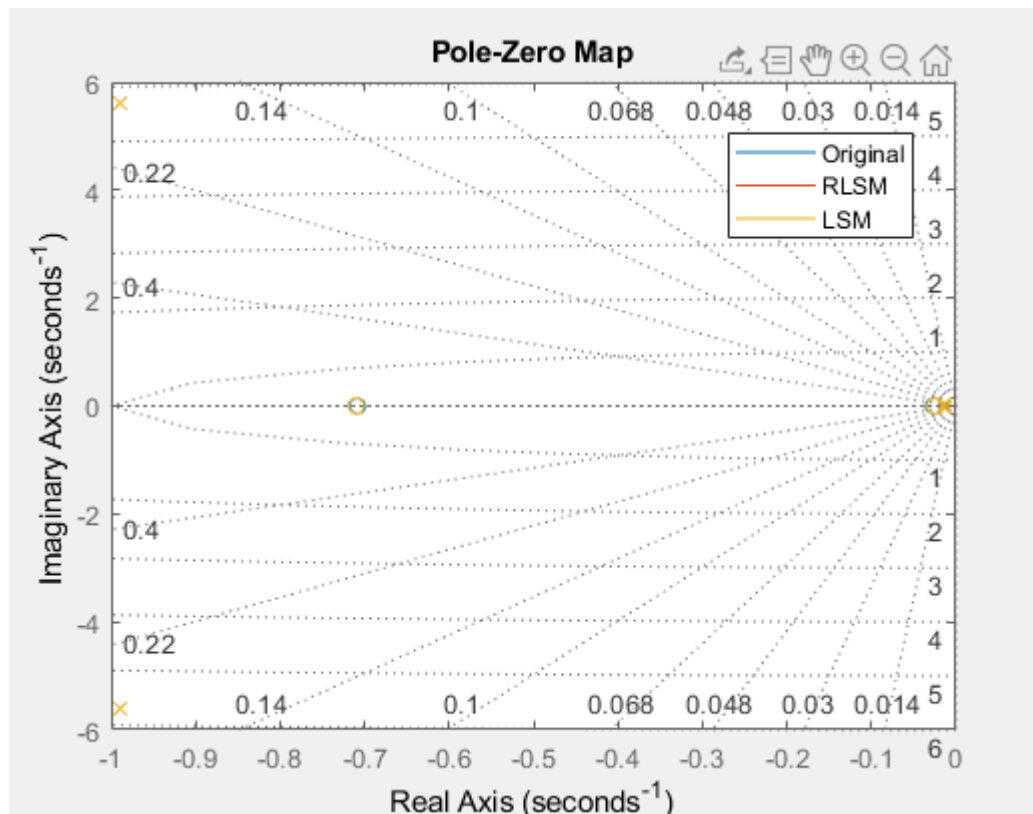


Figure 4.38 Pole zero map for pitch transfer function

Now, the transfer functions resulting from the behavior of the aileron and rudder control surfaces resulting from the lateral motion of an aircraft are compared with both methods. First of all, the transfer function resulting from the behavior of the aileron control surface for the lateral motion with both methods is given in Figure 4.39 below.

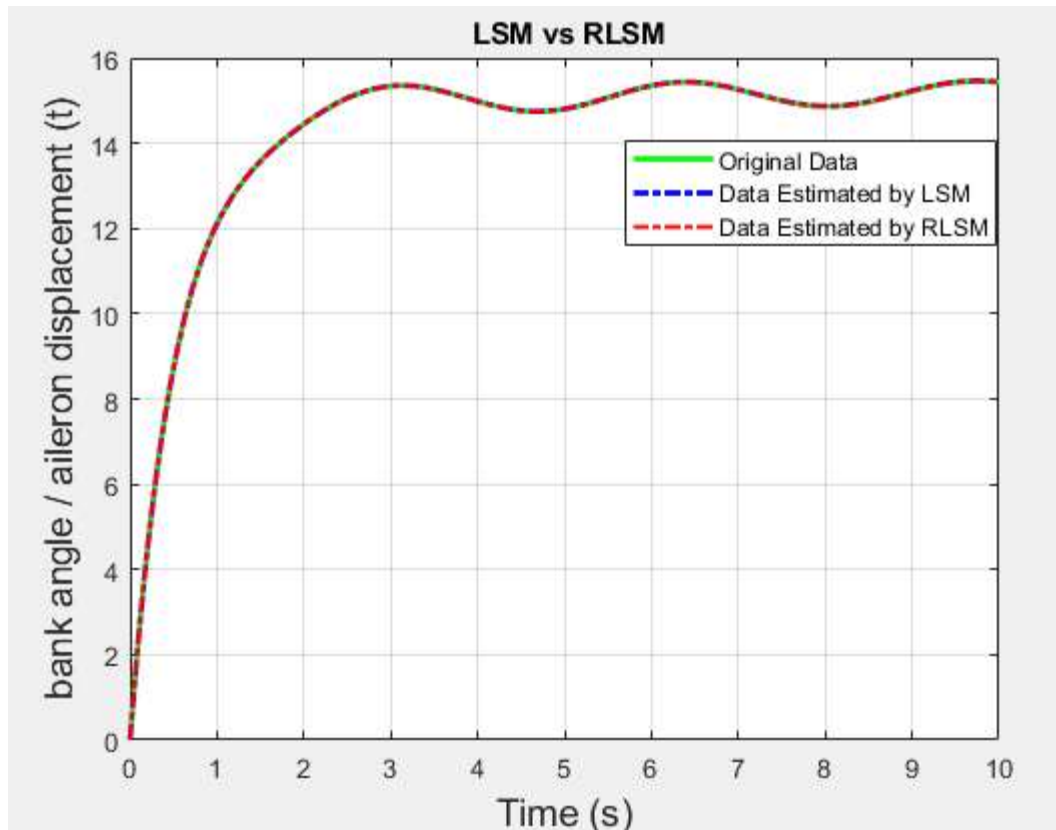


Figure 4.39 Estimated via RLSM and LSM (ϕ/δ_a)

Pole zero map has been extracted as the original forms obtained by LS and RLS methods for the transfer function, which is the ratio of this bank angle to aileron displacement, which is also examined in terms of providing information about the transferred functions or the system examined after the estimated graphs. This pole zero map is given in Figure 4.40 below.

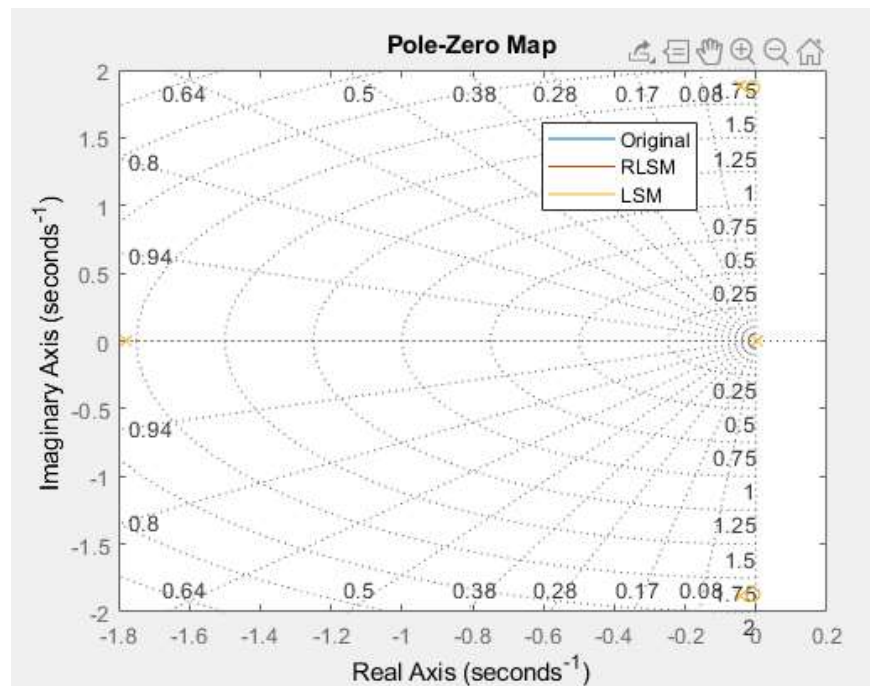


Figure 4.40 Pole zero map for bank angle to aileron displacement

Likewise, the transfer function resulting from the behavior of the rudder control surface resulting from the lateral motion of an aircraft is graphically plotted graphically with both methods, as shown in Figure 4.41 below.

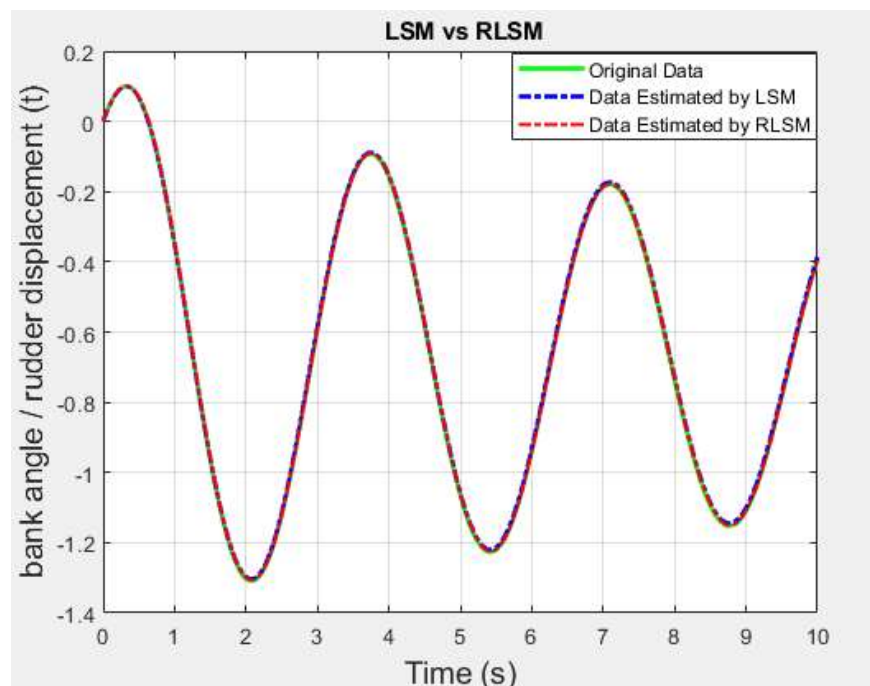


Figure 4.41 Estimated via RLSM and LSM (ϕ/δ_r)

Likewise, for the transfer function, which is the ratio of this bank angle to rudder displacement, which is examined in terms of providing information about the transfer functions or the system examined here, the pole zero map has been extracted as the original forms obtained by LS and RLS methods. This pole zero map is given in Figure 4.42 below.

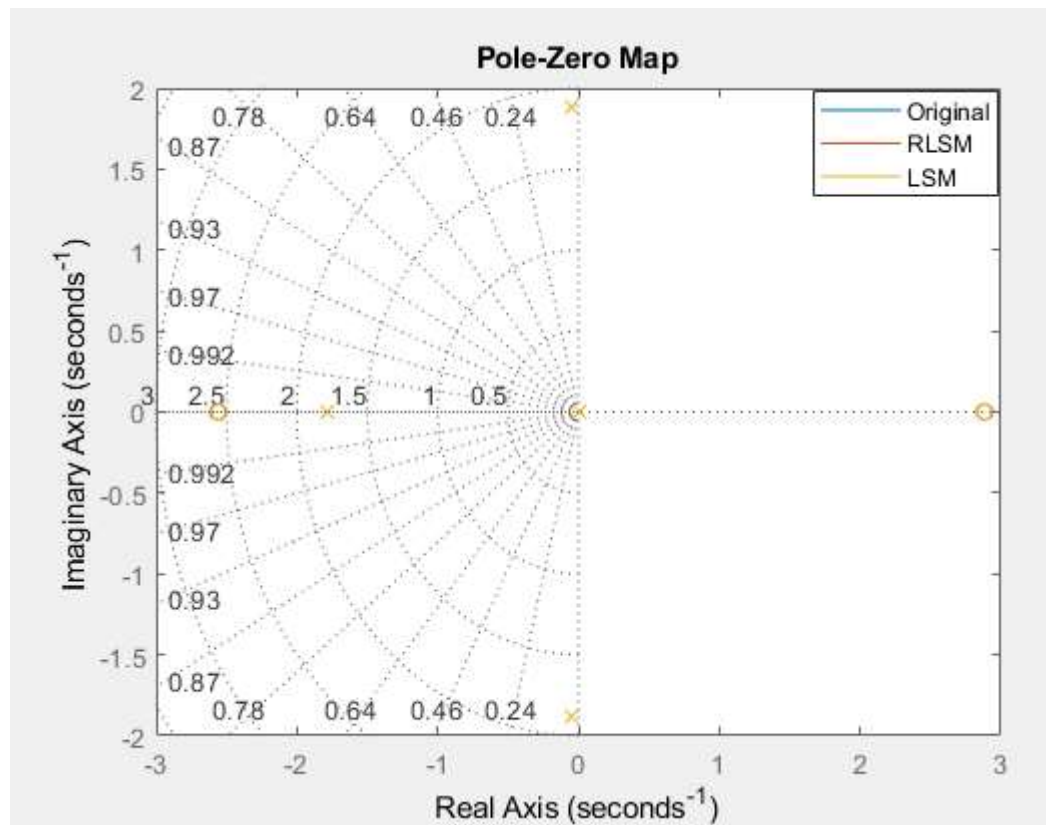


Figure 4.42 Pole zero map for bank angle to rudder displacement

Thus, the unknown parameters in the transfer functions of the aircraft control surfaces were analyzed in time domain by both methods and the transfer functions generated by the new parameters as a result of the estimation were specified. In addition, simulations expressing the result obtained when compared with the original transfer functions of estimation methods examined in MATLAB/Simulink program are shown. In addition to the graphical simulations obtained, it has been given in pole zero maps obtained in MATLAB/Simulink program in order to give information about the systems or the analyzed transfer functions. As a result of simulations, the integral square errors (ISE) table was created in order to observe the error difference of both methods according to the

original data and which method is closer to the original data. the result is given in the Table 4.1. ISE is the statistical information used to see the errors created by integrating the square of the system error throughout the fixed time interval to obtain information about the performance of the systems created.

Table 4.1 ISE table for LSM and RLSM

Parameter Estimation Methods	Elevator Control Surface (ISE)	Aileron Control Surface (ISE)	Rudder Control Surface (ISE)
LSM	0.0001386	0.00009236	0.0003527
RLSM	0.0001354	0.0000348	0.000117

5. ESTIMATION OF DOMINANT PARAMETERS VIA LSM AND RLSM

Many parameter estimation methods were mentioned above, LS and RLS methods were discussed in detail and various analyzes were performed. With both methods, the process of estimating transfer functions extracted according to the behavior of aircraft control surfaces is explained. In this part, the realization process of the estimation of some dominant parameters used in the formation of the transfer functions described and predicted in the above sections will be explained. The dominant parameters estimated here are the parameters of a linear dynamic aircraft model. While finding these aerodynamic parameters, they were compared with the actual aircraft parameters used in the formation of the originally determined transfer functions, and the error rates of the estimated parameters found by both methods were extracted. The parameters studied and tried to be predicted were specified in chapter 3 in the mathematical modeling section during the extraction of transfer functions. Under this chapter, the mathematical explanation of the equations of motion of a linear dynamical aircraft model is expressed and finally, the environment that serves to express some transfer functions has been created by applying the linearization process to these equations. Thus, the prediction of the dominant aerodynamic parameters specified in Equation (3.47), which is expressed from linearized aircraft motion equations, has been realized. In the mathematical operations performed in the process of finding parameters, transfer functions estimated by both methods are used. The parameters were tried to be found by using the Equation (3.52), (3.53) and (3.56) transfer functions specified in the chapter of mathematical modeling. In other words, when finding the parameters, both the pitch transfer function and the transfer function, which is the ratio of the angle of attack to elevator displacement, are used. As a result of the mathematical operations performed on these transfer functions, the parameters are estimated. After the transfer functions used were estimated with LS and RLS methods, the process of finding the dominant parameter was started.

5.1. Estimation Dominant Parameters via LSM

As explained at the beginning of chapter, the process of finding these parameters was carried out by both methods. First, the realization process was carried out with the LS method. Subsequently, the original and estimated versions of the parameters found as a result of this method are expressed. In this chapter, firstly, the transfer function in Equation (4.24) estimated by LS method is processed. This transfer function is the pitch transfer function created as a result of the longitudinal movement of an aircraft. The formation process of this transfer function has been described in the chapters above. In the above operations, this transfer function was estimated using the LS method. In this section, the basic dominant parameters, which are also stated in Equation (3.47), are tried to be estimated in the formation of this transfer function. While performing the estimate operation, was started with the transfer function given in Equation (4.24). However, as observed in the process, there was a difference between the number of equations created and the number of unknown parameters. Since the number of equations obtained here is less than the number of unknown parameters, a result could not be reached. Therefore, the transfer function, which is the ratio of angle of attack to elevator displacement, again resulting from the longitudinal motion of an aircraft, is discussed. In this transfer function, the formation process is explained as in the pitch transfer function. Equation (3.56), which is fully expressed parametrically, is also given. For this reason, before working with this transfer function, estimation was performed with the LS method, as in the other chapters. Thus, before starting the dominant parameter process, estimation process with LS method is explained in the transfer function, which is the ratio of the angle of attack to elevator displacement.

For the estimation process, the model prepared in the MATLAB/Simulink program is given in this transfer function, as shown in Figure 5.1. This model has been implemented differently than the other model used, due to the large number of parameters. Also in the MATLAB program, the algorithm of the LS method is set to estimate the transfer function, which is the ratio of angle of attack to elevator displacement.

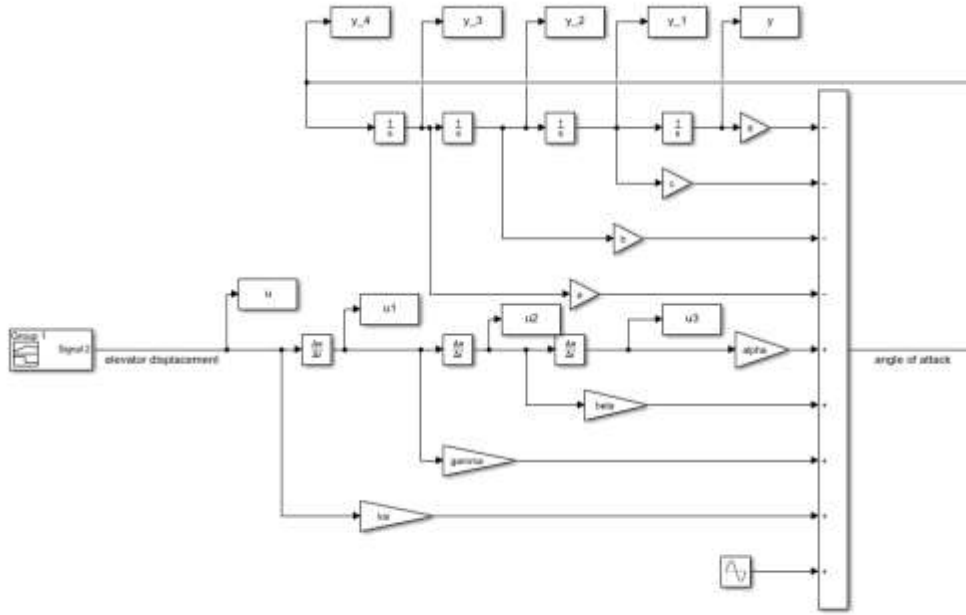


Figure 5.1 MATLAB/Simulink model for α/δ_e

After the model has been created, the transfer function, which is the ratio of the angle of attack to the elevator displacement, is given in Equation (5.1) below for the demonstration of the estimation process, created with the original data.

$$\left(\frac{\alpha}{\delta_e}\right)_{ORJ} = \frac{0.0515s^3 - 23.4487s^2 - 0.621s - 0.0128}{s^4 + 2.0072s^3 + 32.5269s^2 + 0.8638s + 0.0179} \quad (5.1)$$

When the model in Figure 5.1 and the algorithm created in the MATLAB program are run, the estimated transfer function obtained by the least squares method is obtained in Equation (5.1-2) below.

$$\left(\frac{\alpha}{\delta_e}\right)_{LSM} = \frac{0.0515s^3 - 23.4487s^2 - 0.6212s + 0.013572}{s^4 + 2.0071s^3 + 32.527s^2 + 0.8641s + 0.0178} \quad (5.2)$$

Since there is an estimated transfer function, the process of finding the dominant parameters can be started. There are two mathematically obtained transfer functions obtained by LS method. Thus, the number of equations has been increased by the number of unknown parameters. By using these two transfer

functions, solutions are obtained with equation solve commands in the MATLAB program. Thus, below, the values of the dominant parameters originally used and the values found as a result of the estimation process are given in Table 5.1.

Table 5.1 Estimated parameters via LSM

Parameters	Original Values	Estimated via LSM
C_L	0.0642	0.0644
C_D	0.0514	0.0486
$C_{M\alpha}$	-0.4	-0.4144
$C_{M\dot{\alpha}}$	-2	-1.9218
$C_{L\alpha}$	3	2.974
$C_{M\delta_e}$	-0.3	-0.32
$C_{L\delta_e}$	0.2	0.2008

Thus, the dominant parameters obtained have been found. Now the error table has been extracted to see to what extent the parameters approached the original values. this table is given in Table 5.2.

Table 5.2 Error table for parameters via LSM

Parameters	Error Rates
C_L	0.00311
C_D	0.0545
$C_{M\alpha}$	0.0360
$C_{M\dot{\alpha}}$	0.0391
$C_{L\alpha}$	0.0087
$C_{M\delta_e}$	0.066
$C_{L\delta_e}$	0.004

5.2. Estimation Dominant Parameters via RLSM

After the dominant parameters were found with the LS method, the same process was applied this time for the RLS method. Here again, estimated pitch transfer function and transfer function, which is the ratio of angle of attack to elevator displacement, are used. The processes described above in chapter 5.1 are also

applied here. Again, the process was first started by using the RLS method estimated using the pitch transfer function given in Equation (4.44). Then, after the use of the transfer function, which is the ratio of the angle of attack to elevator displacement, this transfer function was tried to be estimated by using the RLS method. While performing the estimate process, Figure 5.1 is used here, as in the LS method. Also here, with the model, the algorithm of the RLS method was created in the MATLAB program. Before proceeding to the dominant parameter finding process, the estimate operation of the transfer function, which is the ratio of the angle of attack to the elevator displacement, created with the original data given in Equation (5.1), was performed with the RLS method. The estimate operation was performed after running the model in Figure 5.1 and the algorithm created in the MATLAB program. Its estimated form is given below in Equation (5.3).

$$\left(\frac{\alpha}{\delta_e}\right)_{RLSM} = \frac{0.0515s^3 - 23.4487s^2 - 0.6214s + 0.0135725}{s^4 + 2.0072s^3 + 32.5269s^2 + 0.8638s + 0.0179} \quad (5.3)$$

Since there is an estimated transfer function, the process of finding the dominant parameters can be started. There are two mathematically obtained transfer functions obtained by RLS method. Thus, the number of equations has been increased by the number of unknown parameters. By using these two transfer functions, solutions are obtained with equation solve commands in the MATLAB program. Thus, below, the values of the dominant parameters originally used and the values found as a result of the estimation process are given in Table 5.3.

Table 5.3 Estimated aerodynamic via RLSM

Paramters	Original Values	Estimated via RLSM
C_L	0.0642	0.0644
C_D	0.0514	0.049
$C_{M\alpha}$	-0.4	-0.4191
$C_{M\dot{\alpha}}$	-2	-2.01
$C_{L\alpha}$	3	2.976
$C_{M\delta_e}$	-0.3	-0.319
$C_{L\delta_e}$	0.2	0.2006

Thus, the dominant parameters obtained have been found. Now the error table has been extracted to see to what extent the parameters approached the original values. this table is given in Table 5.4.

Table 5.4 Error table for parameters via RLSM

Paramters	Error Rates
C_L	0.00311
C_D	0.0466
$C_{M\alpha}$	0.04775
$C_{M\dot{\alpha}}$	0.05
$C_{L\alpha}$	0.008
$C_{M\delta_e}$	0.0633
$C_{L\delta_e}$	0.003

6. CONCLUSION AND RECOMMENDATIONS

In this study, how to use system identification and system identification techniques in the aviation field, examining and analyzing the accuracy of the results. In this context, primarily the parameter estimation method of the MATLAB program, various parameter estimation methods are explained. Some of these are explained in detail and shown with applications in the aviation field. In order to examine and see the system definition, firstly, the system identification tool of the MATLAB program was examined. In this context, the identification of the pitch transfer function obtained as a result of extracting the dynamic aircraft model of an aircraft was performed using this tool. Then, RLS and LS methods, which are examples of online and offline parameter estimation methods, are discussed. By using these methods, the transfer functions resulting from the dynamic aircraft model of an aircraft have been estimated. These defined transfer functions are the transfer functions resulting from the behavior of the aircraft control surfaces as a result of the longitudinal and lateral motion of the aircraft. As a result of these analyzes, estimated transfer functions using both RLS and LS methods are compared and the results are shown. Therefore, as the main purpose of this study, it has been tried to show that the real time parameter estimation method, RLS method, gives better results. In this context, LS method, another parameter estimation method described for comparison, and transfer functions and graphs are compared for both methods. In order to see the comparisons mathematically, the ISE table was created. By looking at this table, it can be seen how close to the original forms of the transfer functions obtained by estimating them. While creating this table, it was created for both methods and the approach was seen in both methods. Thus, when looking at the results, although the RLS method made a certain successful estimation in the LS method, the estimation error rate of the RLS method was found to be less than the LS method.

In general, the obtained transfer functions, graphs, error tables of the methods and the result put forward are explained. The graphics shown and obtained here were created by defining doublet input as input to the model created in MATLAB/Simulink, as outlined above. Thus, as can be seen in the graphs, better

results were obtained with both methods in terms of proximity to the original data. Until this stage, the graphics that came out by using more than one method were interpreted. Before using doublet input, more than one input value has been added to the model. In the first step, single sine value is used. Thus, the estimate values and graphics obtained were found to be very close to each other. Then, the sum of five sinusoidal values of different frequency and amplitude is defined to the model as the input value. With this result, the rate of proximity was higher. Thus, the results have been observed with the change of input values.

After the analysis comments with different input values, the analyzes made with different data numbers are expressed. In the study, appropriate data numbers were used to reach the closest estimate of the results obtained above. However, some analyzes and determinations were made in order to see the effect of the changes in the data numbers. In this context, various changes were made in the number of data in the algorithms applied in the MATLAB program and the results were observed. The evaluation made according to this number of data was also carried out for the LS and RLS methods. Considering that the results obtained above are ideal results, when analyzes were performed with a smaller amount of data than the number of data used in obtaining those results, there was no change in the estimation process performed by the RLS method, while partial divergences occurred in the LS method. These results are given in Figure 6.1, Figure 6.2 and Figure 6.3 below. While performing these results, the same simulation time was applied as above.

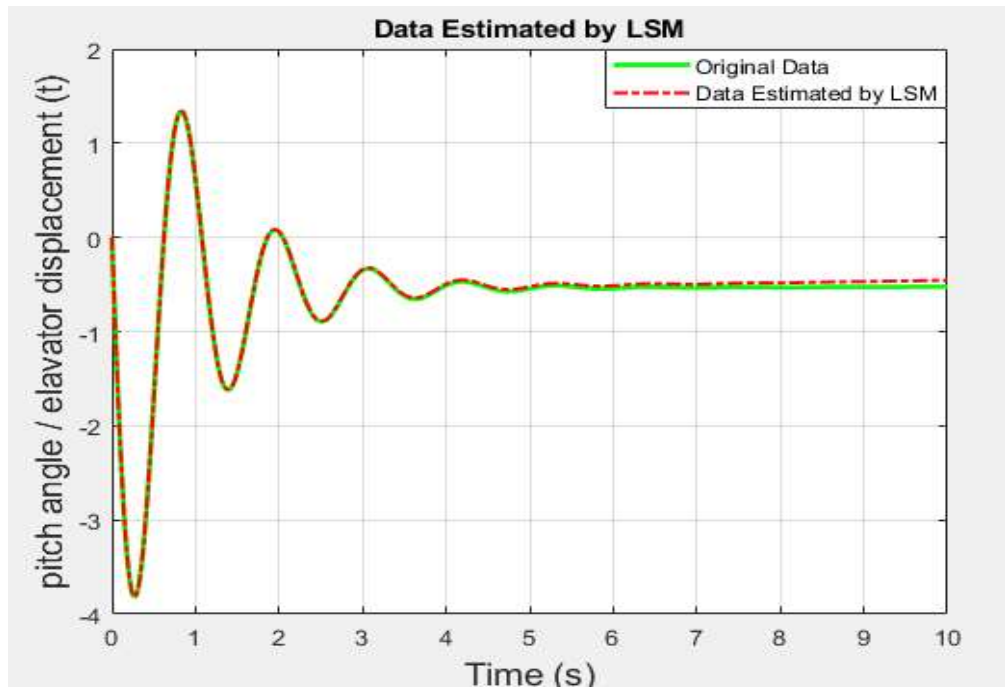


Figure 6.1. Estimated via LSM for decreasing number of data (θ/δ_e)

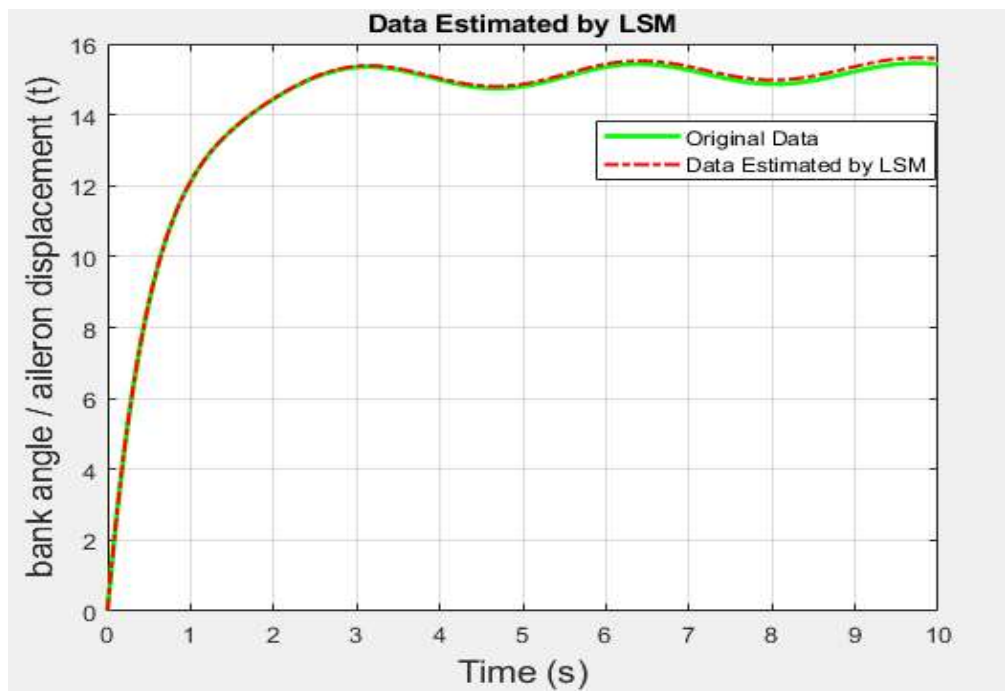


Figure 6.2. Estimated via LSM for decreasing number of data (ϕ/δ_a)

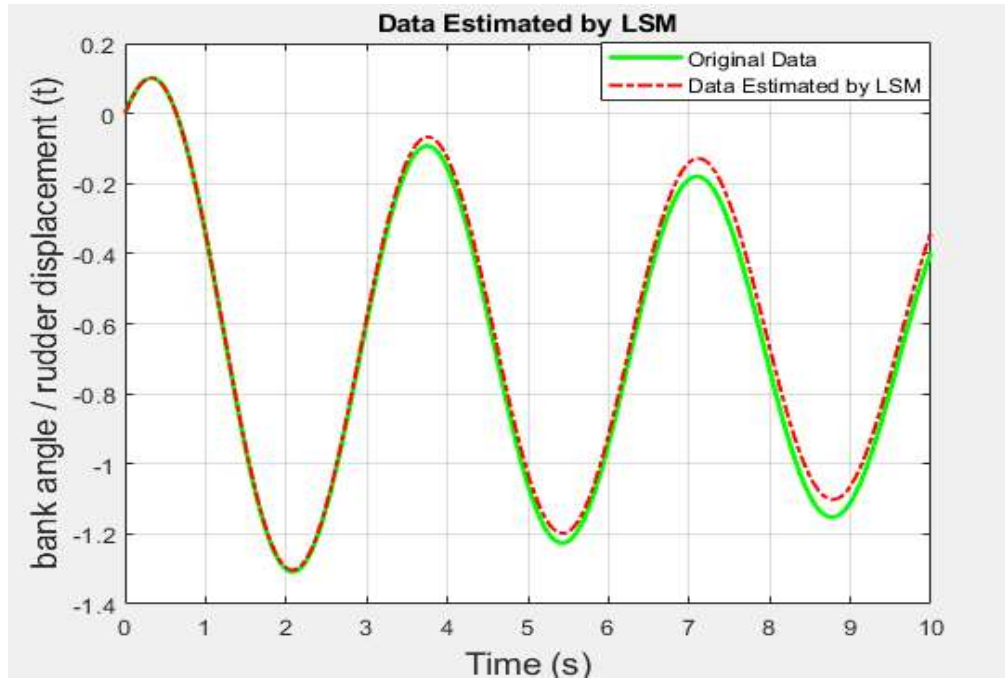


Figure 6.3. Estimated via LSM for decreasing number of data (ϕ/δ_r)

Also, in addition to the results analysis, the results of the analysis for both methods, this time towards increasing the number of data, were shared. Here again, the RLS method performed a successful estimation process. With the increase in the number of data in the LS method, more successful results were acquired in the estimation results obtained. Thus, the behavior of the LS method to increase the number of data is shown in Figure 6.4, Figure 6.5 and Figure 6.6.

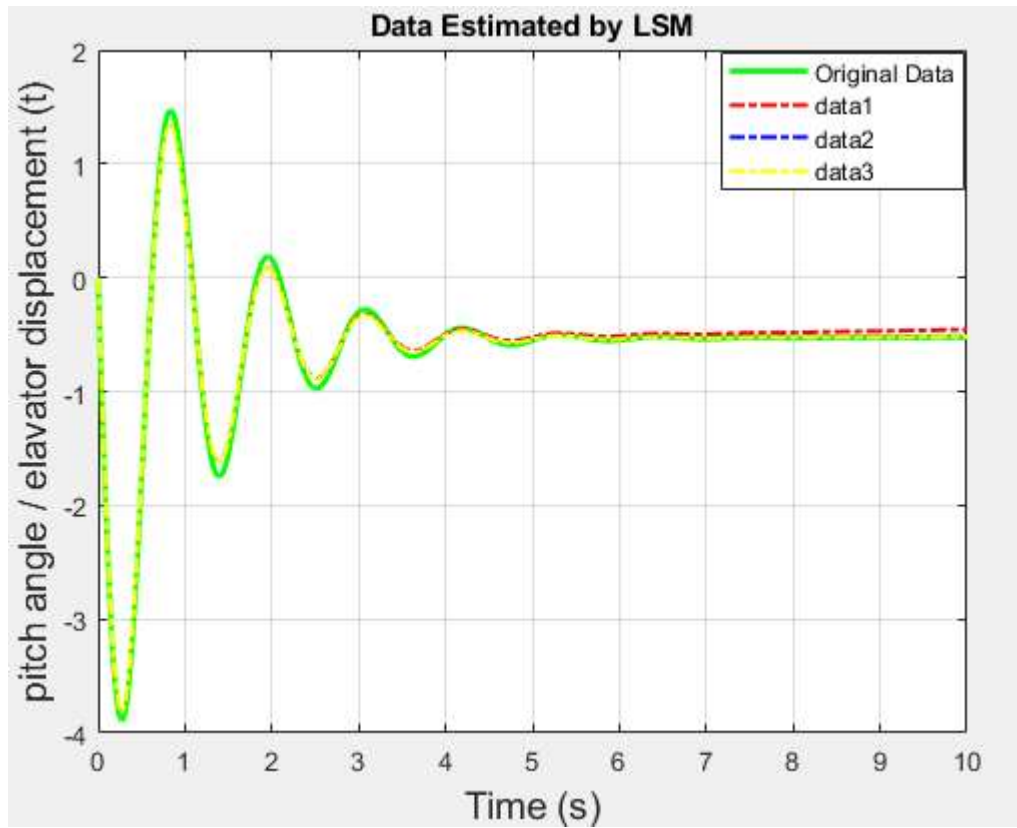


Figure 6.4. Estimated via LSM for increasing number of data (θ/δ_e)

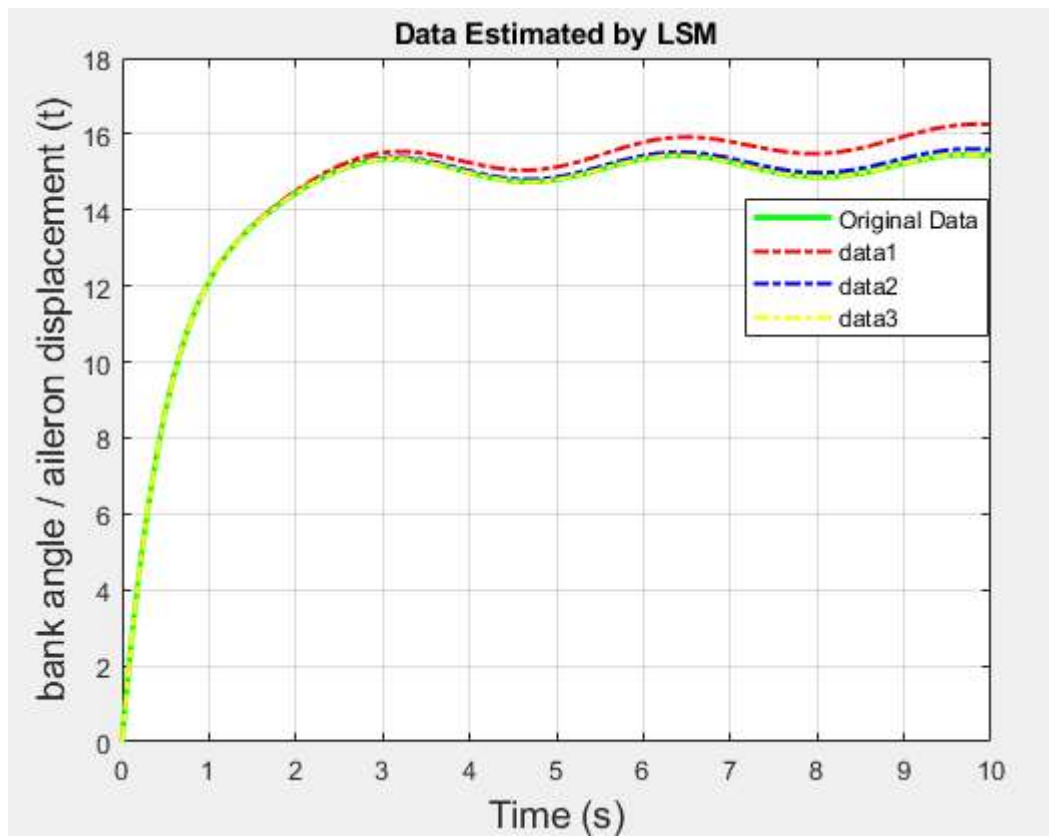


Figure 6.5. Estimated via LSM for increasing number of data (ϕ/δ_a)

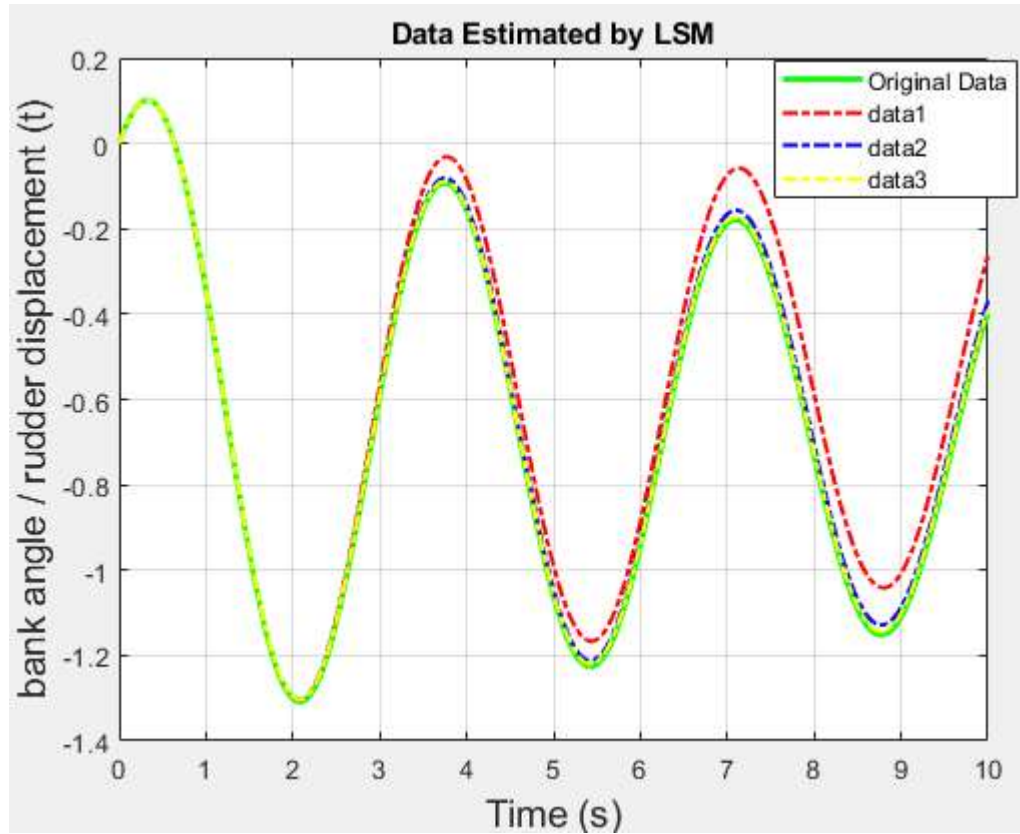


Figure 6.6. Estimated via LSM for increasing number of data (ϕ/δ_r)

Apart from the analysis according to the change in the number of data, a certain amount of error has been applied in order to see the changes in the result of the estimation process in case of breaking the system. In the systems used and examined, the originally used parameters were changed by increasing them starting from 10 percent before starting the estimation process. As the percentage rate increased, the error rate in the estimation result increased as a percentage.

In addition, some step-response properties are also examined in order to see the time responses of these transfer functions. Thus, the system step-response characteristic between the original forms of the transfer functions and the forms estimated by the RLS and LS methods were investigated. In this context, as the step-response characteristics, rise time, settling time overshoot, damping ratio and natural frequency values were examined. The time responses of the systems obtained in all three forms are given in Table 6.1 below. As a result, the time responses of the examined systems, namely the step-response characteristics,

were interpreted by looking at this table, and it was understood that the system responses of the transfer function obtained with RLS were closer to the responses of the original transfer function. Here, among the transfer functions analyzed above, only the time responses of the pitch transfer function are examined. In other words, the properties given in Table 6.1 are the pitch transfer function. Step-response characteristics information could not be obtained because other examined transfer functions displayed unstable behavior starting from their original forms. This situation can be understood by examining the pole-zero maps created in chapter 4 above. Note that the damping ratio and the natural frequencies are depicted for dominant poles of the system given in Equation (4.23) or (4.43), (4.24) and (4.44).

Table 6.1 Step-response characteristic values

Step-Response Characteristic	Original Form	Estimated Form via RLSM	Estimated Form via LSM
Rise Time	47.4256	45.7771	43.7028
Settling Time	297.9623	299.7469	299.8347
Overshoot	19.9879	20.9202	22.3634
Damping Ratio	0.5650	0.5670	0.5560
Natural Frequency	0.0235	0.0234	0.0239

After estimating transfer functions, estimation of some dominant parameters used in the formation process of these transfer functions is explained. the process of finding dominant parameters and the paths followed are expressed in chapter 5. As explained there, the equation number is obtained by using more than one transfer function obtained as a result of the motion equations resulting from the longitudinal motion of an aircraft. Because the number of equations obtained with the pitch transfer function we have in the first place was less than the number of unknowns. Then, the ratio of angle of attack to elevator displacement, another transfer function resulting from longitudinal motion, was deducted. This transfer function has also been estimated by both methods as previously applied to the pitch transfer function. Thus, as the last case, some dominant parameters were found mathematically using the equation solving process in the MATLAB program with these transfer functions obtained from both methods. The

formation of these transfer functions and their connection with the dominant parameters are expressed in the chapter of mathematical modeling. Some dominant parameters were obtained using RLS and LS methods. Separate parameter table has been created with both methods. When looking at these tables, it can be observed that each parameter is close to its original values. Again, during the estimation process of the parameters, the RLS method predicted better than the LS method in terms of proximity to the original values. Separate error tables were prepared to see the estimation closeness of both methods. Here, too, the proximity of the methods to the real data for each parameter is observed. Among these predicted parameters, the C_{MQ} and $C_{D_{cl^2}}$ parameters have been estimated far from their true values. With both methods, these two parameters have a higher error rate compared to other parameters.

After these dominant parameters were found, some changes were made on some of them and they were observed. The purpose of this observation was to see the effect of the change of parameters on the general system. In this context, first of all, the original values of the C_{MQ} parameter and the values that we estimate gave different values to the system. Thus, it has been determined that the effect of the estimated transfer functions obtained initially in general is almost nonexistent. These operations were repeated with another parameter. this time, the effect of $C_{M\alpha}$ parameter was tried to be observed by giving different values from its original value. Thus, it has been observed that this parameter changes in the transfer functions estimated according to different values. It is for this reason that the $C_{M\alpha}$ parameter has a significant effect on whether its value can be changed for the general system.

REFERENCES

- Aström, K.J., Bohlin, T., 1965. Numerical Identification of Linear Dynamic Systems from Normal Operating Records. In: Proc. IFAC Symposium on Self-Adaptive Systems. Teddington, UK.
- Cetin, E., 2018. System Identification and Control of a Fixed Wing Aircraft by Using Flight Data Obtained from X-Aircraft Flight Simulator, Middle East Technical University, Institute of Science, M.Sc. Thesis, 139, Ankara.
- Charles, G., Goodall, R.M., Dixon R., 2008. Condition Monitoring Approaches To Estimating Wheel-Rail Profile. ResearchGate, 7, Berlin, Germany.
- Chen, X., Tomizuka, M., 2014. Advanced Control Systems II (Lecture Notes for ME233). University of California, Department of Mechanical Engineering.
- DeBusk, W.M., Chowdhary, G., Johnson, E.N., 2009. Real-Time System Identification of a Small Multi-Engine Aircraft, Georgia Institute of Technology, Atlanta, GA, USA.
- Evans, C., Fleming, P.C., Hill, D.C., Norton, J.P., Pratt I., Rees, D., Rodriguez-Vazquez, K., 2001. Application of System Identification Techniques to Aircraft Gas Turbine Engines, Control Engineering Practice, 9, 135-148.
- Gauss, C.F., 1809. Teoria Motus Corporum Coelestium in Sectionibus Conicis Solem Ambientium. Reprinted translation: 'Theory of Motion of the Heavenly Bodies Moving about the Sun in Conic Sections'. Dover, New York.
- Grauer, J.A., Morelli, E.A., 2016. Parameter Uncertainty for Aircraft Aerodynamic Modeling using Recursive Least Squares, AIAA Atmospheric Flight Mechanics Conference, 4-8 January, San Diego, California, USA.
- Grauer, J.A., Boucher, M.J., 2020. Aircraft System Identification from Multisine Inputs and Frequency Responses. AIAA Scitech 2020 Forum, 6-10 January, Orlando, F.
- Gupta, A., 2015. Modeling and Control of an Aircraft System, National Institute of Technology Rourkela, M.Sc. Thesis, 66, Odisha.
- Hardier, G., Ferreres, G., Seren C., 2016. A Recursive Estimation Algorithm to Track Aircraft Model Parameters, IEEE SysTol'16, September, Barcelone, Spain.
- Ho, B.L., Kalman, R.E., 1965. Effective Construction of Linear State-Variable Models from Input Output Functions. Regelungstechnik 12, 545-548.

- Howe, R.M., 1980. Control of Aircraft Missiles and Space Vehicles (Lecture Notes for Aero 574). University of Michigan, Department of Aerospace Engineering.
- Jategaonkar, R.V., 2006. Flight Vehicle System Identification: A Time Domain Methodology, AIAA (American Institute of Aeronautics & Astronautics), 629, Reston, Virginia.
- Kamali, C., Pashilkar, A.A., Raol, J.R., 2011. Evaluation of Recursive Least Squares Algorithm for Parameter Estimation in Aircraft Real Time Applications. Aerospace Science and Technology, 15, 165–174.
- Klein, V., Morelli, E.A., 2006. Aircraft System Identification: Theory and Practise, AIAA (American Institute of Aeronautics & Astronautics), 484p, Reston, Virginia.
- McLean, D., 1990. Automatic Flight Control Systems, Prentice Hall, 593, Hemel Hempstead.
- Molugaram, K., Rao, G.S., 2017. Statistical Techniques For Transportation Engineering, Elsevier, 281-292, Amsterdam, Netherlands.
- Qadri, M.T., Zulfikar, R., Ahmed, N., Iftikar, R., Siddiqui, A.A., 2016. Comparative Analysis of LMS (Least Mean Square) and RLS (Recursive Least Square) for Estimation of Fighter Aircraft's Mathematical Model. Journal of Information & Communication Technology 10, 1, 35 – 46.
- Remli, M.A., Mohammed, M.S., Deris, S., Napis, S., Sinnott, R., Sjaugi, M.F., 2017. Metaheuristic Optimization for Parameter Estimation in Kinetic Models of Biological Systems- Recent Development and Future Direction, Current Bioinformatics, 12, 286-295.
- Stevens, B.L., Lewis, F.L., Johnson, E.N., 2016. Aircraft Control and Simulations, Wiley, 749, New Jersey.
- Simmons, B.M., 2018. System Identification of a Nonlinear Flight Dynamics Model for a Small, Fixed-Wing UAV. Virginia State University, Virginia Polytechnic Institute, M.Sc. Thesis, 156, Blacksburg, Virginia.
- Scheper, K.Y.W., Chowdhary, G., Johnson, E.N., 2013. Aerodynamic System Identification of Fixed-wing UAV. August 19-22, Boston, MA.
- Zadeh, L.A., 1962. From Circuit Theory to System Theory, Proceedings of the IRE, 50, 856-865.

BIBLIOGRAPHY

Name Surname : Mehmet ŞAHİN

Education

High School : Prof. Dr. Sabahattin Zaim Anatolian Highschool, 2010

BSc : Istanbul Commerce University, Faculty of Engineering,
Mechatronics Engineering Department, 2017

MSc : Istanbul Commerce University, Graduate School of Natural
and Applied Sciences, Mechatronics Engineering, 2021

Publications

Şahin, M., Kalyon, M., 2021. Estimating Dominant Parameters of Aircraft Linear Dynamical Model via Least Square Method. Istanbul Commerce University Journal of Science, 20 (39), 35-56.